TRENDS IN RAINFALL PATTERN AND SPATIAL VARIATION – CASE STUDY: LANGAT RIVER BASIN

By

PUAH YAN JUN

A dissertation submitted to the Department of Civil Engineering,
Lee Kong Chian Faculty of Engineering and Science,
Universiti Tunku Abdul Rahman,
in partial fulfillment of the requirements for the degree of
Master of Science.
February 2015

ABSTRACT

TRENDS IN RAINFALL PATTERN AND SPATIAL VARIATION – CASE STUDY: LANGAT RIVER BASIN

Puah Yan Jun

Climate change is a global topic that is concerned by researchers in every country. Cyclones, storms and hurricane occurred in 2013 brought heavy precipitation which could cause flooding inland. Thus, analysing rainfall trends becomes popular assessment tools of climate change. This research aimed to determine rainfall trends and spatial variations of Langat River Basin for the period of 1971-2012. Rainfall trend analyses were done by a relatively new method in hydrological analysis, Holt's method, and results were compared with Kendall's Tau and Spearman's Rho test. Since result from Holt's method was shown in graphical form which made it difficult to compare with results from other tests, gradient of the best fitted line was calculated. March, July and November were among the months those have most of the stations with increasing rainfall trends; whilst May and September were the months with the highest number of stations showing decreasing trends. Station 2815001 showed the highest number of months with changing rainfall trends throughout the year. There were seven stations showing upward trends during Northeast Monsoon. Rainfall series were modelled using Additive Holt-Winters method. Rainfall in southern region showed fluctuations. Increasing trends were discovered at stations in the north-eastern

region, central region, western region and south-eastern region except the seasonal analysis at station 45253. Decreasing trend was found in the east. Spatial variations were presented in maps. The study area was partitioned using Thiessen's Polygon method. Most stations showed increasing trend in March, April, July, September and December while more decreasing trends were found in May, Jun, August and October. Similar result was revealed in seasonal rainfall, most stations showed increasing trend in all seasons except SWM (Southwest Monsoon). For analysis of monthly rainfall series, increasing trends were found in whole region except station 2818110. Results from this research can be used in forecasting future rainfall and future water management.

ACKNOWLEDGEMENT

First and foremost, I would like to express my sincere appreciation to my supervisor, Dr. Huang Yuk Feng, who has continually given me guidance on my research. His continuous support, patient, enthusiasm, motivation and also the great knowledge in hydrology field help me a lot during my master study. Hydrology is an unfamiliar topic for me, without his assistance guidance, this thesis would never be materialized.

Also, a special thanks to Dr Chua Kuan Chin, for not only being my co-supervisor and also my special advisor in mathematic field. Thanks for giving me useful and inspiring comments so that I can understand the topic in more detail.

My deepest appreciation goes to UTAR for providing financial support and giving me the opportunity to complete my master study and realize my dreams.

I would also like to thank my parents and family for supporting and supervising me. They always cheered me up when I was facing difficulties.

Finally, I would particularly like to thank the most important person in my life, Shoo Ci Ho. He was always there to encourage and accompany me through the good times and bad.

APPROVAL SHEET

This dissertation/thesis entitled "**TRENDS IN RAINFALL PATTERN AND SPATIAL VARIATION – CASE STUDY: LANGAT RIVER BASIN**" was prepared by PUAH YAN JUN and submitted as partial fulfillment of the requirements for the degree of Master of Science at Universiti Tunku Abdul Rahman.

Approved by:

_____

(Dr. HUANG YUK FENG) Date:……..
Assistant Professor/Supervisor
Department of Civil Engineering
Lee Kong Chian Faculty of Engineering and Science
Universiti Tunku Abdul Rahman

_____

(Dr. CHUA KUAN CHIN) Date:……..
Assistant Professor/Co-supervisor
Department of Mathematical and Actuarial Sciences
Lee Kong Chian Faculty of Engineering and Science
Universiti Tunku Abdul Rahman

LEE KONG CHIAN FACULTY OF ENGINEERING AND SCIENCE

UNIVERSITI TUNKU ABDUL RAHMAN

Date: _____

SUBMISSION OF DISSERTATION

It is hereby certified that ***Puah Yan Jun*** (ID No: ***1207903***) has completed this dissertation entitled "Trends in Rainfall Pattern and Spatial Variation – Case Study: Langat River Basin" under the supervision of Dr Huang Yuk Feng (Supervisor) from the Department of Civil Engineering, Lee Kong Chian Faculty of Engineering and Science, and Dr Chua Kuan Chin (Co-Supervisor) from the Department of Mathematical and Actuarial Sciences, Lee Kong Chian Faculty of Engineering and Science.

I understand that University will upload softcopy of my dissertation in pdf format into UTAR Institutional Repository, which may be made accessible to UTAR community and public.

Yours truly,

_____

(*Puah Yan Jun*)

DECLARATION

I, PUAH YAN JUN hereby declare that the dissertation is based on my original work except for quotations and citations which have been duly acknowledged. I also declare that it has not been previously or concurrently submitted for any other degree at UTAR or other institutions.

_____
(PUAH YAN JUN)

Date _____

TABLE OF CONTENTS

LIST OF TABLES

LIST OF FIGURES

LIST OF ABBREVIATIONS

ADW	Angular Distance Weighting
BR	Buishand Range Test
CUSUM	Cumulative Sum
CV	Coefficient of Variation
DID	Department of Irrigation and Drainage Malaysia
ENSO	El Niño-Southern Oscillation
IDW	Inverse Distance Weighted
IPCC	Intergovernmental Panel on Climate Change
ITM1	Inter-monsoon 1 (September to October)
ITM2	Inter-monsoon 2 (March to April)
MAD	Mean Absolute Deviation
MAPE	Mean Absolute Percentage Error
MMD	Malaysian Meteorological Department
MSE	Mean Square Error
NAHRIM	National Hydraulic Research Institute of Malaysia
NEM	Northeast Monsoon (October to February of the following year)
PCI	Precipitation Concentration Index
PDO	Pacific Decadal Oscillation
PET	Pettitt Test
PKE	Perturbation Kinetic Energy
SNHT	Standard Normal Homogeneity Test
SOI	Southern Oscillation Index
SST	Sea Surface Temperature

SWM	Southwest Monsoon (May to August)
VNR	Von Neumann Ratio Test

CHAPTER 1

INTRODUCTION

1.1 Background of Study

The focus of this study is to investigate the rainfall trends and their spatial variations in Langat River Basin. The river basin occupies the whole southern region of Selangor State and part of the northern region of Negeri Sembilan. Langat River drains westward from the central region of Peninsular Malaysia to the Straits of Malacca with a total basin area of 2200 km^2. It is an important river basin since Putrajaya City, the Federal Administrative Centre of Malaysia, and the Multimedia Super Corridor that covers Cyberjaya and KLIA, are located within this area. Two reservoirs, which are Semenyih Reservoir and Hulu Langat Reservoir, and eight water treatment plants, are found in the river basin. These water sources supply water to two-thirds of Selangor State, and provides freshwater to approximately 1.2 million people within the river basin.

National Water Source Report 2000-2050 from the Economic Planning Unit showed that demand for treated water in Selangor, Kuala Lumpur and Putrajaya is expected to grow between 2% and 3.5% annually (*The Star* 22 July 2010). Furthermore, it is reported that daily water demand of these three areas will reach 4,907 million litres in 2014 whereas the present supply capacity is only 4,431 million litres. Besides that, as reported in the New

Straits Times (Mahmood 2012), about one million people in Selangor, Kuala Lumpur and Putrajaya had been affected by water shortage from the mid of May until July 8. Thus, Pahang-Selangor raw water transfer project was proposed and commenced in the Ninth Malaysia Plan (2006-2010). The construction costs RM9 billion and was mainly planned to overcome the water shortage in Selangor and Kuala Lumpur region due to the rapid commercial and industrial development. The objective of this project is to convey raw water through a transfer tunnel from Pahang to Selangor, Kuala Lumpur and the western part of Negeri Sembilan in order to meet the increasing water demand. It is proposed to pump 1,890 million litres of raw water daily from Sungai Semantan in Pahang to Hulu Langat water treatment facility in Selangor upon completion in 2014.

Global warming, as one of the most serious environmental issues in the last two decades, is strongly believed as a human-induced issue. Climate is the averaged weather condition, which has an impact on living beings in the world. Development is heavily emphasized in the developing countries like Malaysia but rapid urbanization has negative impact on climate. One of the impacts is the urban heat island effect. A city with population more than one million can cause the annual mean temperature to be 1 to 3°C higher than the surrounding areas and air temperature is closely related to rainfall patterns. Malaysia situated in the tropical area where there is no distinct four seasons. However, the characteristic of climate in Malaysia is hot and high humidity. Thus, analysing rainfall trend is one of the limited ways to assess climate change in Malaysia. Associated with global warming and urban heat island effect, patterns in rainfall trend change unconsciously.

1.2 Problem Statement

Malaysia, as a developing country, grows rapidly in both population and economic development. Langat River Basin as the major area for economic growth, a substantial increase in water demand is expected. Rapid development in the southern region of Selangor State especially the District of Hulu Langat, District of Sepang as well as Kuala Langat is expected to be continued in the near future with commencement of hi-tech based industrial operations and other forms of manufacturing activities along with the development of new urban centres. According to the report from Department of Statistic (2011), Selangor was the most populous state of 5.46 million populations with 2.7% population growth rate for the period 2000-2010. Apart from this, Putrajaya, the federal territory with 100% level of urbanization that located within the catchment, had the highest growth rate of 17.8% for the period 2000-2010 and 3.9% annual population growth rate in 2011-2012. With the population density of 674 and 1478 persons per square kilometre in Selangor and Putrajaya, sufficient supply of freshwater is relatively important.

Accelerated land-use change has inevitably destroyed the environment and caused significant impact on climate. Rapid developments such as urbanization and industrialization will lead to a great change of the quantity of water resources in a river basin. Developments in Putrajaya and Cyberjaya have driven the urbanization and industralisation in Langat River Basin. Changes in rainfall pattern could therefore be more obvious in this river basin compared to other river basins in the country. The situation is made to be

worse with the impact of global warming. According to report from NAHRIM (National Hydraulic Research Institute of Malaysia, 2006), projected precipitation for the period 2026-2034 and 2041-2050 is lesser than precipitation in the period 1984-1993 in Selangor area. Even though Pahang-Selangor Inter-state Raw Water Transfer Project is in progress, the Langat 2 water treatment plant project which was the downstream portion of the project had been delayed for 29 months (Ganesh 2012). Current water resources will only be sufficient for people in Selangor, Kuala Lumpur and Putrajaya until 2015.This situation will be worsen if low rainfall continue since the main water resource, Sungai Selangor dam, is dependent on rain.

Considering the above discussion, it is not too far-fetched to say that the availability of water supply resources will be insufficient in the near future. Study of the past and present rainfall trends can provide indication to authorities to plan for appropriate strategies in order to minimize the impact of climate change. Rainfall trend and spatial variation analyses are of the useful and popular ways to assess climate change in a tropical country like Malaysia.

1.3 Objectives

The primary aims of the present study are to examine rainfall trends and spatial variations of the Langat River Basin. Thus, the objectives of this study are:

(i) To examine rainfall trends on particular month or season for selected rainfall stations in the river basin using the Holt's method

and compare result with Kendall's Tau test and Spearman's Rho test.

(ii) To model rainfall series at the 10 selected stations for the whole study period and study the pattern in rainfall trends using the Additive Holt-Winters method.

(iii) To investigate the spatial variations of rainfall in the Langat River Basin from 1970 to 2012.

1.4 Scope of Work

Only Langat River Basin will be focused in this study. Rainfall trend and spatial variation analyses will be carried out based on the recorded rainfall data of the selected rainfall stations within the river basin. The period of study is from 1970 to 2012 depends on data availability at each station. Trend detection will be done in two parts: rainfall trend analysis and rainfall series analysis. The Holt's method, Kendall's Tau test and Spearman's Rho test are employed for rainfall trend detection for series of particular month or season. Then, in rainfall series analysis, the Additive Holt-Winters method is used for modeling and examining rainfall trend for the monthly and seasonal rainfall series throughout the study period.

Spatial variation analysis will be presented in map using the results from rainfall trend analysis and rainfall series analysis. Significant or non-significant positive or negative trend for each region will be shown in different color.

1.5 Significance of Study

Climate issues may be neglected sometimes in urbanization even the side effects could be serious and bring huge impact to the environment, which will indirectly affect the inhabitants and economies. Understanding the future rainfall trends and their spatial variations due to climate change become very important for future climate issues, water resources planning, flood and drought managements, and land use planning, in a river basin. The present study can help in predicting the future rainfall trends and spatial variations for Langat River Basin.

This study provides factual information on how the rainfall patterns change in the heavily developing area. Urbanization should not only emphasize on present development but also for future planning. The projected rainfall patterns in this study will be useful for future water resource and land use planning. Furthermore, analysing the changes in future rainfall patterns can also benefit the policy maker on future water resource planning, natural hazards management and to react wisely to the future changing climate.

CHAPTER 2

LITERATURE REVIEW

2.1 Background

Numerous studies of rainfall trends have been carried out since the raise of climate change issue. In addition, every country in the world is experiencing different changes in rainfall pattern as precipitation is affected by many factors like topography, temperature, wind and so on. Unlike other studies, analysis on rainfall trends needs to be updated to investigate the recent change in climate while long term trends studies are also required to identify the cycle of the trend.

2.2 Climate Change and Rainfall

Climate change is affecting every single region in the world regardless land or ocean. Consequences like extreme temperature, droughts and floods, more frequent natural disaster like hurricane, cyclone are the primary effects. These phenomena will eventually influence agriculture, ecosystems and economies which have direct impacts on human. As cited in Obot et al (2010), climate change affects every facet of the ecological system, inclusive flora and fauna. Thus, researchers are making effort to study on climate change; trends, causes and effects as well as solution of it. An irony issue was raised by

Onyenechere (2010) saying that even though climate change is a global problem, countries that are most vulnerable to its impact are developing countries which contribute the least to this issue. They are the most vulnerable due to the least endowed with resources and lack of high technology to combat the problem. Also, their economies rely heavily on natural resources which are climate sensitive.

Rainfall trend is one of the ways to assess climate change. Many studies on precipitation were done to discover the trend of climate change on the scale of global, continent, country and also catchment. It was claimed that the spatial and temporal distribution of precipitation is crucial to model and predict weather and climate changes (Hatzianastassiou et al. 2008). Precipitation is a climate parameter that has direct impact on ecological system, flora and fauna.

According to report from Intergovernmental Panel on Climate Change (IPCC 2007), precipitation over land of 10°N to 30°N had remarkably increased during the period 1900 to 1950s but it declined after 1970. Conversely, rainfall has decreased in the deep tropics from 10°N to 10°S especially after 1976/1977. A marked note which is worth to be concerned is the increase in the number of heavy precipitation event which can also be found even in areas that experiencing reduction in total precipitation amount. In addition, droughts have become more common since the 1970s due to the decreased land precipitation and raised temperatures that enhance evapotranspiration and drying. Although precipitation is not affected solely by climate change, other natural environmental phenomena which contribute to

the change in rainfall trend might also be influenced by climate change (Takahashi 2011), such as El Niño-Southern Oscillation (ENSO), monsoon and so on.

2.3 Checking and Refilling Missing Data and Homogeneity Tests

In order to enhance the quality of the study, data checking was inevitable in every analysis. For studies of rainfall trend, rainfall series were checked for missing data. In some studies, stations with large missing data were omitted from the study (Cheung et al, 2008; Afzal et al., 2011 and Caloiero et al., 2011). On the other hand, data repairing was sometime applied when missing data was found. Various methods had been used to repair the time series. Some of these methods were filling up the data gap by a neighboring rain-gauge station (Guhathakurta and Rajeevan 2008) and substituting the missing record by the corresponding mean value (Río et al. 2011). However, some methods were also applied such as Inverse Distance Weighted (IDW) interpolation, normal ratio (Suhaila et al. 2010), linear regression (Liu et al. 2008) and so on. IDW interpolation is a simple method which does not require pre-modelling (Basistha et al. 2008). It is an exact interpolator that considers distance between the control point and interpolated point. The shorter the distance, the larger the effect on the output value.

The homogeneity of rainfall data collected from different rain gauges is important in analysing rainfall. Various methods were used by different researcher while there were four tests employed to evaluate homogeneity,

namely standard normal homogeneity test, the Buishand range test , the Pettitt test, and the Von Neumann ratio test (Wijingaard et al., 2003; Sahin and Cigizoglu, 2010 and Kang and Yusof, 2012). The combination of these four absolute tests was first developed by Wijingaard et al., 2003 to assess the homogeneity of European daily temperature and precipitation series. It was commented that relative homogeneity test which was applied with respect to a neighbouring station which was supposed to be homogeneous is more powerful than absolute tests. However, for less dense station network where distance between stations is large, relative testing is inappropriate. The classification of the homogeneity of a particular station was defined as; 'useful' if one or none of the tests reject the null hypothesis: 'doubtful' when the null hypotheses of any two tests are rejected; and 'suspect' if three or all tests reject the null hypothesis. All four methods were tested at 1% significant level.

According to the study by Wijingaard et al.(2003), homogeneity of European daily temperature and precipitation series was tested for the period of 1901-1999. The sub-period of 1946-99 was further analysed to observe the change in the later years. Four absolute tests were applied on annual mean diurnal temperature range, annual mean of the absolute day-to-day temperature differences and annual number of wet days. For the temperature series, it was revealed in the result that 92% of the series during the whole period was classified as 'suspect'. However, in the later period (1946-99), the situation was improved with only 54% of temperature series was labelled as 'suspect'. On the other hand, majority of the precipitation series were classified as 'useful' for both test periods. Significant breaks were found in

winter season around 1950 and 1965 over the Eastern Europe. Consistent with the temperature series, percentage of stations classified as 'suspect' was improved from 14% over the whole period to 9% for the sub-period 1946-99. It was explained that inhomogeneity of the series was normally caused by station relocation as well as changes in observing practice and measuring techniques. Also, by using absolute tests for homogeneity testing was a better choice for sparse density station network as the breaks detected were mainly caused by changes in the observational network which relative tests were insensitive to.

The same tests were adopted by Kang and Yusof (2012) to investigate the homogeneity of the rainfall series in Peninsular Malaysia. 33 stations with less than 10% missing data over Damansara, Johor and Kelantan were selected. All four tests were applied to the annual mean, maximum and median of each rainfall station at 5% level of significance. The same classification method was used in the study. For annual mean and annual maximum series, all stations were found to be 'useful'. Nevertheless, when the annual median series were tested, 4 stations were considered as 'doubtful' and 1 station was labelled as 'suspect'. Besides, it was found that percentage of missing data had no effects on the homogeneity of the series.

2.4 Rainfall Trend and Spatial Variability Analysis

Plenty of studies in precipitation had been done in the past but the objectives and methods used are in a wide variety. Other than studying trends

in annual rainfall amount, spatial variation and rainfall trend analysis can also be done on other indices like extreme rainfall, rainfall intensity, wet spells and so on. Generally, different index are used for different purpose. For example, situation like constant rainfall amount but declining rainy days indicated that more intense rainfall had been receiving in the particular region and higher probability of occurrence of flood events was expected.

2.4.1 Rainfall Trend

Similar to Malaysia, rainfall in India is heavily influenced by the monsoon season. Southwest monsoon season during June to September provides about 75% of the total precipitation over the country and it is the main supplier of fresh water (Guhathakurta and Rajeevan 2008). Long term rainfall series of about 1476 rain-gauge stations were studied in whole India. Besides analysis on annual basis, trends in monsoon season are also a point of interest of the study. Data for the period of 1901-2003 were used and missing data were filled up by neighbouring rain-gauge data. District data were constructed by arithmetic average of data from stations within the district while rainfall for the 36 meteorological subdivisions was obtained by area weighted rainfall. Trends detection was shown by percentage departure from the long period mean and the series were subjected to “low-pass filter” with nine point Gaussian probability curve. Linear regression and “Student t” test were then used to test for significance of the trend. It was found that no significant trend existed in all India monsoon rainfall and monthly rainfall

during monsoon season. However, significant decreasing trends were only observed over three subdivisions but opposite trends were shown in eight subdivisions during monsoon season. More precisely, trends in June and August rainfall were found increasingly in most subdivisions but significant negative trends were detected over central and west peninsular India in July. It was also revealed that decreasing rainfall trends were found in 18 subdivisions during winter and 6 subdivisions over the central part during pre-monsoon season. Instead, during the post-monsoon season, increasing rainfall was shown in most of the subdivisions. It was commented that contribution of major rain producing month in annual rainfall is useful to detect the swift in rainfall pattern spatially and temporally.

Rainfall has great impact on agriculture sector. Economy of Ethiopia, country located in the Horn of Africa, relies heavily on low-productivity rainfed agriculture. Determining timing and amount of rainfall therefore become an important factor. Recent changes in rainfall amount and rainy days were examined by Seleshi and Zanke (2004). Only 11 stations with less than 10% missing data for the period 1965-2002 were selected and these 11 stations were grouped into 5 groups according to the location. Data were first checked by plotting daily time series for each station to identify outliers. Suspected data were then cross-checked with data from neighboring station. Both annual and seasonal analyses were carried out. The three seasons in Ethiopia are main rainy season, Kiremt season (June to September), light rainy season, Belg season (March to May) and the dry season, Bega season (October to February). Six indices were defined and Mann-Kendall test were used to detect whether trends exist. Furthermore, slopes of the trends were evaluated

using least-squares linear fitting. Significant declines were revealed over eastern, southern and southwestern stations in annual and Kiremt season since about 1982. For the light rainy season, two stations in western and central Ethiopia showed increasing trends in the period 1985-2002. For the rainy days analysis, significant decreasing trend was only found in Jijiga station in Kiremt. However, upward trends were observed in 3 stations during Belg. On the other hand, correlation analysis indicated that less Kiremt rainfall over the lowlands was associated with warm South Atlantic Ocean and high pressure over the tropical eastern Pacific Ocean. It was also reported that the rainfall of Ethiopian Highland was positively correlated to both eastern Pacific sea-level pressure and the SOI (Southern Oscillation Index) during the Kiremt season. This report evidenced that ENSO episodes do associate with below-average rainfall during rainy season over the Ethiopian Highlands.

The availability of water resources is important for countries that rely on agricultural sector. Trends of rainfall in Sri Lanka were examined by Jayawardene et al. (2005). Data from 15 stations scattering around the country were retrieved for a time span of 98 to 130 years. Mann-Kendall rank statistic was again performed to test for the trend while Spearman's test was used to confirm the result. In order to evaluate the magnitude of the trend, least-squared regression method was applied. For the whole study period, only three stations showed significant trend from both methods; significant upward trend with 3.15mm/year was found in Colombo while negative trends appeared in Nuwara Eliya (-4.87mm/year) and Kandy (-2.88mm/year). On the other hand, 13 out of 15 stations showed decreasing trends in the short term rainfall study (1949 onwards). However, only four stations revealed significant trends with

the largest magnitude in Batticaloa with -11.16mm/year. Thus, it was suggested that common decreasing trends during the later decades could be an indicator of temporal climate change and might be possibly caused by deforestation, urbanization and so on.

Analyses of precipitation trends were done in Europe too. A study of trend detection of annual and seasonal rainfall in Calabria, a region in southern Italy, was done by Caloiero et al. (2011) to determine the behavior of climatic and hydrological variables. In order to obtain more accurate result, only 109 series with longer than 50 years, at least 5 years within the period of 1991-2000 and 3 years during 1996-2000 were selected. Analysis of trends was done by Mann-Kendall test and parametric linear regression model. While to identify shifts of the time series, the Pettitt form Mann-Whitney test was employed. Also, pre-whitening approach of von Storch's procedure was applied to reduce the serial correlation in the hydrological time series and its effect of changing the rate of rejecting the null hypothesis of no trend. On annual scale, negative trends were found in most part of the study area. Among 109 series, 50 stations revealed significant negative trend and 2 series found significant positive trend by Mann-Kendall test. More negative statistically significant trends were shown in each season except summer. 25 significant positive trends were found uniformly distributed over the territory during summer. It was suggested that the most probable change point years were around 1960-1970 for annual, summer and autumn rainfalls. The estimate of the change year for winter precipitation was 1974 while 1942, 1981 and 1961 would be the change point years for spring.

Furthermore, investigating trends and variability in daily precipitation in Scotland was carried out by Afzal et al. (2011). Temporal change in historic rainfall variability was the main aim of the study. Thus, chosen weather stations were required to have at least 30 years of data with less than 5% missing values. Mann-Kendall test were adopted for trend analyses, sequential Mann-Kendall test was used to detect significant change in a time series and cumulative sum (CUSUM) procedure were then employed to indicate changes in trend. Increasing trends were found in most weather stations except a downward trend was discovered in one in the East for the whole period. Based on the result from CUSUM and sequential Mann-Kendall, turning point was found in one station situated in the west and southwest of the territory. However, more than one turning point was observed in other regions. Variability index was developed to investigate trends in rainfall variability. It was found that higher rainfall variability was showed in most stations in the West and South-west. However, more than one turning point but less variability was found in stations located in northern and eastern region. In the west and southwest of Scotland, increasing trends in rainfall variability were found statistically significant but the trends were not consistent. Around 1980, changing trends of rainfall variability were detected during winter and autumn seasons in the West. For number of annual dry days, both significant increasing and decreasing trends were presented while most of them are downward trends.

Few studies on trends in rainfall were carried out in Iran (Ghahraman and Taghvaeian, 2008 and Soltani et al., 2012). However, not only objectives and focuses of these studies were different, methods used to detect trend were

also not the same.

Annual rainfall trends were determined by Ghahraman and Taghvaeian (2008) by using regression line slope method. Parametric test requires data to be normally distributed which hydrologic data normally do not follow. Thus, "test for normality for a sample size of less than 150" was applied to data from 30 selected stations with equal or less than 50 years and only one station failed the test. In order to have a better picture on how pattern in rainfall trends changes, trend studies were analyzed for the entire record length, 40-year-period (1961-2000) and 30-year-period (1971-2000). For the whole recorded period, significant negative trends were found in seven stations and positive trends were shown in six stations with 95% significance level. Significant positive and negative trends were found in eight and four stations respectively in the 40-year-period. Analysing the period of 1971-2000 data, only negative trends were revealed in three stations. Dependence of trend to data record length was also investigated and it was found that different record length does affect the behavior of the trend.

Not only rainfall trends, trends in rainy days were also examined by Soltani et al. (2012) over Iran in an attempt to detect climate change. 35 stations with at least 30-year records were chosen for trend studies in annual and seasonal scale. Non-parametric Mann-Kendall test and Spearman test were employed to analyse the trends. Since serial correlation might modify the probability of detecting a significant trend, autocorrelation structure of all rainfall series were checked. Also, homogeneity of the time series was tested by Mann-Whitney test to assess shifts in properties of the time series. Most of

the stations are homogeneous at 10% significance level except some stations which were relocated and these stations were omitted from further analysis. Three stations showed negative trends at 1% significance level and two stations found positive trends at 5% significance interval for annual analysis. For seasonal analysis of spring, insignificant negative trends were found in stations located over the southern and north-northwestern region but significant positive trend was observed in one station in the central. Only three stations showed significant negative trend in all summer months while significant positive trend in only one station was detected in autumn. Significant positive trends were found in two stations in December whereas significant negative trends were also showed in two stations in January and February. For trends in number of rainy days, two stations found significant decreasing trends and upward trends were shown in ten stations by Mann-Kendall test. Similar to the result from rainfall total, majority of positive trends were found in December while negative trends were mostly found in April.

A shorter-period study was done in Nigeria, country that situated in the northeastern Africa (Obot et al 2010). Nigeria was segmented into six parts and 30-year-rainfall trends were analysed for the whole territory. Besides analyzing for the whole 30-year-period, data were categorized into two segments which are 1978-1997 and 1988-2007 to verify interdecades trends. The lag1 serial correlation coefficient was first tested and null hypothesis was rejected if it is affected by the serial correlation effect. Prewhitening process was applied to the series to avoid serial effect of time series. Mann-Kendall test was used to evaluate the rainfall trends. Since Mann-Kendall method does

not provide information on rate of change, nonparametric Sen's method was employed to estimate slope of the trend. Prewhitening process was only applied for series in Maiduguri (North East). There was only one out of six regions showed significant trend. The increasing trend was found in Maiduguri which has the least amounts of rainfall throughout the country. It was formally witnessed a downward trend but increasing rainfall has taken place. In the second sub-division (1988-2007), results from the two methods showed contradicting signs in three regions. It was suggested that longer data range should be employed to find out the changes that occurred in all of the North East zone of Nigeria and see whether there is any cycle in it.

As shown above, non-parametric tests (Mann-Kendall and Sen's T tests) are widely used for detection of rainfall trends since no assumption for probability distribution of the series is needed. Another rank-based non-parametric test, the Spearman's rho test, was also applied in detecting trends in hydrological data while this test had been found to be as powerful as the Mann-Kendall test (Yue, 2002 cited in Yue and Pilon, 2004). On the other hand, some parametric methods like linear regression model were also be used. The power of parametric and non-parametric tests in detecting trend has been analyzed by Bayazit and Önöz (2003). The comparison of parametric linear regression method and the non-parametric Mann-Kendall test was made with Monte Carlo simulation for various probability distributions. T-test was found to be slightly more powerful when the distribution is normal. However, when it came to a skewed probability distribution, Mann-Kendall test had more power. It was also noticed that the power ratio of t-test decreased with the increase of the coefficient of skewness.

Another study of comparison of the power of the t-test, Mann-Kendall, bootstrap-based slope and bootstrap based Mann-Kendall tests was carried out by Yue and Pilon (2004). Monte Carlo simulation was once again used to generate time series for a given distribution type having pre-selected characteristics. All tests were applied to the generated data and the power of each test was observed. It was found that the power of ranked-based tests (Mann-Kendall and bootstrap-based Mann Kendall tests) was much higher for non-normally distributed series. It was suggested that slope-based tests could be employed to assess significance of trends for approximately normally distributed data. On the other hand, rank-based test was shown appropriate to be used for trend detection since the higher power in detecting trends in non-normal series and similar power to detect trend for normal distributed series.

As seen in many studies which used Mann-Kendall test to detect trends, prewhitening procedures were applied to the series (Deni et al., 2010, Obot et al., 2010 and Caloiero et al., 2011). It was commented that the serial correlation in the hydrological time series altered the variance of Mann-Kendall statistic and increased the chance of rejecting null hypothesis and affect the findings. Thus, the lag1 serial correlation coefficient would first have to be tested and prewhitening procedures have to be performed if found. Even though prewhitening procedure is useful in removing possibility of finding a significant trend when there is no trend, accepting the null hypothesis of no trend with a high probability when a trend actually exists is the drawback of the process. Thus, a study of whether or not prewhitening to be applied was done by Bayazit and Onoz (2007). The analysis was performed by 20000 normally distributed time series generated by AR(1) model with 5

different lag1 correlation coefficients and sample size of n=25, 50, 75, 100 with mean 1 and the 5 distinct coefficient of variation (CV). Eight known slopes were attached to the linear trends. Then, Mann-Kendall test with and without prewhitening were applied to these series. It was concluded that prewhitening would not be necessary when the coefficient of variation is very low (CV=0.1) for all sample size. Also, prewhitening should be eliminated in the case that sample size is larger than 70 and the slope of the trend is larger than 0.005.

Instead of checking trends, non-stationarity in precipitation and temperature was also investigated to provide significant evidence of climate change (Kamruzzaman et al. 2011). The study was carried out in the Murray Darling Basin which produces one third of food supply in Australia. Two analyses were carried out on monthly rainfall and average maximum temperature time series in ten selected stations. Taking into account of seasonal variations, the Pacific Decadal Oscillation (PDO) and the Southern Oscillation Index (SOI), the multiple regression models for rainfall and temperature were developed. The residuals from the regression which represented the random variation about the fitted values were first investigated. Then, the CUSUM technique was also applied to the residuals and evidence of non-stationarity in both precipitation and rainfall was discovered. Next, Holt-Winters method was adopted since it allowed the underlying mean, trend and seasonal components change over time. Thus, this method was used to track shifts in the parameters of a time series. It was revealed that reduction in rainfall was accompanied by negative SOI but there was no trend found in both PDO and SOI series. Furthermore, in Holt-Winters

analysis, negative trend was found in agreement with the previous analysis.

2.4.2 Spatial Variation

Spatial variation of rainfall were usually analysed with rainfall trend. Both outcomes create a better picture of the distribution of rainfall over certain time period. Also, forecasting of future rainfall might be more accurate with historical spatial variation and rainfall trend found in the particular region.

According to a study in Spain by del Río et al. (2011), annual, seasonal and monthly rainfall trends were analysed for the period of 1961-2006. The location of Spain, in the Mediterranean basin and eastern part of Atlantic, makes it highly sensitive to variations in the amount and distribution of rainfall. Due to the wide variation, series from a total of 563 weather stations scattering the whole Spain were acquired. After eliminating 10 stations which failed non-parametric Kruskal-Wallis homogeneity test, mean precipitation values for the whole study period were computed for each station to provide better interpretation on seasonal distribution. The mean values were used to produce a map which showed the wettest season in a specific area. Geostatistical interpolation techniques were applied to show spatial distribution of rainfall trends. In order to have more information on the rainfall trend, slope of the linear regression model by least square method represented magnitude of the trends. On the other hand, non-parametric Mann-Kendall test was applied to test the significance of the trends. Half of the Spain covering the western part received more rainfall in winter while autumn was the rainiest

season in the southeastern part which facing Mediterranean. Only a small part of northeastern part had the highest precipitation in summer while there was most rainfall received in spring season in the middle part of Spain. On monthly scale, it was revealed that most stations showed negative trends in first half year except May and more than 45% of stations found significant trends in February and June. On the contrary, positive trends were detected in May, August, September and October. Negative trends were found in winter rainfall and were significant in central and western area while most of the country showed decreasing trend in spring. Summer rainfall trended downward especially in southern and northeastern Spain. The only increasing rainfall season was autumn in western Spain.

Sicily is located at the south of Calabria, Italy. Spatial distribution of rainfall trends was investigated in Sicily which situated in the middle of Mediterranean Sea by Cannarozzo et al. (2006). Rainfall data of 247 stations which are homogeneous and complete for the period of 1921-2000 were used. Method of spatial interpolation was adopted to create complete data set. A modified version of Oliver's precipitation concentration index (PCI) was used to determine temporal distribution and value obtained that below 10 indicate uniform monthly rainfall distribution in the year while 11-20 represent seasonality. Mann-Kendall test was used to detect trends in annual, monthly and seasonal rainfall. IDW interpolation was also used to determine the confidence levels and the slope of the trend spatially. Then, Regional Average Kendall's S was applied to find out whether there are regional trends in rainfall. In order to determine the critical value for the percentage of stations that expected to show trends by chance, bootstrap approach was employed. It

was shown in their findings that negative trend could be found in most rain gauges where 62% of the stations showed significant trend. Only one significant positive trend was detected in a station located in the North West. Greatest number of downward trends was discovered in winter season with 60% significant trends found. It was claimed that winter contributes most precipitation during a year so decrease in rainfall in winter was the reason of negative trend in annual rainfall. Result from IDW method showed that presence of trend might be shown over southwestern part of Sicily with high confidence level and followed by the eastern part. Indeed, great number of significant negative trends was observed in these areas during winter especially over western region in January. PCI revealed that the spatial variation in Sicily was found in a generally steady situation. Outcome from bootstrap procedure had double confirmed the result that significant negative trend was exhibited in annual rainfall in Sicily from 1921 to 2000.

Australia, a country as well as a continent, located at the southern and eastern hemisphere with tropical climate at the northern part of it. Precipitation in Australia exhibits a high degree of variability since it is affected by sea surface temperature (SST), tropical cyclone, ENSO and also monsoon. A comprehensive study of trends in Australian rainfall was carried out by Taschetto and England (2009). The period of 1970-2006 was studied and it was argued that the 37-year-period was long enough to resolve multi-decadal timescales. Standardized rainfall time series were used with the comparison of regions with different variances to calculate trends. It was found from the spatial pattern analysis that trends in annual precipitation were characterized into two regions where increasing rainfall was generally found in the West

while opposite trend was observed in the East. Similar situation was shown in summer and autumn. However, negative winter precipitation trends were found in most of the territory except southern Australia. During spring, positive trends could only be detected in some parts of northeastern and northwestern Australia. Focusing on tropical Australia, contrasting trends were discovered from December to May (austral summer to austral autumn). Thus, it was explained that these patterns in trends were partially caused by changes in the Asian-Australian monsoon. Regarding to the drought events over tropical Australia, a possible factor highlighted was the negative trends in the SOI which make precipitation shift eastward together with warm waters. To assess climate change effectively, trends in extreme event were also analyzed. Spatial distribution of daily rainfall standard deviation per year and per season was shown to determine the variations in rainfall. Similar trends were found in standard deviation where Western Australian was dominated by positive values and negative values were found in the east. However, negative trend does not mean less variation if the annual mean also decreases. Hence, bootstrap method was applied to the beginning (1970-1980) and the end (1990-2000) decades. It was revealed that a decrease in rainfall was shown over east coast while increased precipitation was observed over west coast. For the trends in extreme rainfall event, trends in very heavy rainfall in annual and seasonal scale were found more frequent than that of moderate and heavy events. Particular in trends in very heavy rainfall, decrease over eastern region and increase in the west were discovered. In addition, strong positive trends in rainfall in the northwest were credited to the very heavy rainfall events.

2.5 Factors Affecting Rainfall

As shown in the previous session, there are many factors affecting rainfall. However, only monsoon, tropical cyclone, ENSO and urbanization will be discussed as they affect rainfall in Malaysia.

2.5.1 El Niño-Southern Oscillation (ENSO)

ENSO is a 3 to 5 years oscillation of atmospheric pressure pattern and warming surface waters which occurs in the equatorial Pacific Ocean. Not only concerning temperature, ENSO also involves changes in trade winds, tropical circulation and precipitation (IPCC, 2007). According to IPCC Fourth Assessment Report (2007), the nature of ENSO varies over time. From the late 19th century through the first 25 years of the 20th century, strong ENSO activities occurred. Then, it started again about 1950. As cited in the report, there was a shift in climate during 1976-1977 and was associated with the notably change in El Niño evolution. El Niño heated SSTs to above-normal in the eastern and central equatorial Pacific and tends to become longer and stronger; it then had great impact on most tropical monsoons. Besides, it also dominated variation in disaster like tropical cyclones, hurricanes and typhoons. Since the mid-1970s, significant upward trends were shown in estimates of the potential destructiveness of hurricanes and such trends are strongly correlated with tropical SST. Positive trends were also detected in longer lifetimes and greater storms intensity.

ENSO event could not be taken into account since it is a special event occurred in cycle. In addition, ENSO induces the Southeast Asia rainfall anomalies. Thus, decrease or increase of rainfall during ENSO period should be excluded since it does not belong to the general rainfall trend.

The region of Maritime Continent is situated in the center of the Indo-Pacific sector. Thus, the climate variability in this region links to the large-scale atmosphere-ocean variability. Also, ENSO-induced drought and flood often involve in this region especially the Indonesian region.

Rainfall anomalies in Malaysia were also assumed to be in associated with ENSO. A study focusing on mechanisms of Malaysian rainfall anomalies was done by Tangang and Juneng (2004) using monthly data of nearly 50 years. Among the 12 stations that located in or near coastal area, 6 of the stations were selected from East Malaysia while the remaining was from Peninsular Malaysia. In order to compare the differences in the behavior of Malaysian and Indonesian anomalous rainfall, a single Malaysian rainfall index (called MalayP) was created. The average value of rainfall from all stations produced an index which was weighted towards the stations with higher variability. Then, the anomalous MalayP was correlated with the anomalous SST and horizontal winds over the Indian and Pacific Oceans to determine the relationship between the Malaysian anomalous rainfall and large-scale forcing associated with ENSO. The behavior of Malaysian anomalous rainfall was found to be consistent with the northward migration of the ENSO-related coherence in the Maritime Continent. During March to May, the dying phase of an ENSO event was resulted in no relationship between the

Malaysian anomalous rainfall and the SSTs in the surrounding seas. From June to August, higher ENSO coherence was experienced in the Indonesian region (south of the Equator) so Malaysian anomalous rainfall was correlated with local air-sea interaction. Then, owing to the broadening ENSO-related coherence to the north, behaviors of anomalous rainfall in both regions were found to be similar during September to November. Diminishing ENSO-Indonesia rainfall relationship and the augmenting ENSO-Malaysia rainfall relationship were observed during December to February due to the continuing northward migration of ENSO-related coherence. Therefore, anomalous rainfall in Malaysia was partly caused by the ENSO event. Thus, unusual rainfall during ENSO years has to be eliminated when investigating the existence of trends in annual rainfall amount.

2.5.2 Tropical Cyclone

Behaviour of tropical cyclone has also changed in associated with rising in SST and climate change. A study of changes in tropical cyclone number, duration and intensity in a warming environment by Webster et al. (2005) evidenced the statistically significant increasing trend found in both annual frequency and duration over North Atlantic Ocean at 99% confidence interval while such trend occurred simultaneously with the significant positive trend in SST. Trends in numbers of tropical storms and hurricanes, number of storm days and the hurricane intensity distribution were identified for each tropical ocean basin by using 5-year running average plot. In the warming SST

environment, no trend in number of tropical cyclone and the number of cyclone days in the time series was observed. Instead, a worrying upward trend was found in the number of hurricanes in categories 4 and 5 which are the strongest hurricanes. It has almost doubled in number from 50 per pentad in the 1970s to near 90 per pentad during the last decade and these changes happen in all ocean basin. Deeper understanding of the role of hurricane was suggested by using longer data record.

It was claimed that tropical cyclone activity over north Indian Ocean and western north Pacific/South China Sea has strong impact on rainfall over South and Southeast Asia (Takahashi, 2011). Thus, long-term changes in rainfall and tropical cyclone activity over South and Southeast Asia were studied. Since rainfall in seasonal transition periods (March to May, September to November) is associated with tropical cyclone activity, it was the main period of focus. The study period of 1951 to 2007 was divided into three periods, namely P1 (1951-1969), P2 (1970-1988) and P3 (1989-2007). Then, the perturbation kinetic energy (PKE) was used to estimate tropical cyclone activity. It was revealed that increase in rainfall in May around Myanmar over the last 40 years was caused by the enhancement of tropical cyclone activity. Thus, monsoon over western Indochina became earlier. Decrease in rainfall over western Indochina was shown over the last 40 years in November due to the weakening of tropical cyclone. Also, owing to the change of tropical cyclone activity, it was found that decrease of rainfall in September and increase of that in October made rainy season over northern Vietnam lengthen. Also, it was suggested that continuous analysis and cross-check should be carried out to confirm the changes.

2.5.3 Monsoon System

Concerning the changes in climate models, every element that affects Earth's climate has to be taken into account. Changes in monsoon rainfall are of great scientific and societal importance since their rain affects over two-thirds of the world population (Wang and Ding, 2006). Using the method of summer-minus-winter precipitation, we can measure the precipitation intensity. Wang and Ding (2006) conducted their study on global monsoon precipitation by using the method above. For the entire study period of 56 years, a decreasing trend was presented in the global monsoon index particularly before 1980. Such downward trend was significant in both global and northern hemisphere monsoon index at 95% confidence interval with the greatest amplitude of decrement in Africa. Nevertheless, increasing monsoon strength can be seen over northwest Australia. It was suggested that monsoon strength might reflect the regime shift but there is still much to learn about the causes of observed trends in the global monsoon.

Rainfall of most countries in the tropical area is affected by monsoon. As there is no distinct season in tropical countries, monsoon is then used to distinguish seasons. As mentioned in the study in India (Guhathakurta and Rajeevan, 2008), the two monsoon seasons are called northeast monsoon season and southwest monsoon seasons. Rainfall trends affected by monsoon seasons in Malaysia will be discussed in details later.

2.5.4 Urbanization

Urbanization, one of the important land use and land cover changes within watersheds, has serious impact on the whole process of the hydrological cycle such as reducing infiltration, frequency of floods and surface runoff (Du et al., 2012 and Liu et al., 2012). Hydrological effects of urbanization in Qinhuai River basin were investigated by Liu et al. (2012). Some characteristics of Qinhuai River were found similar to Langat River basin; it occupies an area of 2,631km^2 and rapid development of urbanization was actualized in recent years. With the subtropical wet monsoon climate, average temperature and annual average precipitation were found to be 15.4°C and 1047.8mm, respectively. Using linear regression analysis, increase of annual rainfall and flood season rainfall was shown due to the urban heat island effect. Also, the distribution of rainfall was observed to be concentrated during the main flood season. Increasing trends of rainfall were detected in both downtown and suburb, with greater magnitude found in downtown. It was also observed that the gap of rainfall received in downtown and in suburb was getting wider. Furthermore, urban island effect was found to be more obvious.

Juahir et al. (2010) investigated the relationship between hydrological trend and land use changes in the Langat River Basin. Spatial and temporal changes in land use areas, discharge and direct runoff were studied using non-parametric methods. Precipitation data were analyzed as rainfall affects the discharge volume which flows into the river and indirectly influences pollutant

transport through the rainfall-runoff process. Cumulative area for five land use activities namely agriculture, forest, urban, waterbody and others were studied to find the relationship with meteorological parameters. Significant increasing trend in annual maximum/minimum ratio was shown at Dengkil station which was found with enormous changes in land use in the surrounding. However, Lui station, with a little land use changes, showed no significant trend on annual maximum/minimum ratio. Thus, it is evident that there is a relationship between regional variability in discharge and land use or land cover changes in the study area.

2.6 Analysis of Rainfall Pattern in Malaysia

Malaysia situated at a region that is freed from natural hazards. Few destructive disasters that occur in Peninsular Malaysia are landslides, floods and droughts. It was found by Ratnayake and Herath (2005) that there was a strong relationship between rainfall and landslides. Furthermore, floods and droughts had happened in the recent years over Peninsular Malaysia. Thus, several studies of rainfall trends were carried out in Malaysia.

A recent study by Wong et al. (2009) investigated the rainfall variability in Peninsular Malaysia for the period of 1971 to 2006. Rainfall in Malaysia is greatly affected northeast monsoon (NEM), from November to March, and southwest monsoon (SWM), from May to September. The available data were first interpolated by using Shepherd's angular distance weighting (ADW) procedure and Thiessen polygon methods. Sixteen

representative stations scattered over Peninsular Malaysia were selected and classified into east coast, inland and west coast. Harmonic analysis was applied to examine the periodic characteristics of rainfall time series. Spearman's rank test was used to detect the existence of trends in rainfall. Finally, spatial variation was determined by evaluating the coefficient of variance within a specific region. For whole Peninsular Malaysia, maximum rainfall was received at the end of the year during NEM. An interesting finding showed that both maximum (December) and minimum (February) monthly rainfall were observed during SWM season. As expected, from the harmonic analysis, two peaks of rainfall received were shown every year in all 3 regions. 55% of rainfall was received during NEM and SWM contributed 31% to the annual rainfall over east coast region. For the west coast region, only 41% and 37% of mean annual rainfall was contributed during SWM and NEM. Nevertheless, 80% of mean annual rainfall was received during monsoon season in the inland region. Even though it was reported that rainfall patterns in Peninsular Malaysia were not manipulated by the ENSO events, rainfall variability in individual regions was affected. No significant trends were found in annual and monsoon rainfall in the east coast and inland area. Instead, increasing trend of 2.0mm/year was found in November rainfall in the west coast region. Upward trends with 9.33mm/year and 6.2mm/year for mean annual and mean NEM rainfall were exhibited for the same area. However, it was claimed that significant trends in mean annual and mean NEM rainfall might be caused by the accumulation of insignificant increasing trend in other months. Although largest mean rainfall was observed in east coast, the spatial variation of rainfall was more uniform throughout the year. For the inland

area, large spatial variability was detected in February. Larger spatial variability was shown in the west coast region especially during NEM. It was noted that the magnitude of the spatial rainfall variation in the Peninsular Malaysia was governed by the topography and monsoon winds. However, no significant long-term spatial rainfall variation trends were showed for all three regions.

Since monsoon is one of the manipulators that affects rainfall in Peninsular Malaysia, a study focusing on seasonal trends in rainfall data was done by Suhaila et al. (2010). The study period was about the same as study by Wong et al. (2009) due to the availability of data in Malaysia. In spite of that, segmentations of monsoon months and stations were different. SWM season and NEM season were defined as the period of May to August and November to February, respectively. Furthermore, rainfall data for the period of 1975 to 2004 from 30 rain gauge stations were categorized into four regions, specifically northwest, west, southwest and east over Peninsular Malaysia. Data checking for the homogeneity was done by standard normal homogeneity test, Buishand test range test, Pettitt test and Von Neumann ratio test and 30 data series used were found to be homogeneous. Several weighting methods were used to estimate the less-than-10% missing data, namely IDW, normal ratio, correlation and so on. Trends in five rainfall indices (total amount of rainfall, frequency of wet days with at least 1mm of rain, rainfall intensity, frequency of wet days exceeding the 95^{th} percentile and rainfall intensity exceeding the 95^{th} percentile) had been investigated in this study. Mann-Kendall statistical test was the only test used in this study to detect significant trend. Spatial pattern of mean values during SWM showed that northwestern

region was the wettest region since large values were shown in all 5 indices. It was disclosed that eastern region was the driest part in Peninsular Malaysia due to the smallest mean values found in 4 indices (except rain intensity). Since the coast that facing the NEM flow tends to be wetter, spatial rainfall patterns were in a totally opposite result where eastern region became the wettest region during NEM season. Negative trends (with few significant trends) were detected in total rainfall amount and frequency of wet days in most stations during SWM but opposite results were found during NEM. Upward trends in rain intensity were observed in most stations during both seasons except few negative trends shown during NEM. For the extreme events of frequency of wet days, decreasing trends were found in 11 stations in both SWM and NEM. Lastly, negative trends in extreme rain intensity were generally found during SWM but both upward and downward trends were observed during NEM. It was explained that conflicting trends found in the west and east coast were caused by the mountain range in the middle of Peninsular Malaysia.

After considering trends in the five rainfall indices, wet spell and dry spell over Peninsular Malaysia during monsoon seasons were also a point of interest since these extreme events might cause severe floods and droughts. Two studies focusing on wet spell and dry spell separately were done by Deni et al. (2009, 2010). For the period of 1975 to 2004, 32 and 36 stations scattered across the peninsular were selected and were categorized into four sub-regions to study trends in wet spells and dry spells, respectively. Data checking, repairing missing values as well as trends detecting procedures were performed by the similar methods used in study by Suhaila et al. (2010).

Despite this, methods used to identify the slopes of the trends were different. Ordinary least square method was applied in the wet spells study while a set of improved procedures were employed in the study of dry spells. Prewhitening procedures were first applied to the data series to test for the serial correlation effect. After detecting trends, slopes of the trends were analyzed by Theil-Sen's estimator. The five out of six indices tested in both studies included maximum consecutive number of wet (dry) days, mean length, persistency of wet (dry) events and the frequency of short (consecutive of 1-3 days) and long (consecutive of more than 3 days) durations of wet (dry) spells length. The remaining index for wet spells study was the variability of the length of wet spells while trends in total number of dry days were examined in the other study.

A wet day was defined as a day with the minimum rainfall amount of 0.1mm. Consistent with the previous study by Suhaila et al. (2010), eastern region was found to be the wettest region during NEM since high values were found in all indices except the frequency of short durations of wet spells length in that area. Mean of annual maximum duration of wet day was shown in the range of 6 to 14 days in most areas during NEM while only 4 to 9 days were found during SWM. On the other hand, short wet spells were found more frequent during SWM but frequent longer duration of wet spells was only found in one station. During NEM, decreasing trend was found in annual maximum of wet spells over the peninsular. However, positive trends were observed in mean, variability and persistency of wet spells in the eastern region as well as frequency of short wet spells in west coast. All indices were trended downward in the East of peninsular during SWM. On the contrary,

positive trends were detected in all indices except frequency of long and short wet spells in the west. It was noticed that significant decreasing trend in frequency of long wet spells was discovered in most stations in both monsoon seasons in the 30 years period. Moreover, regional trend analysis revealed that increasing trends in maximum duration of wet spells were observed over northwestern and western region during both NEM and SWM. Also, trends in persistency of two consecutive wet spells were found decreasing in all regions. In the southern part, negative trends were exhibited in mean, variability, maximum duration and the persistency in both monsoon seasons.

Since Malaysia's climate is classified as hot and high humidity, dry day was defined as a day with rainfall amount of less than 1mm instead of 0.1mm. Once again consistent with the findings from Suhaila et al. (2010), the driest region was represented by northwestern Peninsular Malaysia with higher value found in all indices (except the frequency of short spells) compared to other regions during NEM. Besides northwestern region, high value in the mean of total dry days was also seen in southwestern area. During SWM season, stations located around 102.5°E and 3°N were found to be the driest evident by high values in total number of dry days and mean length of dry spells. However, stations that located at the higher latitude and southeastern area were slightly wetter during May to August. Significant serial correlation was failed to found in most stations in all six indices except five stations in the eastern region showing significant serial correlation in the frequency of short dry spells during NEM. Thus, prewhitening procedures were applied. It was concluded that negative trends could be found in total number of dry days, maximum duration of dry spells, mean length of dry spells and the persistency

of two consecutive dry days in most stations over the peninsular during NEM. Similar direction but significant trends in the four indices were detected in northwestern and western areas. It was remarkable that increasing trends in the four indices were shown (but only significant in the northwestern area) during SWM. From November to February, instead of the significant decreasing trend found in the frequency of long dry spells, positive trends in frequency of short spells were shown in most stations which exhibited the same outcome in regional analysis. On the other hand, decreasing trends were observed in frequency of the both short and long dry spells over most stations in Peninsular Malaysia during SWM. The only significant trend was discovered negatively in the frequency of short dry spells over the southwestern area. An important outcome from the study was that negative trends were showed in most of the dry spell indices during NEM but opposite trends in most indices studied were found during SWM season.

2.7 Analysis on River Basin Scale

In a study of precipitation trends in Spain, it was claimed that river basins are the most appropriate spatial scale for assessing the climate change on water resources as they are the natural hydro-climatic units (Gonzalez-Hidalgo et al., 2010). According to study by Kumar and Jain (2011), analysis of rainfall trend on different spatial scales was needed to construct the climate scenarios comprehensively. Using these scenarios, problems associated with floods, drought and the availability of water can be solved accordingly. Instead

of investigating trends in rainfall data only on regional scales, some studies divided the study area according to the drainage area of major rivers.

Spatial variations of summer precipitation trends in South Korea for a period of 33 years were investigated by Chang and Kwon (2007). Precipitation provides fresh water in East Asia. Rainfall during the summer monsoon season contributes approximately two thirds to its annual precipitation. There are five major basins in Korea and data from 187 stations were acquired to identify trends in precipitation amount, intensity and also heavy precipitation events. Homogeneity test of Worsley likelihood ratio, the cumulative deviations and Bayesian procedures were used. Rain intensity was calculated using total summer (monthly) precipitation amount divided by total number of precipitation days during the same period while heavy precipitation event was represented by those with daily precipitation amounts greater than 30 and 50mm. Trends of all three indices were detected by Kendall's τ test. In order to identify spatial dependence in precipitation trend among all stations, Moran's I were employed. It was found that all 187 stations show increasing trends in precipitation and precipitation intensity during June to September. For rainfall amount, 55% of all stations showed significant increase with 95% confidence level but none of the significant upward trend was found in station in Youngsan river basin (Southwest Korean). Highest percentage of significant increase was found in June over northern and central western region. Significant increasing trends in rainfall intensity were only shown in 59 stations. In particular, negative trends were found in 24 stations indicating the increase in number of summer rainy days. In accordance with significant increase in rainfall amount in June, precipitation intensity trends were

increased significantly in 41 stations. For the number of heavy precipitation events, positive trends were found in all stations but significant trends could only be detected in less than half of the stations covering over coastal, northern and southeastern area. Weak to moderate positive spatial autocorrelation were detected with the highest in June rainfall amount and August precipitation intensity. It was suggested that longer period data should be employed so that cyclical pattern in rainfall trend could be observed.

Since rainfall variability in the watershed has the most effect on agriculture, a research over 13 watersheds covering most but not all of the country was done by Cheung et al (2008). It was suggested that analyses of rainfall trends based on watershed provide an approximation of the amount of rainfall and associated runoff since the excess of rainfall will eventually be confined to the watershed. Also, it was assumed that rainfall patterns were homogeneous over a particular watershed so watersheds were defined as a unit to do analysis. Four analyses were performed in the study; they are interstation and watershed correlation analyses, watershed and national level analysis, seasonal rainfall analysis and comparison with previous rainfall studies. Pairwise correlation procedure was performed to ensure the homogeneity of rainfall in different stations within a particular watershed. Then, pairwise correlation coefficients were averaged to calculate the mean watershed correlation coefficient. Thiessen polygons were also applied to discern probable areas that experiencing trends recorded by different rain gauges. A 25% rule that omits yearly data for any watershed which has lost data from at least 25% of its gauge stations was implemented to avoid misrepresentation. Annual watershed rainfall was regressed on time to detect the changes in

rainfall on watershed level. One-sample t-test was employed to test for significance. The watershed's CV was used to examine the variability of annual rainfall in each watershed. Both CV and regression analysis with all observations were also used in a single regression to find rainfall changes for the whole country. Similar procedures were carried out for seasonal analysis. Lastly, to compare with other studies, all available annual rainfall observations without implementing 25% rule were used and watershed units were combined to make comparison with studies on rainfall trends in regional scales. It was revealed that most watersheds showed high correlation coefficients except watersheds 1 and 4. This suggested that finer scale should be applied for these two watersheds. During the study period (1960-2002), neither watershed level nor national level analysis discovered significant change in annual rainfall. However, significant decrease of rainfall in Kiremt season was found in 4 out of 13 watersheds. Rainfalls of all watersheds were actually decreasing during June to September but positive change was revealed from Belg season; this made annual rainfall remain unchanged. It was claimed that use of inappropriate data will lead to unrepresentative and contradictory outcomes. Also, study area should be defined in a geographically meaningful manner such that obtains a more useful result.

Considering year 1951 to 2004, trends in both rainfall amount and rainy days were investigated by Kumar and Jain (2011). Daily gridded rainfall data at 1°×1° resolution based on 1803 stations were used and only 10% or less missing data were allowed. The whole territory of India can be divided into 22 river basins and all analyses were performed on river basin scale. In this study, rainy day was defined as a day with rainfall of 2.5mm or more

within 24 hours. Beside annual investigation, seasonal analysis was done according to winter (December to February), pre-monsoon (March to May), monsoon (June to September) and post-monsoon (October to November). After calculating the coefficient of variance, it was found that high variability of rainfall and rainy days was found in every season except monsoon. Result from mean annual rainfall showed that two basins in northwestern region receive minimum rainfall while another two coastal basins (WFR1 and WFR2) at the West receive the most rainfall. Magnitude of the trend was determined by Sen's estimator and Mann-Kendall test was used to test the statistical significance of the trend in the time series. From spatial distribution analysis, it was found that more annual rainfall but less rainy days was observed in WFR1 which indicated that the rainfall intensity was much larger compared to other basins. On annual scale, increasing trends in 6 river basins and negative trends in 15 river basins were found and only one river basin showed no trend. It was suggested that no trend was found in Ganga basin because the average rainfall was measured over a large area where similar number of negative and positive trends exist over sub-basins. Downward trends were observed in most stations in pre-monsoon and monsoon season while opposite trends were found in 13 basins during post-monsoon and 18 basins during winter. However, most trends were found insignificant. In terms of rainy days, 15 decreasing trends were found but only 3 of them are significant. Out of seven decreasing trends, only two were found significant during pre-monsoon. Downward trends were detected in most stations during monsoon while only two were significant. For post-monsoon season, no trends were shown in most stations but one significant decreasing trend was revealed.

Only a few studies of rainfall trends were done on the basis of water catchment in the past. However, there has been a growing interest in the study of precipitation on a much smaller scale (Caramelo and Orgaz, 2007).

A case study was done at catchment scale in the Grand-Duchy of Luxembourg, a country in Western Europe, by Pfister et al. (2004). Since several serious flooding events had happened at the beginning of the 1990s, investigations of the causes have been carried out. Long rainfall and temperature data ranging from 1854-2003 were used. A coherence test was applied on both data sets as data checking. Similar to most studies, non-parametric Kendall test was used to assess trends in rainfall series. Five-year moving average of annual rainfall was calculated to indicate fluctuations over the study period. It was revealed that mean values of only 550 and 680mm were found in 1940s and 1970s. The maximum total annual rainfall was found in 1980s with a mean 5-year moving average of 1050mm and this average value dropped to less than 800mm afterwards. Statistically significant positive trends in winter rainfall totals and also maximum duration of a single rainfall event were shown in most stations. On the contrary, decreasing summer rainfall was detected during 1950s to 1990s. To analyze the changes in rainfall in the 150 years, intercomparison of 1855-1884 (19^{th} century) and 1967-1996 (20^{th} century) was done. Although no clear trend was detected, it could be concluded that higher level of annual rainfall was observed in the second half of the latter century.

Another small-scale analysis of precipitation data trends was done by Karpouzos et al. (2010) in Aison River basin in the Northern Greece with an

area of about 1232km^2. The precipitation records for a rather short period of 1974 to 2007 were being studied. However, it was clarified that a record length of 25 years was enough to ensure the statistical validity of the trend result in climate change research (Burn and Elnur, 2002). Double mass curve method was applied to all time series to test for homogeneity while modified Thiessen Polygon method was used to calculate areal precipitation. Then, Mann-Kendall test for trend identification, Sen's estimator of slope for trend magnitude estimation and Sequential Mann-Kendall test for determination of starting point of trend were performed. The distribution-free CUSUM test was also employed to test for the existence of abrupt change in the time series. To avoid the serial correlation effect, autocorrelation test was performed and no lag-1 serial correlation coefficient was found to be significant. Results from the seasonal analysis were as followed; negative trends (with one significant) were found in most stations during spring, weak increasing trends were observed at three stations during summer, slightly downward trends in autumn rainfall were showed over three stations and upward trends were detected at three stations during winter. Insignificant downward trends were seen in three stations located at the lower altitudes in annual analysis. A remarked finding was highlighted that weak upward trend was found in a station with positive trends found in all four seasons. Generally, rainfall trend in the whole region was represented by a dim negative trend with -3.71mm/year due to the downward trends revealed during autumn, winter and spring. From the sequential Mann-Kendall test, it was noticed that apparent decrease in annual precipitation was reflected in all stations during 1987 to 1993. Also, significant downward trend in spring rainfall was found around the year 2003

but further investigation which considers data of the forthcoming years should be done. In addition, no significant step change was identified during the study period in both annual and seasonal analysis.

2.8 Concluding Remarks

As climate change issue is getting serious, researchers in every country are trying the best to seek for evidence and methods to minimize the impact on living beings. From the previous literature, it was noticed that there are only a few rainfall trend analysis carried out in river basin scale. Particularly in Malaysia, most of the studies were focusing on the whole peninsular. There is only one rainfall trend analysis in Langat River Basin which emphasized on urbanization. Also, the most popular method in rainfall trend analysis is the Mann-Kendall test. However, the result found using such method summarizes trend for the whole study period and it might not provide an actual scenario of rainfall distribution. Modelling rainfall not only can simulate the real scenario but also forecasting future rainfall. Forecasted rainfall is useful in future water management and flood/drought prevention.

CHAPTER 3

METHODOLOGY

3.1 Study Area

Langat River Basin is the chosen study area in this present study. The catchment area extends from 2°45'N to 3°20'N latitudes and 101°20'E to 102°0'E longitudes located at the central west of the Peninsular Malaysia (Figure 3.1). It has an area of about 2,200km^2. The main stream, Langat River, originates from the western slope of Banjaran Titiwangsa (main range dividing Peninsular Malaysia in the middle right through) and flows southwestern into the Malacca Strait. Besides, two tributaries also drain through the Langat River Basin; they are the Semenyih River and the Labu River. The river basin has a population of approximately 1.2 million living in Cheras, Kajang, Bangi, Government Centre of Putrajaya, Cyberjaya and others. Two reservoirs (at Semenyih and Hulu Langat) and eight water treatment plants (Sungai Lolo, Sungai Pangsoon, Ampang Intake, Sungai Serai, Sungai Langat, Cheras, Bukit Tampoi and Salak Tinggi) are served as clean water providers in the river basin. Besides, the Langat Reservoir also has a function of generating power supply within the Langat Valley.

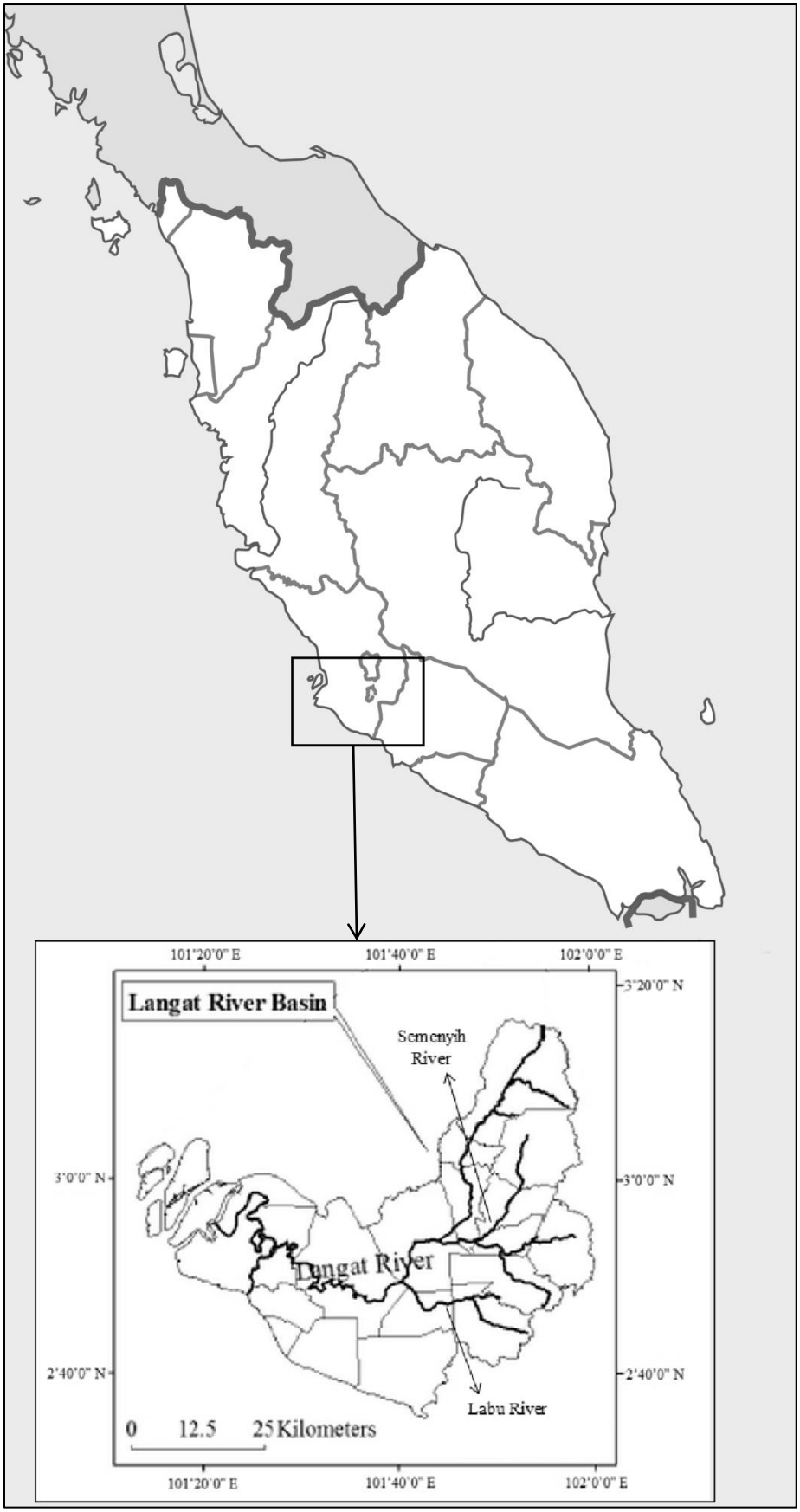

Figure 3.1: Location of the Langat River Basin in Peninsular Malaysia

Similar to the climate in Malaysia, climate of Langat River is equatorial-monsoon with high but uniform annual temperature and high humidity (with mean annual rainfall of 2079.1mm). Although it is located at the western region of Peninsular Malaysia, rainfall in this area is heavily affected by both SWM and NEM seasons. Generally, seasons in this area can be categorized by monsoon and inter-monsoon seasons, which are Southwest Monsoon (May to August), inter-monsoon (September to October and March to April) and Northeast Monsoon (November to February). NEM which blows over South China Sea brings heavy rainfall to Peninsular Malaysia while SWM is a drier period for the whole country. Even though Langat River Basin is located in the west coast region, rainfall received during SWM is still lesser than rainfall received during NEM due to the lower wind speed of SWM.

3.2 Research Procedures

The analyses of trends in rainfall pattern and spatial variation in Langat River Basin will be carried out based on the following procedures:

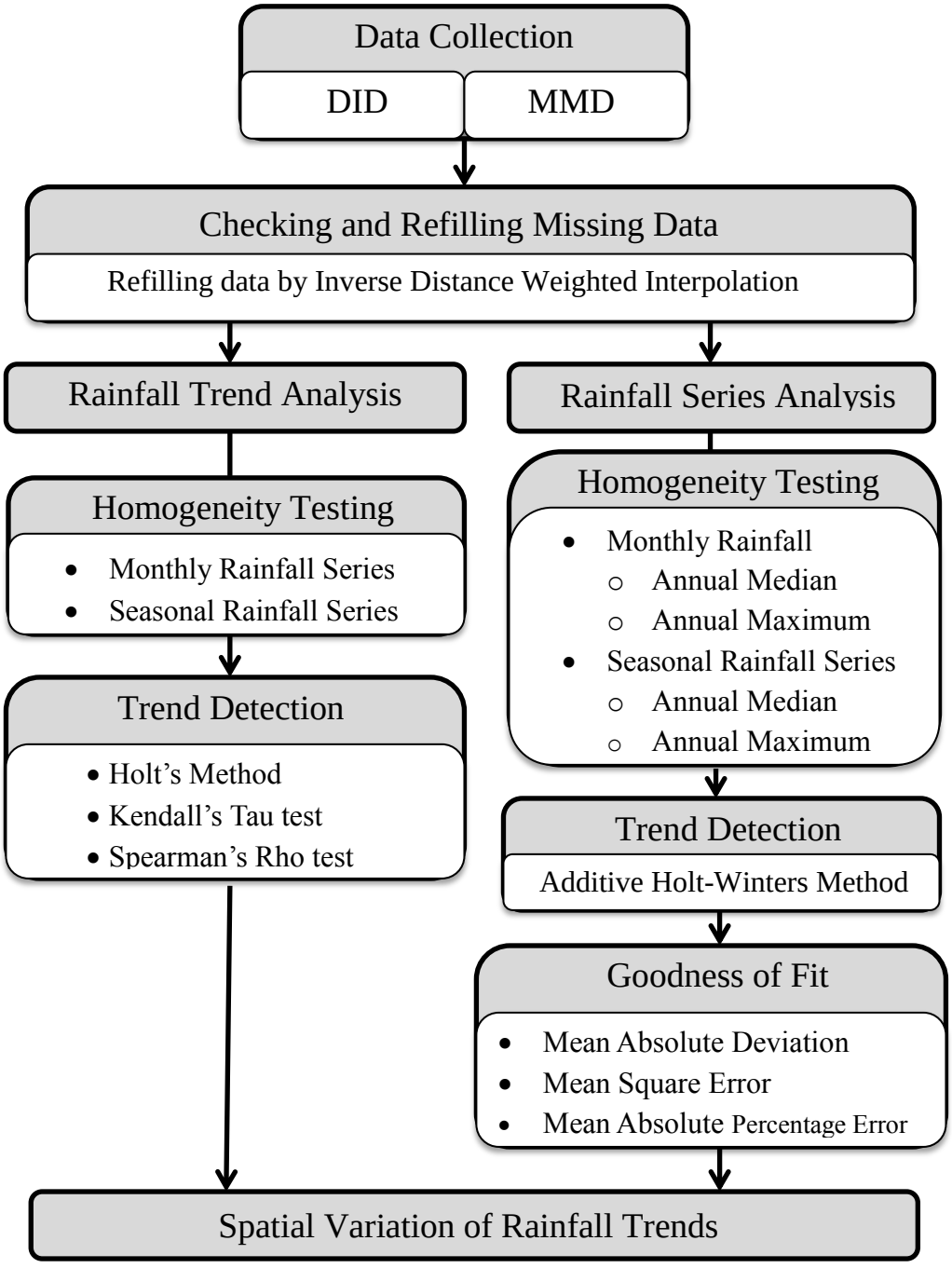

Figure 3.2: Flowchart of the research procedures

3.3 Data Collection

Historical rainfall data utilized in the present study were collected from DID (Department of Irrigation and Drainage Malaysia) and MMD (Malaysian Meteorological Department). Hourly and daily rainfalls were obtained and monthly, seasonally and yearly data are calculated by using daily precipitation. In order to investigate the rainfall trend effectively, rainfall time series of more than 25 years should be used. Therefore, only time series of 6 stations from DID and 4 stations from MMD spanning the period of 1970-2012 were employed to investigate the changes in rainfall pattern and spatial variation. Locations of the 10 selected stations were presented in Figure 3.3. All utilized stations name, the coordinates of the stations and the periods of analysis were listed in Table 3.1.

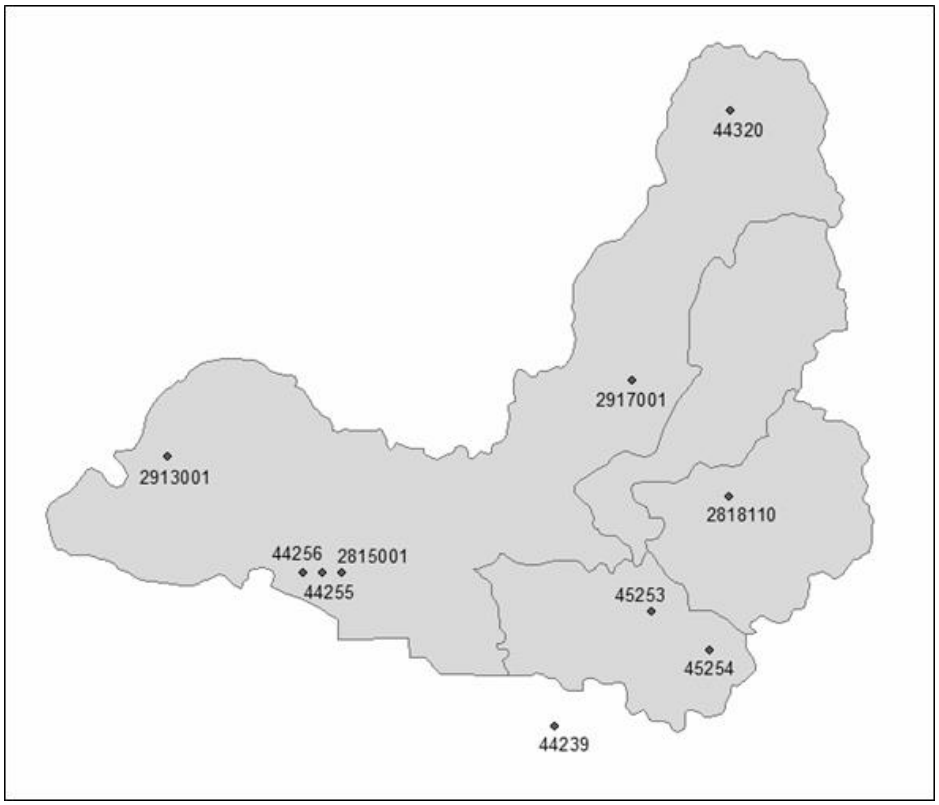

Figure 3.3: Locations of the 10 selected stations in Langat River Basin

Table 3.1: List of station code, name, study period, latitude and longitude

Station Code	Station Name	Study Period	Duration (years)	Longitude	Latitude
2815001	Pejabat JPS Sg Mangg	1970-2012	43	101°32'E	2 °49'N
2818110	SMK Bdr Tasik Kesuma	1972-2012	41	101°52'E	2 °53'N
2913001	P/KWLN P/S Telok Gong	1973-2012	39	101°23'E	2 °55'N
2917001	RTM Kajang	1975-2012	37	101°47'E	2 °59'N
44239	Sepang Estate	1974-2012	38	101°43'E	2 °41'N
44255	Pusat Pertanian Teluk Datuk	1983-2012	29	101°31'E	2 °49'N
44256	Banting Oil Palm Research Station	1981-2012	32	101°30'E	2 °49'N
44320	Ampangan Ulu Langat	1984-2012	29	101°52'E	3 °13'N
45253	New Labu Estate	1985-2012	28	101°48'E	2 °47'N
45254	Kirby Estate	1984-2012	29	101°51'E	2 °45'N

3.4 Data Checking and Missing Data Imputation

The first step of data checking is to check whether there is missing value of data. Rainfall time series of more than 10% missing data is excluded from the study to ensure the accuracy of the rainfall trend found. Data repairing will be done by Inverse Distance Weighted (IDW) interpolation method if missing data of less than 10% is found. Basic statistics like mean, standard deviation, median and coefficient of variance of each time series will be evaluated to check the general characteristic of the data.

3.4.1 Inverse Distance Weighted Interpolation

Missing data at a particular rainfall station can be estimated by Inverse Distance Weighted (IDW) Interpolation method. The IDW method makes use of data and distance from neighboring stations. Considering the station with missing data as the central, divides the surrounding area into four quadrants.

Then, rainfall data from the nearest station to the central in each quadrant is acquired for estimating missing data for the central station:

$$P_x = \frac{\sum_{i=1}^{N} \frac{P_i}{d_i^2}}{\sum_{i=1}^{N} \frac{1}{d_i^2}} \quad (1)$$

where P_x is the estimate of rainfall for the central station, N is the number of surrounding station, P_i is the rainfall values of the i-th rainfall station used for estimation and d_i is the distance from the i-th rainfall station to the central.

3.5 Homogeneity Tests

Rainfall data used in studies of rainfall trends should only be affected by weather and climate. However, other factors like location of the station, station environment, observing practices and instruments will also influence the homogeneity of rainfall time series. Thus, homogeneity testing of rainfall data is performed before further investigating. Four homogeneity tests are applied to the rainfall data, namely standard normal homogeneity test (SNHT), the Buishand range test (BR), the Pettitt test (PET) and the Von Neumann ratio test (VNR). Due to the low density of station network in Langat River Basin, these four absolute tests were chosen since they are more sensitive on detecting inhomogeneities caused by simultaneous change in the observational network (Wijingaard et al., 2003). On the other hand, the relative tests were not suitable in this study as high positive correlation among stations is required (Kang and Yusof, 2012). All four absolute tests are applied to the time series respectively. The null hypothesis for all four tests is the same which

indicating the annual values Y_i of the testing variable Y are independent and identically distributed. On the other hand, the alternative hypothesis for the SNHT, the Buishand range test and the Pettitt test is that a step-wise shift in the mean, a break, in the time series is present. These three tests are location-specific tests which can help in detecting the year where a break probably exists. Under the alternative hypothesis of the fourth test, the Von Neumann ratio test assumes the series tested is not randomly distributed.

The criteria used in the present study is similar to the one proposed by Wijingaard et al. (2003). With at least three out of four tests reject the homogeneity, the time series is categorized as "suspect". If two tests reject the homogeneity, then the time series is known to be "doubtful". The time series is "useful" when only one or zero test rejects the homogeneity. Critical values of each homogeneity tests were given in Table 3.2.

Table 3.2: The 5% critical values for the four homogeneity tests as a function of n

n	T_0 (SNHT)	$R/\sqrt{n}$ (BR)	X_E (PET)	N (VNR)
20	6.95	1.43	57	1.30
30	7.65	1.50	107	1.42
40	8.10	1.53	167	1.49
50	8.45	1.55	235	1.54

T_0, $R/\sqrt{n}$, X_E and N are the test statistics of the standard normal homogeneity test, the Buishand range test, the Pettitt test and the Von Neumann ratio test, respectively.

3.5.1 Standard Normal Homogeneity Test (SNHT)

Standard normal homogeneity test is more capable in detecting breaks near the beginning and the end of a series. However, it assumes the annual

series are normal. The statistic can be calculated as followed:

$$T_k = k\overline{z_1^2} + (n-k)\overline{z_2^2}, k = 1,2,\dots,n \qquad (2)$$

where

$$\overline{z_1} = \frac{1}{k}\sum_{i=1}^{k}\frac{(Y_i - \bar{Y})}{s} \text{ and } \overline{z_2} = \frac{1}{n-k}\sum_{i=k+1}^{n}\frac{(Y_i - \bar{Y})}{s} \qquad (3)$$

And Y_i is the annual series to be tested where *i* is the year from 1 to *n*, $\bar{Y}$ is the mean and *s* is the standard deviation.

If the series contains a break at the year *K*, then T_k comes to a maximum near the year *k*=*K*. Thus, the test statistic is

$$T_0 = \max_{1\le k\le n} T_k \qquad (4)$$

The null hypothesis is rejected if T_0 is greater than the critical value. Critical values depending on the sample size *n* is given in Table 3.2.

3.4.2 The Buishand Range Test (BR)

The Buishand range test is sensitive to breaks in the middle of a series but it assumes the Y_i values are normally distributed. The adjusted partial sum is

$$S_0^* = 0 \text{ and } S_k^* = \sum_{i=1}^{k}(Y_i - \bar{Y}), k = 1,2,\dots,n \qquad (5)$$

The values of S_k^* will fluctuate around 0 if the series is homogeneous. On contrary, the value of S_k^* reaches a maximum or a minimum near the year *k*= *K* if there is a break in year *K*. The 'rescaled adjusted range' R can be obtained by

$$R = \frac{\left(\max_{0 \le k \le n} S_k^* - \min_{0 \le k \le n} S_k^*\right)}{s} \quad (6)$$

to calculate the significance of the change in the mean. The critical value of $\frac{R}{\sqrt{n}}$ is listed in Table 3.2 to accept or reject the null hypothesis.

3.5.3 The Pettitt Test (PET)

Similar to the Buishand range test, the Pettitt test is capable to detect break in the middle of the series. However, since the Pettitt test is based on the rank, it does not require normality assumption of the data. Also, the non-parametric rank-based Pettitt test is less sensitive to outliers than other tests.

The statistic can be evaluated by

$$X_k = 2\sum_{i=1}^{k} r_i - k(n+1)\,, k = 1,2,\dots,n \quad (7)$$

Where r_i is the rank of Y_i.

X_k shows maximum or minimum if the break occurs near the year $k = E$:

$$X_E = \max_{1 \le k \le n} |X_k| \quad (8)$$

The critical values of X_E is given in Table 3.2.

3.5.4 The Von Neumann Ratio Test (VNR)

Instead of detecting breaks in the series, the Von Neumann ratio test examines whether the series is randomly distributed. The test statistic calculates the ratio of mean square successive difference to the variance:

$$N = \frac{\sum_{i=1}^{n-1}(Y_i - Y_{i+1})^2}{\sum_{i=1}^{n}(Y_i - \bar{Y})^2} \qquad (9)$$

The expected value *N* is 2 when the series is homogeneous. The value of *N* tends to be lower when there is a break in the series. The value of *N* rises above 2 when the series has rapid variations in the mean. The critical values for *N* are shown in Table 3.2.

3.6 Trend Detection

Most of the methods used for trend detection are only capable to find a general trend in single direction throughout the whole study period. However, rainfall time series might have more than one change in the study period. Changes in rainfall pattern do not necessary be increasing or decreasing throughout the entire study period, it can also be fluctuating. Instead of finding rainfall trend, modelling rainfall is an alternative to observe rainfall pattern for a certain period of time.

Holt-Winters method is an exponential smoothing method, which was initially used for forecasting sales for inventory control. There are few advantages of the exponentially weighted moving average: the decreasing

weight on historical data, the simplicity of the method and less data is required. Holt (1957) extended the exponential weighted moving averages for series with no trend, or linear trend and non-seasonal series, or series with seasonal variation in additive or multiplicative patterns. Winters (1960) concluded that this exponential forecasting model not only provides better forecasting compared to some other forecasting methods, it also reacts more efficiently when there is a sudden shift in the time series. Also, result from Holt-Winters method can be used in forecasting future rainfall.

The analysis was separated into two parts. The first part studied rainfall trend of a particular month or season over the study period. The result can help us to examine the rainfall pattern and distribution of every month or season. This analysis was done by Holt's method and the results obtained were compared with the results from two well-known non-parametric rank-based tests, which are Kendall's Tau test and Spearman's Rho test. The second part modelled monthly and seasonal rainfall series. Rainfall variations from year to year can be observed with regular rainfall pattern. Overall rainfall trend at each station can be determined using Additive Holt-Winters method.

3.6.1 Rainfall Trend Analysis

The first part analysis is aimed to find the rainfall pattern of a particular monthly and seasonal over the study period. The Holt's method is an extended single exponential smoothing, which is capable for detecting trend in different time periods. The Holt's method was used for modeling monthly and

seasonal rainfall time series for each station in the study. Non-parametric rank-based tests are popular to use in detecting trend in hydrologic data in the recent years. Even without making assumption about the data distribution, non-parametric rank-based tests are still powerful in trend detection. Also, these methods are less influenced by the outliers in the data. Due to the reason stated, the well-known Kendall's Tau test and Spearman's Rho test are commonly used in analyzing rainfall trend.

3.6.1.1 The Holt's Method

The model selected for the first part of analysis is the Holt's algorithm with trend but without seasonal variation. Since the monthly (seasonal) rainfall series was formed by a particular month (season) of every year, there is no seasonal variation the series. It is assumed that there is a linear trend in the time series and this assumption is valid for rainfall series as there should be a significant or insignificant trend in the rainfall series. Rainfall series with absolutely no trend is unlikely to be happened.

The estimate of the level (L_t) and growth rate (trend, b_t) of the time series at time *t*, are given by

$$L_t = \alpha Y_t + (1-\alpha)(L_{t-1} + b_{t-1}) \quad (10)$$

$$b_t = \beta(L_t - L_{t-1}) + (1-\beta)b_{t-1} \quad (11)$$

$$F_{t+m} = L_t + b_t m \quad (12)$$

The two parameters α and β control the smoothing for the estimate of the level and slope at the current time point, respectively. The weights α and β are

selected by minimizing the value of Mean Square Error (MSE) over observations (this process will be done using R programming) and the values of α and β are between 0 and 1. MSE is a measurement of error between the forecasted model and the observed model. In other words, a model (with a specific set of values of α and β) that gives the minimum value of MSE would be the most accurate forecasted model. If the values of α and β are close to zero, it means that little weight is placed on the most recent observations when making forecasts of future values.

In equation (10), the current estimate of the level is adjusted for the trend of the previous period. The last estimated value of trend (b_{t-1}) is added to the last smoothes value (L_{t-1}) to eliminate lag and bring L_t to the approximate level of the current data value. The smoothing parameter α controls the estimate of level with weighting the most recent observations with a weight value of α and the most recent forecast value with a weight of $(1-\alpha)$ for smoothing purpose. Since there is a trend in the time series, the next value will be either higher or lower than the current one. Then, the estimate of trend in equation (11) is expressed as the difference between the last two smoothed values of level. Since randomness might exist, the smoothing parameter β is multiplied to the trend in the last period $(L_t - L_{t-1})$ while the previous estimated value of trend is multiplied by $(1-\beta)$.

The initialization process for the Holt's algorithm requires two estimates for the first smoothed values for level, L_1 and trend, b_1:

$$L_1 = y_1 \tag{13}$$

$$b_1 = y_2 - y_1 \tag{14}$$

Trends of the time series are plotted to show how rainfall trends changed in the study period. The gradient of the regression line is calculated to compare with the results from the other two tests described hereafter.

$$m_{b_t} = \frac{\sum_{t=1}^{n}(x_t - \bar{x})\left(b_t - \bar{b}\right)}{\sum_{t=1}^{n}(x_t - \bar{x})^2} \tag{15}$$

where m_{b_t} is the gradient of the trendline, b_t is the trend value at year x_t while $\bar{x}$ and $\bar{b}$ are the mean value of the corresponding.

3.6.1.2 The Kendall's Tau Test

All annual, monthly and seasonal analysis of rainfall trend can be done by Kendall's Tau test. The null hypothesis assumes that there is no trend in the rainfall series while the alternative hypothesis is that there is a trend in the underlying data. Confidence interval of 95% is considered.

The Mann Kendall statistic, S, is described as

$$S = \sum_{i=1}^{n-1}\sum_{j=i+1}^{n} sign(y_j - y_i) \tag{16}$$

Where y_i and y_j are the data value at time *i* and *j*, respectively, n is the length of the data set and

$$sign(y_j - y_i) = \begin{cases} 1 & if\ (y_j - y_i) > 0 \\ 0 & if\ (y_j - y_i) = 0 \\ -1 & if\ (y_j - y_i) < 0 \end{cases} \tag{17}$$

The statistic *S* is approximately normally distributed when $n \geq 8$ with mean equals to zero and variance as

$$\sigma^2 = \frac{n(n-1)(2n+5)}{18} \tag{18}$$

Thus, the standardized test statistic Z_{MK} is computed by

$$Z_{MK} = \begin{cases} \frac{S-1}{\sigma} & if\ S > 0 \\ 0 & if\ S = 0 \\ \frac{S+1}{\sigma} & if\ S < 0 \end{cases} \tag{19}$$

which follows a standard normal distribution. Positive values of Z_{MK} suggest increasing trend while negative values of Z_{MK} indicate downward trend. Then, the magnitude of the trend slope can be estimated by

$$\beta = Median\left[\frac{(y_j - y_i)}{(j-i)}\right] \ for\ all\ i < j \tag{20}$$

where y_j and y_i and the data value at time *j* and *i*, respectively.

As reviewed in Chapter 2, prewhitening process was performed in some studies since the presence of serial correlation will alter the probability of rejecting the null hypothesis. Thus, before applying the Kendall's Tau test, the lag-1 serial correlation coefficient is first tested by applying

$$r_1 = \frac{\frac{1}{n-1}\sum_{t=1}^{n-1}(y_t - \bar{y})(y_{t+1} - \bar{y})}{\frac{1}{n}\sum_{t=1}^{n}(y_t - \bar{y})^2} \tag{21}$$

If $r_i > 0.1$, then the Kendall's Tau test should be applied on the prewhitened time series. The prewhitening procedure is

$$x_t = y_t - r_1 \cdot y_{t-1} \tag{22}$$

3.6.1.3 The Spearman's Rho Test

Another widely-used method in hydrologic trend detection is the non-parametric rank based Spearman's Rho test. The null hypothesis assumes that there is no correlation between the order in the time series and increase or decrease in magnitude of those data. It is noted that a 5% significant level is used for the two-tailed test.

The coefficient of rank correlation r_s is computed by

$$r_s = 1 - \frac{6\sum d_i^2}{n(n^2-1)} \tag{23}$$

where

$$\sum d_i^2 = \sum_{i=1}^{n} [R(X_i) - R(Y_i)]^2 \tag{24}$$

and n is the number of pairs while (X_i, Y_i) is the pair observation and $R(X_i)$ and $R(Y_i)$ is the number of rank, from smallest to largest in order of magnitude, $R(X_i) = 1$ if X_i is the smallest observed value of X (similar rule is applied to Y).

The test statistic is then evaluated with

$$t_t = r_s \sqrt{\frac{n-2}{1-r_s^2}} \tag{25}$$

The test statistic has the Student's t distribution with (n-2) degree of freedom. The null hypothesis of there is no trend in the time series is accepted when the t_t does not lie in the critical region.

3.6.2 Rainfall Series Analysis

The second part of rainfall analysis modelled the rainfall in monthly and seasonal basis. Rainfall series that consists of 12 months (or 4 seasons) are modelled using Additive Holt-Winters Method to study the rainfall pattern at each station for the whole study period. The accuracy of generated model is then measured by mean absolute deviation (MAD), mean square error (MSE) and mean absolute percentage error (MAPE).

3.6.2.1 Additive Holt-Winters Method

The Additive Holt-Winters Method is capable in forecasting from historical value. It assumes that the rainfall series exhibits a linear trend with constant seasonal variation. Similar to the rainfall trend analysis, monthly (seasonal) rainfall series with absolutely no trend is unlikely to happen. As rainfall in Malaysia is mainly affected by monsoon system, there is a pattern in annual rainfall distribution. The assumption of constant seasonal variation in rainfall series is thus validated. The Additive Holt-Winters Algorithm takes into account level, trend and seasonality. As it is one of the exponential smoothing methods, this method is useful in detecting trend at different time point. Thus, this algorithm can also be used to refill missing data from historical data. The estimate of the level (L_t), growth rate (trend, b_t) and seasonal pattern (S_t) at time t are computed using the following equations:

Level: $$L_t = \alpha(Y_t - S_{t-s}) + (1-\alpha)(L_{t-1} + b_{t-1}) \quad (26)$$

Trend: $$b_t = \beta(L_t - L_{t-1}) + (1-\beta)b_{t-1} \quad (27)$$

Seasonal: $$S_t = \gamma(Y_t - L_t) + (1-\gamma)S_{t-s} \quad (28)$$

where α, β and γ are smoothing constants between 0 and 1 and s represents the number of seasons in a year (s =12 for monthly data). The smoothing constants can be chosen by minimizing the value of mean square error of the historical data (This process will be done by using R programming). The L_{t-1} and b_{t-1} are the estimate of level and trend at time $t-1$, respectively, while S_{t-c} denotes the estimate of seasonal factor in time $t-c$, c represents the number of periods in a year (c = 12 for monthly data, c = 4 for quarterly data).

Finally, the forecasted value, F_{t+m} can be evaluated by

$$F_{t+m} = L_t + b_t m + S_{t-s+m} \quad (29)$$

The initialization for the Holt's Algorithm requires three estimates for first smoothed value for level(L_1), trend(b_1) and seasonal variation(s_1):

$$L_s = \frac{1}{s}(Y_1 + Y_2 + Y_3 + \cdots + Y_s) \quad (30)$$

$$b_s = \frac{1}{s}\left(\frac{Y_{s+1} - Y_1}{s} + \frac{Y_{s+2} - Y_2}{s} + \cdots + \frac{Y_{s+s} - Y_s}{s}\right) \quad (31)$$

$$S_1 = Y_1 - L_s, S_2 = Y_2 - L_s, \ldots, S_s = Y_s - L_s \quad (32)$$

Thus, increasing growth rate, b_t represents an upward rainfall trend while decreasing growth rate shows downward trend.

Since the rainy season is concentrated in few specific consecutive months (due to the monsoon season) but not the particular months, seasonal rainfall series might provide a better picture of the rainfall trend for the study

period. Results from monthly and seasonal analysis were presented together for comparison purpose.

3.6.2.2 Goodness of Fit

Goodness of fit is a measurement of the accuracy of the forecasted model to actual value. Three standard error measures, namely MAD, MSE and MAPE of the forecasted model throughout the whole study period were calculated to examine the fitting of the model. For all three measures, the smaller the value, the better the forecast accuracy. In each equation below, Y_t and $\widehat{Y_t}$ denote the actual data and forecasted value, respectively, while *n* is the number of observations.

3.6.2.2.1 Mean Absolute Deviation

Mean absolute deviation (MAD) calculates the average of the absolute value of error terms regardless whether the error is an overestimate or underestimate. It is calculated as followed:

$$MAD = \frac{\sum_{i=1}^{N} |Y_t - \hat{y}_t|}{n} \quad (33)$$

3.6.2.2.2 Mean Square Error

Mean square error (MSE) is the average value of the squared individual errors; this is a commonly-used measurement of dispersion between forecasted value and actual observation. However, due to the squared error term, the value of MSE will be magnified and cause misleading conclusion.

$$MSE = \frac{\sum_{i=1}^{N}(Y_t - \hat{y}_t)^2}{n} \quad (34)$$

3.6.2.2.3 Mean Absolute Percentage Error

Mean absolute percentage error (MAPE) is a better error measurement compared to MSE since it does not magnify large errors as MSE does. However, the drawback of this measurement is that MAPE will go to extreme when the actual observation is small (close to zero) as the denominator is the actual data Y_t.

$$MAPE = \frac{\sum_{t=1}^{N}\left(\frac{Y_t - \hat{y}_t}{Y_t}\right)}{n} \times 100\% \quad (35)$$

Lewis (1982) had developed a scale to judge the accuracy of the forecasted model using MAPE, as shown in Table 3.3.

Table 3.3: A scale of judgement of forecast accuracy (Lewis, 1982)

MAPE	Judgement of Forecast Accuracy
Less than 10%	Highly Accurate
11% to 20%	Good Forecast
21% to 50%	Reasonable Forecast
51% or more	Inaccurate Forecast

3.7 Spatial Variation

Spatial variation of rainfall trend in the Langat River Basin is presented in map. The study area will be partitioned using Thiessen polygon which takes a weighted average of the measurements based on the size of each polygon. Even though it does not truly represent the range of the gauges, it is a preliminary tool that can be used to identify spatial variation of rainfall trend in small areas. It is assumed that each polygon possesses the same characteristic of rainfall trend as the represented rainfall station. Thiessen polygon is developed as followed:

(i) Each rainfall station is considered as the measurement point.

(ii) Draw a circle around every measurement point and find the perpendicular bisector between each pair of neighboring rainfall stations.

(iii) Each polygon is built by connecting all perpendicular bisectors around the measurement point.

(iv) Every polygon will be represented by significant or non-significant positive trend or significant or non-significant negative trend.

CHAPTER 4

RESULTS

4.1 Rainfall Trend Analysis

The first part of the analysis started with rainfall trend analysis of a particular month or season. The rainfall series is composed by a specific month (or season) of every year. Homogeneities of each series were tested before trend analysis. The results are discussed in two parts, monthly trend analysis and seasonal trend analysis. Since results from the Holt's test were presented in graph form, the best fitted line was plotted to indicate whether the trends are going upward, downward or no trend. Also, in order to make comparison with results from the Kendall's Tau test and Spearman's Rho test, gradient of the best fitted line was estimated.

4.1.1 Monthly Trend Analysis

According to the criteria proposed by Wijingaard *et al.* (2003), 101 out of 120 monthly series were categorized as "useful", 14 series are "doubtful" while the remaining 5 monthly series were labeled as "suspect". Results of homogeneity tests were shown in Table 4.1. A noticeable result from homogeneity tests was that almost all monthly series failed the Von Neumann ratio test. This result suggested that the series is not randomly distributed and it might be caused by the refilled missing data.

Table 4.1: Result of homogeneity tests of monthly rainfall series

Station	Test	Jan	Feb	Mar	Apr	May	Jun	Jul	Aug	Sep	Oct	Nov	Dec
2815001	SNHT	0	0	0	0	0	0	0	0	0	0	0	1
	BR	0	0	0	0	0	0	0	0	0	0	0	0
	PET	0	0	0	0	0	0	0	0	0	0	0	0
	VNR	1	1	1	1	1	1	1	1	1	1	1	1
2818110	SNHT	0	0	0	0	0	0	0	0	0	0	1	0
	BR	0	0	0	0	1	0	0	0	0	0	0	0
	PET	0	0	0	0	1	0	0	0	0	0	0	1
	VNR	1	1	1	1	0	1	1	1	1	1	1	1
2913001	SNHT	0	0	0	0	0	0	0	0	1	0	0	0
	BR	0	0	0	0	0	0	0	0	0	0	0	0
	PET	0	0	0	0	0	0	0	0	0	0	0	0
	VNR	1	1	1	1	1	1	1	1	0	1	1	1
2917001	SNHT	1	0	0	0	0	0	0	0	0	0	0	0
	BR	0	0	0	0	0	0	0	0	0	0	0	0
	PET	1	0	0	1	0	0	0	0	0	0	0	0
	VNR	1	1	1	0	1	1	1	1	1	1	1	1
44239	SNHT	0	0	0	0	0	0	0	0	0	0	0	0
	BR	0	0	0	0	0	0	0	0	0	0	0	0
	PET	0	0	0	0	0	0	0	0	0	0	0	0
	VNR	1	1	1	1	1	1	1	1	1	1	1	1
44255	SNHT	0	0	0	0	0	0	0	0	0	1	0	0
	BR	0	0	0	1	0	0	1	0	0	0	0	0
	PET	0	0	0	1	0	0	1	1	0	0	0	0
	VNR	1	1	1	1	1	1	1	1	1	1	1	1
44256	SNHT	1	0	0	0	1	0	0	0	0	0	0	1
	BR	0	0	0	0	0	0	0	0	0	0	0	0
	PET	0	0	0	0	1	0	0	1	0	0	0	0
	VNR	1	1	1	1	1	1	1	1	1	1	1	1
44320	SNHT	1	0	0	0	0	0	0	0	0	0	0	0
	BR	0	0	0	0	0	0	0	0	0	0	0	0
	PET	0	0	0	0	0	0	0	0	0	0	0	0
	VNR	1	1	1	1	1	0	1	1	0	1	1	1
45253	SNHT	0	0	0	0	1	0	0	0	0	0	0	0
	BR	0	0	0	0	0	0	0	1	0	0	0	1
	PET	0	0	0	0	1	0	0	1	0	0	0	0
	VNR	1	1	1	1	0	1	1	1	1	1	1	1
45254	SNHT	0	1	0	0	0	0	0	0	0	0	0	0
	BR	0	0	0	0	0	0	0	0	0	0	0	0
	PET	0	0	0	0	1	0	0	0	0	0	0	0
	VNR	1	1	1	0	1	1	1	1	1	1	1	1

"0" indicated the test was passed;
"1" indicated the test was failed.

Based on the graph plotted using the trends of monthly time series by the Holt's method, the best fitted lines were drawn, as illustrated in Figure 4.1 (other trend plots were showed in Appendix B). The gradient of the best fitted line was calculated in order to compare with results from Kendall's Tau and Spearman's Rho tests. From January rainfall analysis, there are 5 increasing

trends at stations 2913001 (Figure 4.1), 2917001, 44255, 44320 and 45254 showed from Holt's method, as shown in Table 4.2. Increasing trends at stations 2913001, 2917001 and 44320 were confirmed by Kendall's Tau and Spearman's Rho tests. A consistent result of decreasing trend from all three tests was also found at station 2815001.

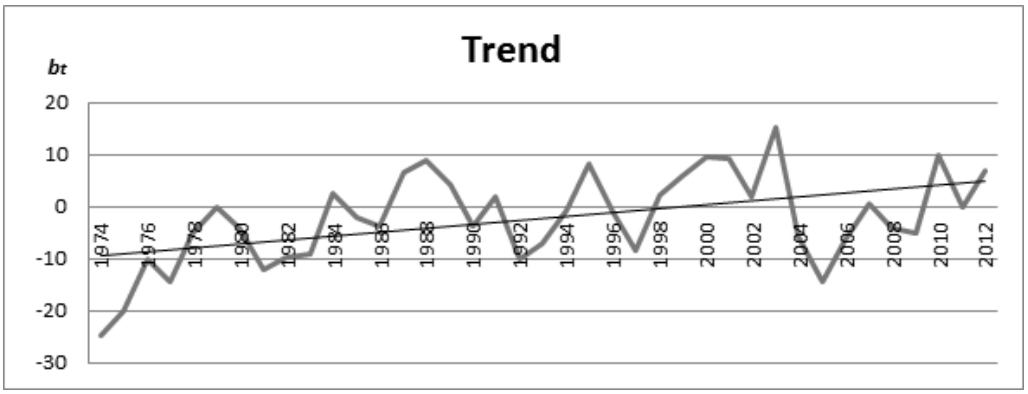

Figure 4.1: Example of trend plot of January series using Holt's method at station 2913001

Table 4.2: Result of monthly rainfall analysis using Holt's Method (m_{b_t}), Kendall's Tau (Z_{MK}) and Spearman's Rho (t_t)

Station Code	January			February			March		
	m_{b_t}	Z_{MK}	t_t	m_{b_t}	Z_{MK}	t_t	m_{b_t}	Z_{MK}	t_t
2815001	-0.038	-0.544	-0.070	-0.871	-0.209	-0.022	0.150	0.314	0.041
2818110	-0.127	0.550	-0.044	0.000	0.000	0.041	-0.487	0.056	-0.094
2913001	0.369	1.355	0.416	0.402	-1.113	0.115	0.159	0.000	0.269
2917001	0.019	2.184	0.611	-0.417	0.798	0.477	0.487	0.772	0.459
44239	-0.142	0.327	0.029	0.522	0.352	0.041	-0.076	-0.427	0.071
44255	0.096	-0.169	0.013	0.880	-1.069	-0.188	-0.502	1.570	0.286
44256	-0.443	0.730	0.129	-0.492	-0.114	-0.033	-0.350	0.308	0.071
44320	0.790	1.144	0.233	2.513	0.732	0.156	1.063	1.932	0.371
45253	-0.795	0.929	0.164	-0.209	0.257	0.039	1.433	-0.099	-0.037
45254	0.885	-0.810	-0.197	2.820	-1.369	-0.261	1.107	0.356	0.061

Table 4.2 continued: Result of monthly rainfall analysis using Holt's Method (m_{b_t}), Kendall's Tau (Z_{MK}) and Spearman's Rho (t_t).

Station Code	April			May			June		
	m_{b_t}	Z_{MK}	t_t	m_{b_t}	Z_{MK}	t_t	m_{b_t}	Z_{MK}	t_t
2815001	0.165	-0.774	-0.163	-0.124	-0.335	-0.053	0.110	-0.021	0.016
2818110	0.109	0.595	0.110	0.515	-0.734	-0.207	0.118	-0.550	-0.144
2913001	0.892	-0.411	0.220	-0.163	-0.919	0.147	-0.224	0.218	0.293
2917001	-0.347	2.062	0.537	-0.262	0.151	0.327	-0.034	-0.528	0.257
44239	0.041	-0.427	-0.075	-0.179	0.453	-0.074	-0.278	0.532	0.062
44255	-0.020	0.892	0.189	0.038	-1.035	-0.175	0.423	-0.071	-0.007
44256	0.256	0.892	0.169	-1.230	-1.541	-0.254	-0.761	0.600	0.096
44320	0.000	0.694	0.145	0.392	-0.544	-0.069	-0.919	-0.217	0.024
45253	-1.299	-0.059	0.006	3.200	-2.549	-0.464	-0.675	0.296	0.079
45254	1.121	0.506	0.121	-0.159	-1.594	-0.310	1.184	-0.356	-0.038
Station Code	July			August			September		
	m_{b_t}	Z_{MK}	t_t	m_{b_t}	Z_{MK}	t_t	m_{b_t}	Z_{MK}	t_t
2815001	0.145	1.151	0.198	-0.187	-0.293	-0.056	0.947	-1.151	-0.153
2818110	-0.900	-1.089	-0.181	-0.134	1.202	0.079	0.215	-0.775	0.159
2913001	0.396	-0.315	0.223	-0.922	0.363	0.300	1.639	-1.524	0.084
2917001	0.920	-0.377	0.260	0.169	1.861	0.549	0.816	1.333	0.456
44239	0.167	0.290	0.083	-0.683	0.895	0.057	0.744	-0.754	0.150
44255	2.041	1.285	0.241	1.579	2.248	0.389	0.745	-0.844	-0.167
44256	0.124	-0.503	-0.059	-0.168	2.092	0.363	0.652	0.000	-0.010
44320	1.536	-0.807	-0.146	-0.593	1.482	0.295	-2.298	-0.459	-0.151
45253	0.188	-0.573	-0.119	-0.117	-1.442	-0.265	-0.594	-0.834	-0.186
45254	0.167	0.394	0.100	-1.255	0.206	0.030	-1.570	-0.375	-0.034
Station Code	October			November			December		
	m_{b_t}	Z_{MK}	t_t	m_{b_t}	Z_{MK}	t_t	m_{b_t}	Z_{MK}	t_t
2815001	0.812	-0.356	-0.061	-0.294	-0.251	-0.026	0.353	1.047	0.163
2818110	0.831	0.011	0.130	-0.149	0.011	0.154	0.000	1.629	0.162
2913001	-1.422	0.000	0.255	1.136	0.478	0.241	-0.331	1.433	0.391
2917001	-0.308	0.779	0.422	-0.221	1.333	0.435	0.480	0.578	0.379
44239	-1.591	-1.131	-0.101	-0.703	1.282	-0.183	0.068	0.000	0.203
44255	-0.450	0.094	0.001	-0.245	0.694	0.118	-0.033	0.994	0.156
44256	0.291	-0.442	-0.108	0.539	1.054	0.185	0.722	0.306	0.068
44320	-0.884	0.296	0.034	2.641	0.573	0.068	1.696	-0.533	-0.107
45253	1.204	-0.917	-0.206	0.818	0.417	0.156	0.342	0.292	0.117
45254	-1.864	0.138	0.008	0.704	0.296	0.054	0.156	0.020	-0.001

	Increasing trend by all three tests.
	Decreasing trend by all three tests.

In February rainfall, consistent results by all the three tests were found at station 2815001 (decreasing trend), station 44239 (increasing trend), station 44256 (decreasing trend) and station 44320 (increasing trend), as listed in Table 4.2. It was noticed that station 2818110 showed no trend from Holt's test and Kendall's Tau test but very insignificant positive trend from Spearman's Rho test.

For rainfall analysis in March, four stations (2815001, 2917001, 44320 and 45254) exhibited consistent increasing trends by the three tests. However, in April, only three increasing trends at stations 2818110, 44256 and 45254 found by the Holt's test were also supported by the other two tests, as shown in Table 4.2. From the results of Kendall's Tau and Spearman's Rho tests, significant increasing trend (2.062 and 0.537, respectively) was revealed at station 2917001 in April rainfall. However, Holt's test gave an opposite result (-0.347). March and April fall into ITM2, which is considered a wet season for the study area. Since all consistent results showed upward trend, future rainfall in the river basin is likely to be increasing.

There are three stations showing consistent results by the three tests for May, which are stations 2815001, 44256 and 45254, with decreasing trends. A noticeable contradicting result was also discovered in May rainfall. A significant decreasing trend was found by Kendall's Tau test with value of -2.549 and Spearman's Rho test with value of -0.464 at station 45253; while Holt's test had showed a clear increasing trend with a significant value of 3.200.

There are four stations, namely stations 2815001, 44239, 44255 and 45254 had shown consistent result with increasing trends by all the three tests in July rainfall. Besides that, the Holt's test showed only one downward trend (-0.900) at station 2818110, and this had been agreed by the Kendall's Tau and Spearman's Rho tests. For August rainfall analysis, only two increasing trends were found by Holt's test, and both were supported by the other two tests. Out of the remaining eight decreasing trends, consistent results by the three tests can only be found at stations 2815001 and 45253.

All three tests had discovered consistent results of downward trends at stations (44320, 45253 and 45254) located in the eastern region in September rainfall, as shown in Figure 4.2-4.4. Only two stations in October rainfall show consistent result by all three tests, as compared to November where there are six stations show consistent result. All five increasing trends (stations 2913001, 44256, 44320, 45253 and 45254) found by the Holt's test were supported by the other two tests, while consistent result of decreasing trend was only showed at station 2815001 for rainfall analysis of November. Finally, there are four stations show increasing trend by the three tests in December.

As a whole, result in monthly rainfall trend analysis indicated that March, July and November show most of the stations (at least 5 stations) have consistent results (either increasing or decreasing) by the three tests, with the highest of six stations in November, as shown in Table 4.2. It was also noticed that most of the stations show increasing trends in these three months.

On the other hand, January, February, August, September and December have moderate number of four stations with consistent results;

while May and October have only three and two, respectively. There was no station in June. It was also found that May and September have the highest number of stations (three stations each) show decreasing trends by all the three tests. The results imply that in May and September, the river basin is more likely to go through a dry period in the future as all 3 tests gave the same result. On the other hand, more increasing trends were found in January, November and December, monsoon months of NEM (wettest season). The wet season is getting wetter in the Langat river basin. According to this trend, future rainfall is expected to be increasing.

In terms of station basis, station 2815001 was the station with the highest number of months with changing rainfall trends throughout the year, as supported by all three tests. From monthly rainfall analysis, decreasing trends were found in January, February, May, August and November (five months); while increasing trends were shown in March, July and December (three months). Furthermore, high number of months with changing trend was also found at station 45254, which includes four increasing trends (March, April, July and November) and two decreasing trends (May and September). Among the ten stations, station 44255 has the least number of months (July and August) with changing trends. Other stations show moderate number of months with the range of 3-5 months.

It was noticed that contradicting results were found when different methods were used. The inconsistent results might be caused by few reasons. Firstly, since Kendall's Tau and Spearman's Rho are rank-based tests, the magnitude of increment or decrement is not taken into account. However,

Holt's test considers both the direction and the magnitude. For example, for May rainfall at station 45253, although the number of decreasing rainfall (compared to previous year) is more than the number of increasing rainfall, the magnitude of each increasing rainfall is much larger than the magnitude of each decreasing rainfall. Thus, increasing trend was shown from Holt's test but Kendall's Tau and Spearman's Rho tests showed downward trend. Besides, the two rank-based tests only show general trend for the whole study period. For rainfall pattern with decreasing trend in the earlier period and increase afterward, a generalized positive or negative trend would be shown, which does not reflect the real scenario of the rainfall pattern. A good example is the November rainfall trend analysis at station 2818110 (Figure 4.2).

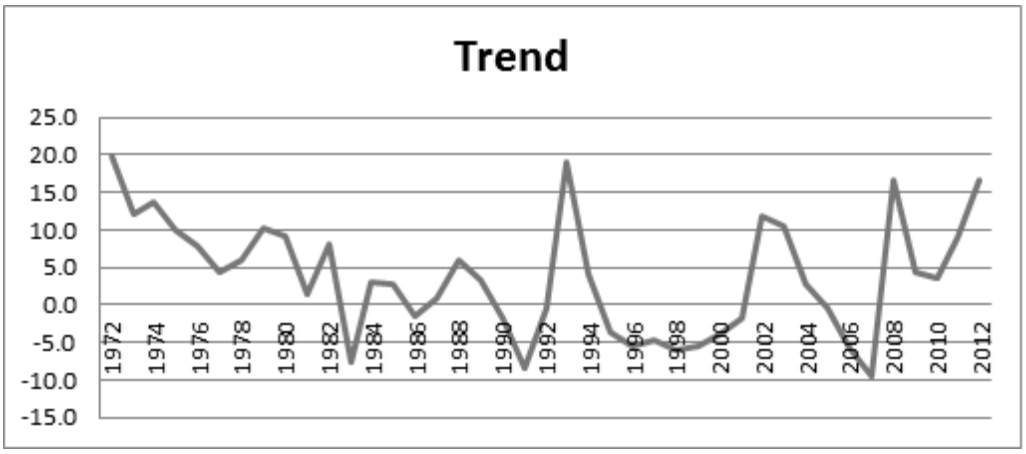

Figure 4.2: Trend plot of November series using Holt's test at station 2818110

4.1.2 Seasonal Trend Analysis

Seasonal rainfall series was composed by summing up monthly rainfall. The four seasons indicated here were Southwest Monsoon (SWM, May to August), Northeast Monsoon (NEM, October to February of the

following year) and two inter-monsoons (ITM1, from September to October; and ITM2, from March to April). From homogeneity tests, it was found that 28 out of 40 seasonal series were "useful", 8 of the series were "doubtful" and the remaining 4 series were categorized as "suspect", as presented in Table 4.3. Similar to the result of homogeneity testing on monthly series, most of the seasonal series were not randomly distributed as they failed the Von Neumann ratio test.

Table 4.3: Result of homogeneity tests of seasonal rainfall series

Station	Test	SWM	ITM1	NEM	ITM2	Station	Test	SWM	ITM1	NEM	ITM2
2815001	SNHT	0	0	0	0	44255	SNHT	0	1	0	1
	BR	0	0	0	0		BR	1	0	0	0
	PET	0	0	0	0		PET	0	0	0	1
	VNR	1	1	1	1		VNR	1	1	1	1
2818110	SNHT	0	0	0	0	44256	SNHT	0	1	1	1
	BR	1	0	0	0		BR	0	0	0	0
	PET	1	0	0	0		PET	0	0	0	1
	VNR	1	1	1	1		VNR	1	1	0	1
2913001	SNHT	0	0	0	0	44320	SNHT	0	0	0	0
	BR	0	0	0	0		BR	0	0	0	0
	PET	0	1	0	0		PET	0	0	0	1
	VNR	1	1	1	1		VNR	1	1	1	1
2917001	SNHT	0	1	0	0	45253	SNHT	0	0	0	0
	BR	0	0	0	0		BR	0	0	0	0
	PET	0	1	1	1		PET	1	0	0	0
	VNR	1	1	1	1		VNR	1	1	1	1
44239	SNHT	0	0	0	0	45254	SNHT	0	0	0	0
	BR	0	0	0	0		BR	0	0	0	0
	PET	0	0	0	0		PET	0	0	0	0
	VNR	1	1	1	1		VNR	1	1	1	1

"0" indicated the test was passed;
"1" indicated the test was failed.

During SWM, five increasing trends were reported at stations 2917001, 44239, 44255, 45253 and 45254 by Holt's test. However, only three series (2917001, 44239 and 44255) produced the same result when analyzing using the other two tests, as shown in Table 4.4. Significant downward trend was found at station 45253 by Kendall's Tau (-2.193) and Spearman's Rho (-0.413) test but opposite trend had been found by the Holt's test (1.303). Other

consistent results of decreasing trends were also showed at stations 2818110 and 44256 in SWM rainfall. For rainfall analysis in ITM1, the only significant decreasing trend (-3.702) was revealed at station 45254, which was supported by both the non-parametric tests (-0.296 and -0.064). Among the eight increasing trends by Holt's test, consistent and statistically significant upward trend was showed from Kendall's Tau test (1.961) and Spearman's Rho test (0.533) at station 2917001. All three tests had discovered that rainfall at station 2818110 trended upward during the study period.

Table 4.4: Result of seasonal rainfall analysis using Holt's Method (m_{b_t}), Kendall's Tau (Z_{MK}) and Spearman's Rho (t_t)

Station Code	SWM			ITM1		
	m_{b_t}	Z_{MK}	t_t	m_{b_t}	Z_{MK}	t_t
2815001	-0.421	0.440	0.060	1.841	-0.837	-0.116
2818110	-0.163	-1.045	-0.216	0.544	0.056	0.042
2913001	0.000	0.339	0.290	0.667	-1.476	0.091
2917001	**1.194**	0.779	**0.400**	0.217	**1.961**	**0.533**
44239	**0.770**	0.578	0.096	0.091	-1.307	-0.204
44255	**4.321**	0.749	0.143	0.180	-0.131	0.000
44256	-1.584	-0.178	-0.019	1.192	-0.748	-0.127
44320	-0.144	0.469	0.126	0.000	0.296	0.049
45253	**1.303**	**-2.193**	**-0.413**	1.184	-1.543	-0.300
45254	**0.037**	-1.407	-0.265	-3.702	-0.296	-0.064
Station Code	NEM			ITM2		
	m_{b_t}	Z_{MK}	t_t	m_{b_t}	Z_{MK}	t_t
2815001	**0.856**	-0.282	-0.056	0.395	0.272	0.021
2818110	**0.015**	0.571	0.089	-0.453	0.550	0.034
2913001	**1.345**	0.048	0.209	1.093	-0.073	0.273
2917001	-1.065	**2.027**	**0.567**	0.911	1.478	**0.523**
44239	**0.217**	1.530	0.111	0.131	-0.805	-0.126
44255	**0.542**	0.169	0.003	-0.407	1.606	0.294
44256	**0.447**	0.782	0.138	-0.027	1.184	0.239
44320	**5.146**	1.087	0.188	1.295	1.782	**0.393**
45253	**0.921**	1.293	0.212	-0.016	-0.731	-0.154
45254	**0.745**	-0.178	-0.050	2.437	0.769	0.158

	Increasing trend by all three tests.
	Decreasing trend by all three tests.

For NEM rainfall analysis, nine out of ten stations have showed increasing trends by Holt's test. Except for stations 2815001 and 45254, consistent results were obtained for all stations by Kendall's Tau and Spearman's Rho tests. Increasing trend at station 2917001 was found statistically significant by Kendall's Tau test (2.027) and Spearman's Rho test (0.567). However, trend in the opposite direction was shown from Holt's test (-1.065). In ITM2, the three tests had showed consistent results for five stations, with increasing trends at stations 2815001, 2917001, 44320, 45254 and decreasing trend at station 45253, as shown in Table 4.4.

Overall result from seasonal rainfall trend analysis indicated that seven out of the ten stations showed increasing trend by all the three tests in NEM. This result is consistent with the result obtained from monthly rainfall trend analysis, where NEM consists of November, December, January and February, has shown the highest number of stations with increasing trends by the three tests.

4.2 Rainfall Series Analysis

The second part of rainfall analysis was carried out in the form of monthly and seasonal series. The monthly series was composed by 12 months of every year of the study period; while the seasonal series consisted of the four seasons of each year. Results from the Additive Holt-Winters method were presented in graph and results of monthly and seasonal series were shown together for comparison. The rainfall trends were discussed based on

the location of each station.

4.2.1 Homogeneity Tests

Similar tests were applied to the maximum rainfall and annual median of the series to test whether the monthly or seasonal series is homogeneous. It was found that 15 out of 20 monthly series were homogeneous at 95 % significance level, as shown in Table 4.5. Out of the five remaining, four series (median and maximum at station 2917001, median at station 44255 and maximum at station 44256) were found to be "suspect" and one (maximum at station 44255) was found under "doubtful" category. It was noticed that the monthly series at station 44255 were labeled as "suspect" and "doubtful" when testing on annual maximum and annual median rainfall, respectively. This result suggested that monthly rainfall series of station 44255 might not be suitable for further analysis ("suspect" in annual maximum and "doubtful" in annual median).

Table 4.5: Result of homogeneity tests at each station

Station Code	Study Period (n)	Critical Value	Tests	Monthly Series		Seasonal Series	
				Median	Max	Median	Max
2815001	43	*8.205*	SNHT	1.738	3.811	4.074	1.62
		1.536	BR	1.01	1.212	1.113	0.906
		187.4	Pettitt	106	146	94	96
		1.505	VNR	1.957*	1.439	2.068*	1.904*
2818110	41	*8.135*	SNHT	6.6	6.906	5.058	6.718
		1.532	BR	1.492	1.095	1.55*	1.119
		173.8	Pettitt	150	162	136	124
		1.495	VNR	1.458	2.026*	1.642*	1.817*
2913001	39	*8.055*	SNHT	4.731	0.92	4.3	1.19
		1.527	BR	1.111	0.688	1.258	0.985
		161	Pettitt	76	86	100	82
		1.483	VNR	1.449	2.568*	1.9*	2.202*

Table 4.5 continued: Result of homogeneity tests at each station.

Station Code	Study Period (n)	Critical Value	Tests	Monthly Series		Seasonal Series	
				Median	Max	Median	Max
2917001	37	*7.965*	SNHT	9.212*	5.557	9.955*	8.495*
		1.521	BR	1.504	1.228	1.572*	1.564*
		149	Pettitt	204*	152*	212*	196*
		1.469	VNR	1.455	1.674*	1.503*	1.501*
44239	38	*8.01*	SHNT	3.446	2.199	2.779	2.669
		1.524	BR	0.846	0.935	0.754	1.23
		155	Pettitt	105	97	68	108
		1.476	VNR	1.975*	1.925*	2.346*	2.045*
44255	29	*7.58*	SHNT	7.474	9.805*	7.583*	4.863
		1.493	BR	1.58*	1.513*	1.502*	1.188
		102	Pettitt	124*	110*	102	84
		1.408	VNR	1.357	1.443*	1.676*	2.293*
44256	32	*7.74*	SHNT	11.765*	8.892*	10.979*	5.929
		1.506	BR	1.373	0.831	1.109	0.911
		119	Pettitt	84	109	91	58
		1.434	VNR	1.168	1.663*	1.694*	2.19*
44320	29	*7.58*	SHNT	4.595	6.456	4.158	3.662
		1.493	BR	1.009	1.183	1.092	0.851
		102	Pettitt	84	68	80	42
		1.408	VNR	2.258*	1.708*	2.255*	2.281*
45253	29	*7.58*	SHNT	3.414	1.657	6.757	2.496
		1.493	BR	1.054	1.076	1.202	1.313
		102	Pettitt	62	50	100	58
		1.408	VNR	1.608*	2.112*	1.927*	1.983*
45254	29	*7.58*	SHNT	4.532	3.123	2.85	2.048
		1.493	BR	1.141	1.337	1.186	0.92
		102	Pettitt	62	76	64	80
		1.408	VNR	1.7*	1.658*	1.84*	2.126*

* significant at $\alpha = 0.05$.

For seasonal rainfall series, 15 series were categorized as “useful”. Two “suspect” (stations 2917001 and 44255) and two “doubtful” (stations 2818110 and 44256) series were found when testing on annual median. Only one “doubtful” series was showed at station 2917001 when annual maximum

was used as testing variable. As seasonal rainfall series at station 2917001 was inhomogeneous regardless testing on annual median or annual maximum rainfall, this station was eliminated from further investigation.

4.2.2 Goodness of Fit

Accuracy of the generated model was measured by MAD, MSE and MAPE. There is no existing criterion to indicate how well the generated model performs for MAD and MSE. However, value of MAPE can be interpreted according to the "Scale of Judgement of Forecast Accuracy" (as shown in Chapter 3, Figure 3.3). Results of MAD, MSE and MAPE for the whole study period were listed in Table 4.6.

Table 4.6: Values of average rainfall, MAD, MSE and MAPE of monthly and seasonal analyses at each station for the whole period

Stations Code		Average	MAD	MSE	MAPE
44239	Monthly	170.9	65.5	6955.8	0.68
	Seasonal	509.7	119.3	23591.5	0.35
44255	Seasonal	476.8	133.8	27587	0.32
44256	Monthly	170.7	72.4	9478.6	0.78
	Seasonal	511.3	141.2	39189.8	0.3
44320	Monthly	215	84.8	10621.4	0.75
	Seasonal	640.8	161.8	42235.9	0.29
45253	Monthly	174.3	76.2	9665.6	0.77
	Seasonal	517	152	34403.6	0.35
45254	Monthly	180.7	79.4	10314.9	0.87
	Seasonal	536.5	154.3	42869.4	0.31
2815001	Monthly	147.7	66.6	7323.3	1.14
	Seasonal	440.8	142.5	34206.2	0.48

Table 4.6 continued: Values of average rainfall, MAD, MSE and MAPE of monthly and seasonal analyses at each station for the whole period

Stations Code		Average	MAD	MSE	MAPE
2818110	Monthly	162.5	64.2	6918.4	0.88
	Seasonal	485.8	133.5	28138.6	0.34
2913001	Monthly	160	70.7	8810.3	1.82
	Seasonal	475.6	133.5	29556.5	4.07
2917001	Monthly	567.3	78.1	10189.2	0.86

As shown in Table 4.6, values of MAD of monthly series ranged from 64.2 to 84.8, indicating that the forecasted rainfall had a deviation of 64.2mm to 84.8mm rainfall. For instance, the largest value of 84.8 was found at station 44320, so the forecasted rainfall at this station was averagely more or lesser of 84.8mm rainfall every month while the average rainfall was 215mm. Figure 4.3 showed the boxplot of monthly rainfall series over the 29 years at station 44320 and the average monthly rainfall was described in line. For seasonal rainfall series, the value of MAD was found in the interval between 119.3mm to 161.8mm. The MAD value of forecasted seasonal rainfall was 161.8mm at station 44320 which has an average seasonal rainfall of 640.8mm. Comparing accuracy of monthly and seasonal model, the MAD value is 39.44% of the average rainfall for monthly series, while the percentage decreased to 25.25% for seasonal rainfall series at station 44320. The same situation could be seen at every station. Therefore, it was concluded that the generated seasonal rainfall model was better than the monthly rainfall model when MAD was used as the indicator of goodness of fit of the model.

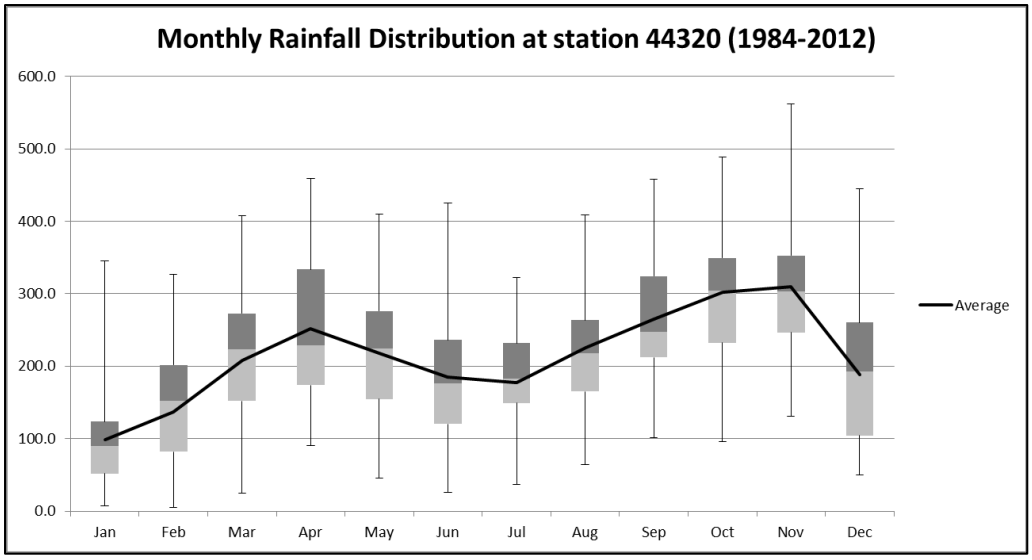

Figure 4.3: Boxplot of monthly rainfall at station 44320

As mentioned in Chapter 3, the value of MSE will accentuate when the error is large due to the squared error term. Hence, the MSE value was generally larger than MAD value, as shown in Table 4.6. For this study, minimum MSE was used to optimize smoothing parameters of Holt-Winters method for each station. The values of MSE for the monthly rainfall series were large, which lied between 6918.4 and 10621.4. As for seasonal rainfall series, the values ranged from 23591.5 to 42869.4.

Compared to MSE, MAPE would be a better indicator of goodness of fit of the model since it does not magnify when the errors are large. However, there are some disadvantages of this indicator. Firstly, when the actual data is zero, the denominator becomes zero, which is known as “undefined”. Then, if the actual data is less than 1, the value of MAPE would become large. The values of MAPE found in this part were compared to the scale of judgement, which was developed by Lewis (1982). The MAPE values shown in monthly series were unsatisfactory with values from 64.93% to 182.25%, and these values are labeled as “Inaccurate Forecast”.

Generated seasonal rainfall series presented a better result where most of the MAPE values fell in 29.15% to 47.57%. All MAPE values in the interval of 21% to 50% are “Reasonable Forecast”. The only exception was station 2913001. The MAPE values of monthly and seasonal analysis were 182.25% and 406.53%, respectively. Refering to the boxplot of rainfall distribution at station 2913001 (Figure 4.4), there were few months with very low rainfall (close to 0) and the range of the monthly rainfall was wide (for example, the minimum and maximum rainfall in October were 23mm and 615.5mm). For seasonal rainfall series, a special case of seasonal rainfalls with 0.6mm caused the uncommonly large MAPE. With exception of station 2913001, the forecasted seasonal rainfall series was proven a better model as compared to monthly rainfall series.

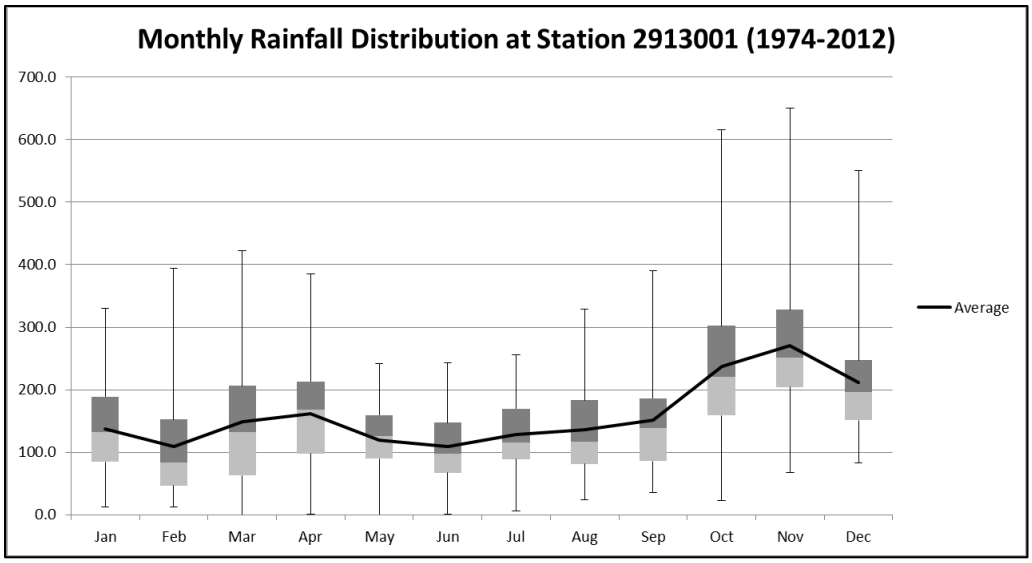

Figure 4.4: Boxplot of monthly rainfall at station 2913001

4.2.3 Monthly and Seasonal Series Analysis

Trends of monthly and seasonal rainfall series at each station were plotted to show the changes in rainfall pattern for the study period. In the western region of the study area, station 2913001, is the nearest station to the west coast. Refer to Figure 4.5, it was noticed that rainfall at this station generally trended upward but decreased during the period of April 2001 to April 2005. From seasonal analysis, the rainfall trend was also increasing but with more fluctuations. Similar to monthly analysis, rainfall decreased from ITM2 2001 to ITM1 2005.

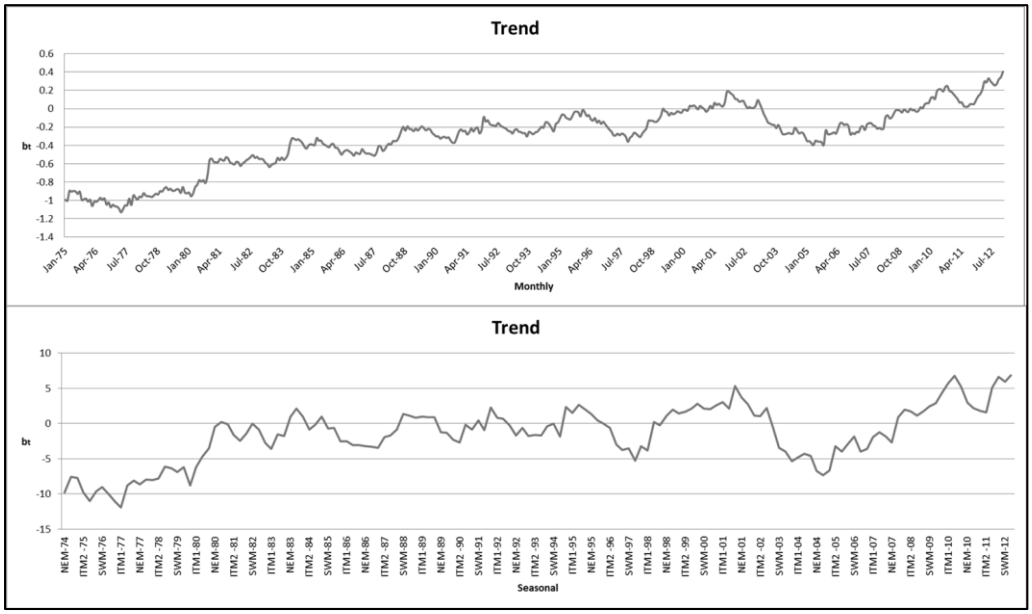

Figure 4.5: Trend plots of monthly and seasonal rainfall at station 2913001

The three nearby stations, stations 2815001, 44255 and 44256 also represented rainfall stations from western region. Station 2815001 has the longest rainfall data with 43 years among all nine stations. Both monthly and seasonal analyses get the similar result in rainfall series analysis (Figure 4.6); an increasing rainfall trend was shown from 1971 to mid of 1996 and

remained consistent with a turning point in September 2005. Stations 44255 and 44256, which located next to station 2815001, have shorter periods of data (29 and 32 years, respectively). Monthly rainfall series analysis at station 44255 was excluded since the monthly rainfall series was inhomogeneous. As shown in Figure 4.7, rainfall decreased during the earlier period but increased thereafter in seasonal analysis. As for station 44256, increasing rainfall trend was revealed during the whole study period in both monthly and seasonal analysis, as shown in Figure 4.8. Comparing results from these three nearby stations in the overlapped period, it was found that similar results were shown at stations 2815001 and 44255 but not at station 44256.

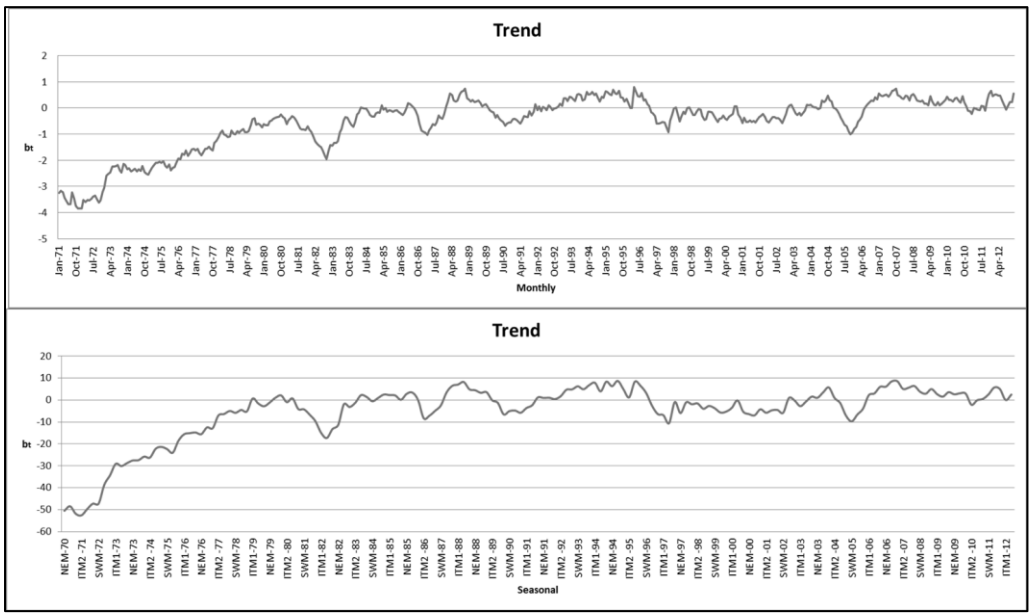

Figure 4.6: Trend plots of monthly and seasonal rainfall at station 2815001

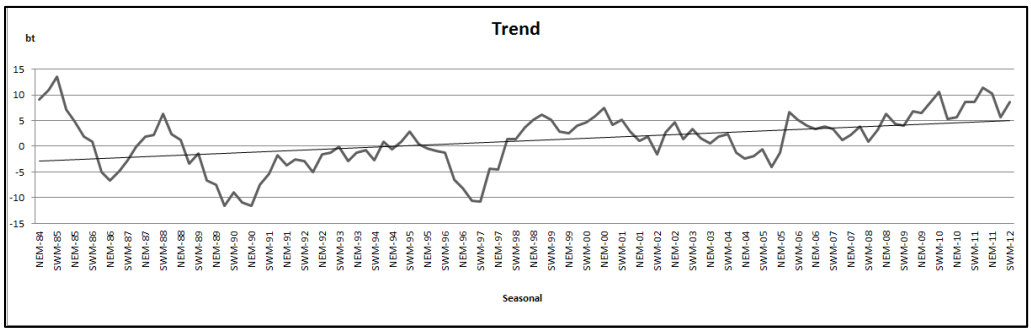

Figure 4.7: Trend plots of monthly and seasonal rainfall at station 44255

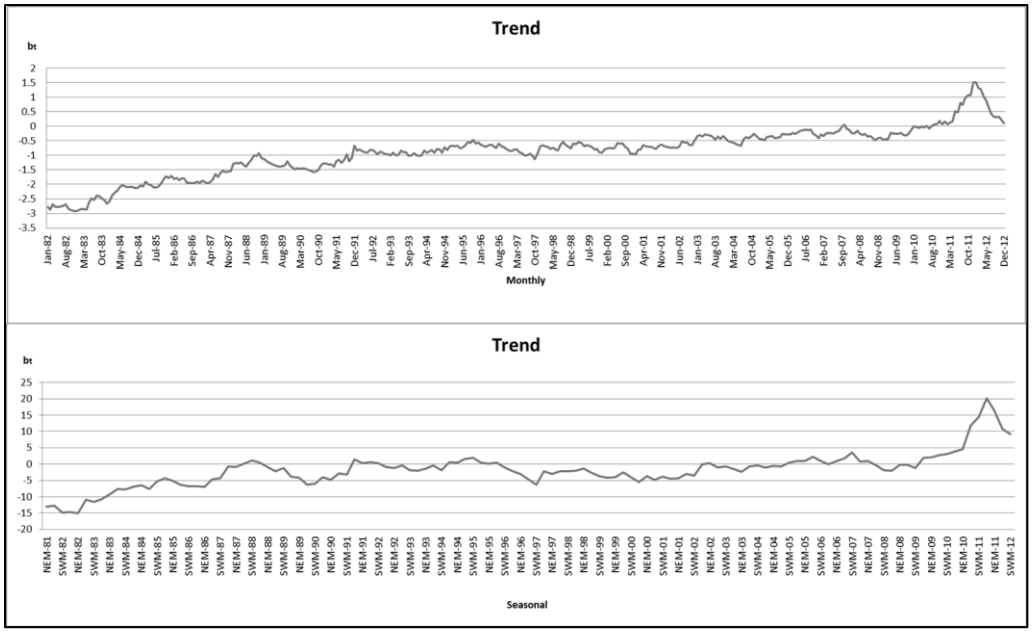

Figure 4.8: Trend plots of monthly and seasonal rainfall at station 44256

There is only one station in the southern region, which is station 44239. From Figure 4.9, there were two turning points in the rainfall trend; monthly rainfall increased from 1975 to 1988 and hit 2 minima point in October 1991 and March 2005, upward trend was shown afterward. On the other hand, seasonal analysis discovered a downward trend from 1975 to SWM 1991 and turned into slightly increasing trend until 2012.

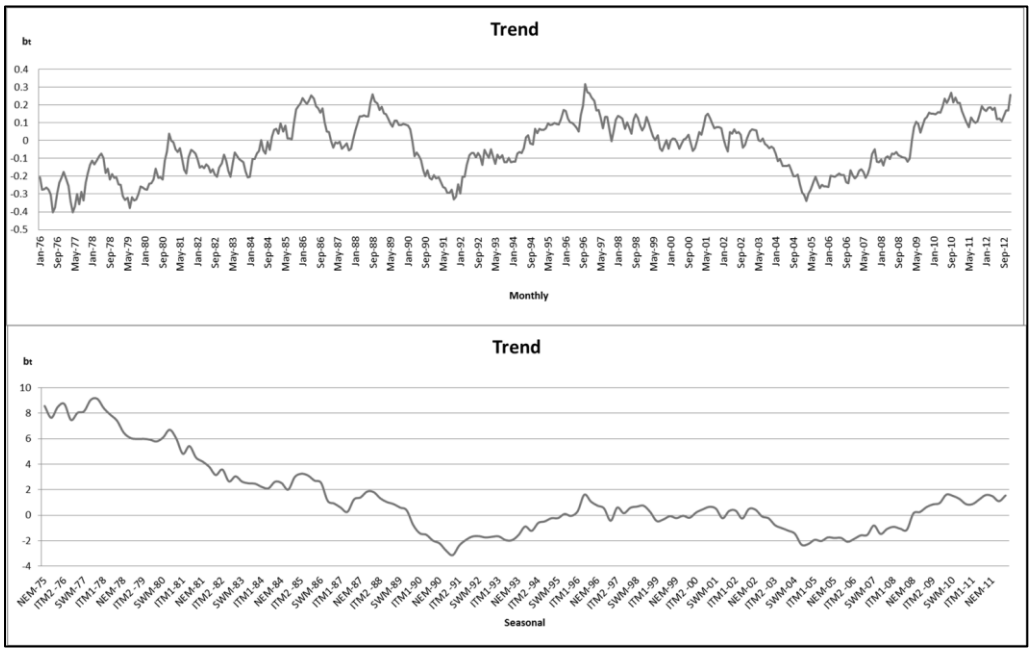

Figure 4.9: Trend plots of monthly and seasonal rainfall at station 44239

Stations 45253 and 45254 situated in the southeastern region. Monthly rainfall at station 45253 exhibited a generally increasing trend during the whole study period (Figure 4.10). Instead of upward trend, result from seasonal analysis showed trend in the opposite direction. Figure 4.11 showed the increasing trend in both monthly and seasonal analysis at station 45254 throughout the study period.

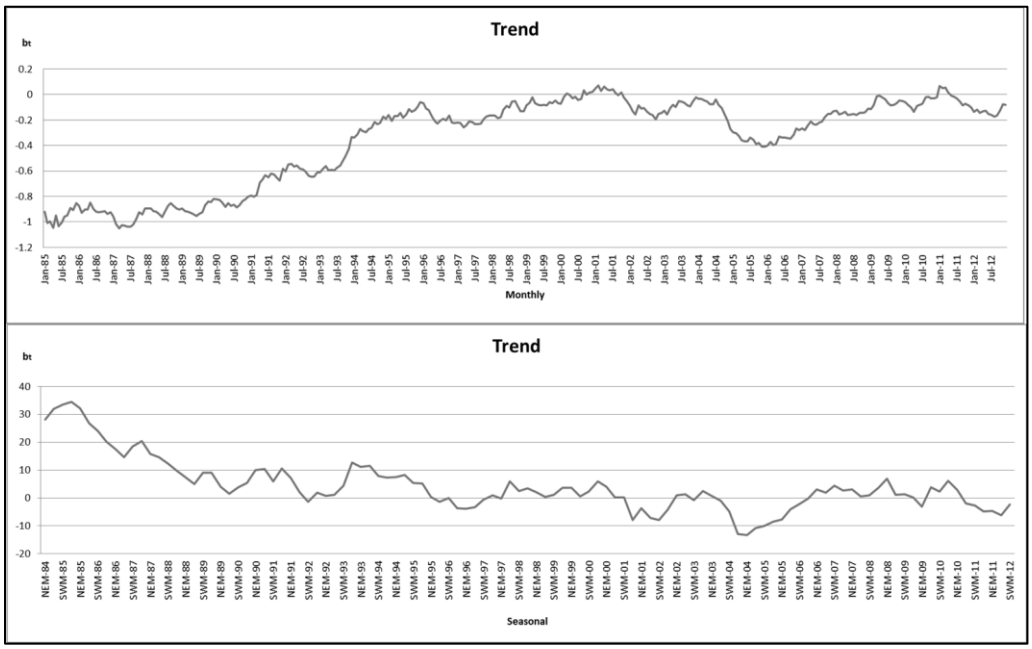

Figure 4.10: Trend plots of monthly and seasonal rainfall at station 45253.

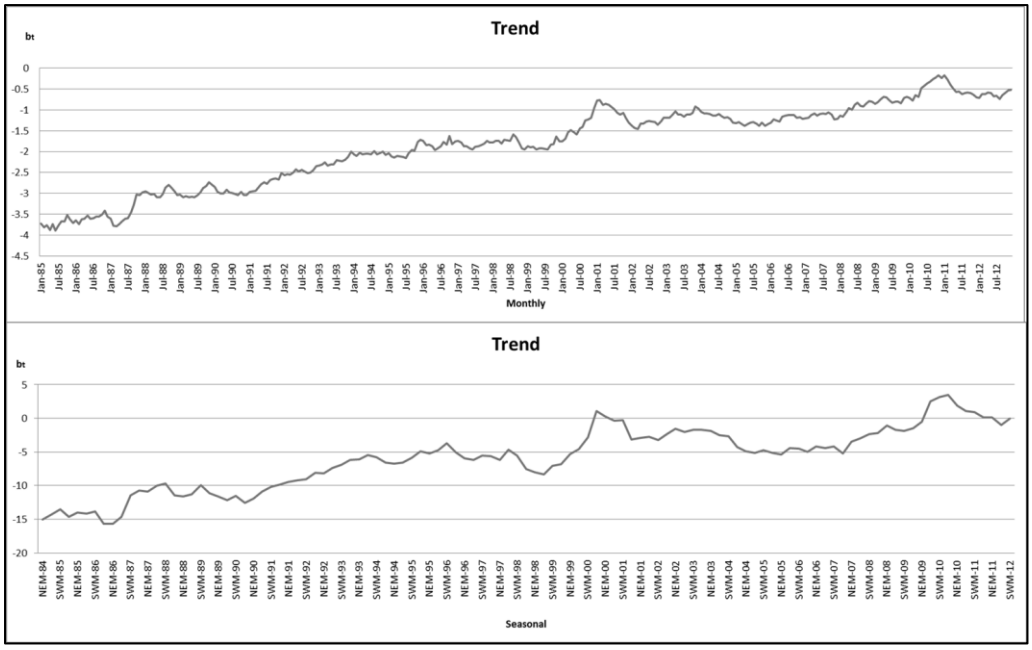

Figure 4.11: Trend plots of monthly and seasonal rainfall at station 45254.

The only representative of eastern region is station 2818110. Similar results were found in monthly and seasonal analysis, as shown in Figure 4.12. Steep decreasing trends were shown during the period of 1972 to 1977 and remained consistent afterward.

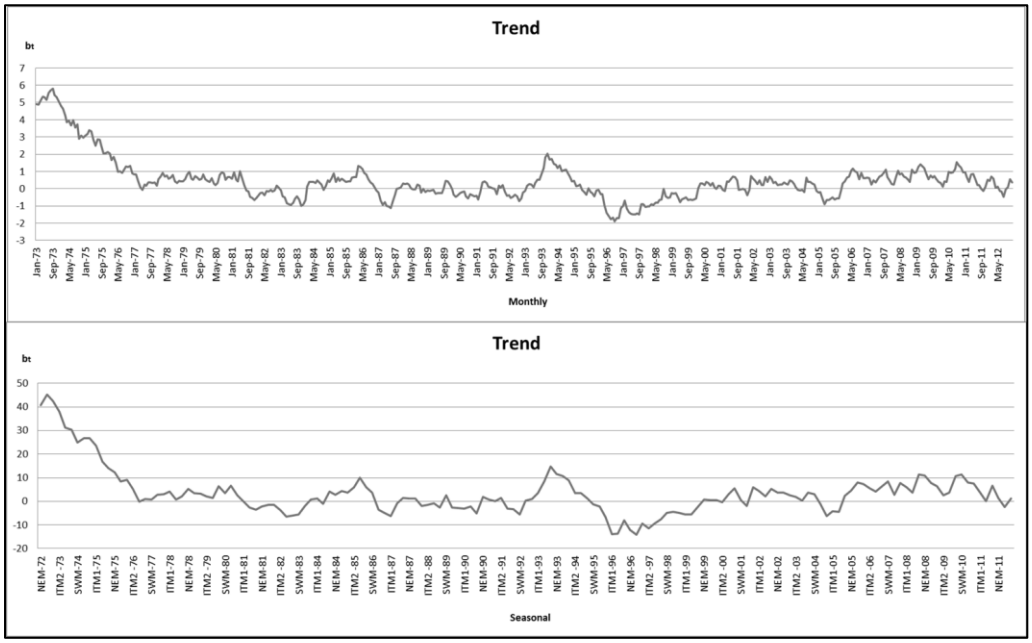

Figure 4.12: Trend plots of monthly and seasonal rainfall at station 2818110

For station 44320 that represented the northeastern region, rainfall pattern in seasonal analysis was similar with the result from monthly analysis but in a "smoother" form (Figure 4.13). Increasing trend was found during the entire study period but it was more obvious in the earlier period, 1984 to 1993.

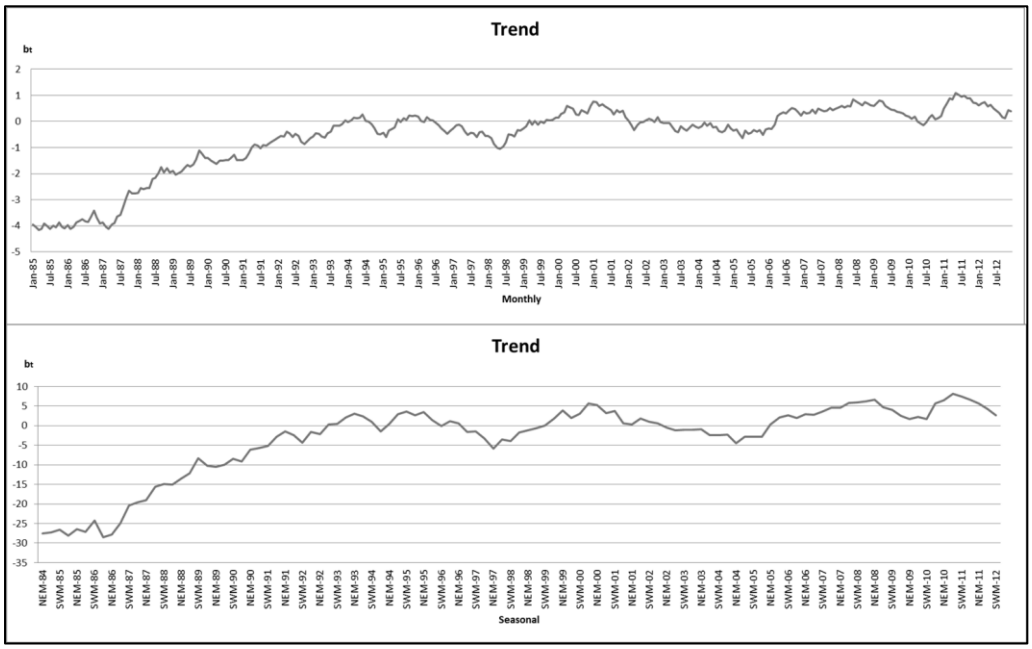

Figure 4.13: Trend plots of monthly and seasonal rainfall at station 44320.

Station 2917001, located in the central part of the study area, was eliminated from seasonal rainfall series analysis due to the inhomogeneity in both annual median and annual maximum rainfall. It was noticed that in Figure 4.14, monthly series analysis showed increasing trend in earlier period (1977 to 1995) and remain consistent in the later period (May 1995 to 2012).

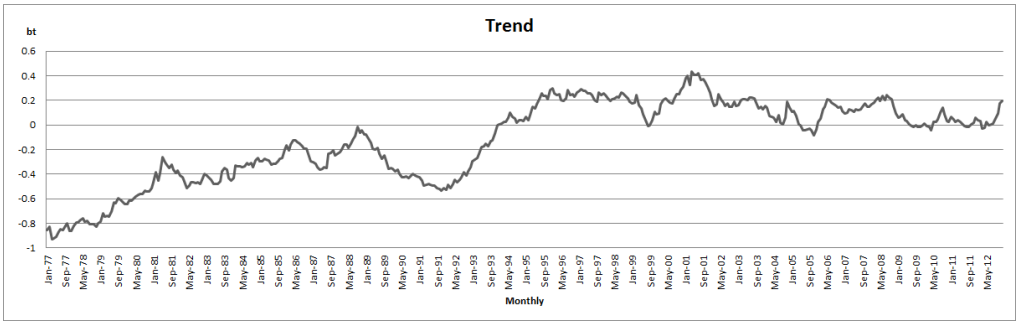

Figure 4.14: Trend plots of monthly rainfall at station 2917001.

4.3 Spatial Variation

Spatial variation of rainfall trend was presented in map. The Langat River Basin was partitioned into eight parts based on the location of the rainfall stations using Thiessen Polygon. Each part was represented by one station. Result from Holt-Winters method was used to develop the map.

4.3.1 Monthly Rainfall Trend Analysis

Figure 4.15 showed the spatial variation of monthly rainfall trend. It was discovered that insignificant increasing trends were shown in the most western, northeastern and the most southeastern parts in January rainfall. For February rainfall, significant increasing trends took place in the northeastern and southeastern parts while insignificant decreasing trends were shown in the middle part of the study area. All except the eastern and southern parts showed increasing trends in March rainfall.

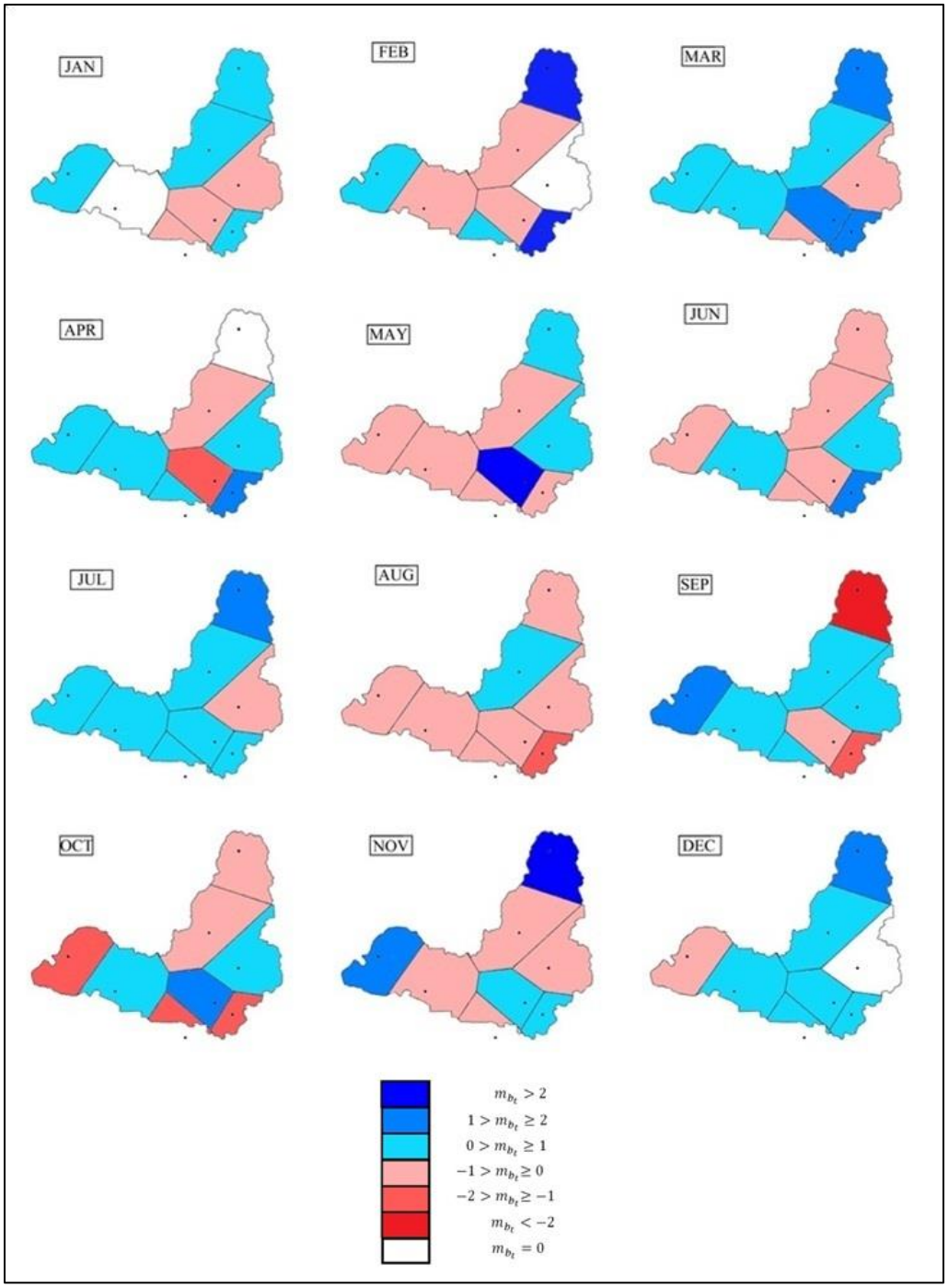

Figure 4.15: Spatial variation maps of monthly rainfall trend analysis

For April analysis, downward trends were only found in two parts and no trend was found in the northeastern part, as shown in Figure 4.15. Out of the divided eight partitions, five showed insignificant decreasing trends in May rainfall. However, significant increasing trend was revealed in one part of

the southeastern region. Refer to Figure 4.15, there were also five parts showed insignificant downward trends from rainfall analysis in June but the three with opposite trends were found in the western and eastern parts.

In July rainfall, all regions showed increasing trends except one part in the western region. In contrast, only one increasing trend was discovered in the western region in August. From spatial variation map of September, upward trends once again took place in most parts of the Langat River Basin. Significant downward trend was shown in the northeastern region.

As shown in Figure 4.15, decreasing trends with gradient from -2 to -1 were found in the western, southern and southeastern regions in October rainfall. Increasing trends were only found in three parts located in the middle of the study area. For November rainfall, significant increasing trend was discovered in the northeastern part. The other upward trends were shown in the western and southeastern region. Six out of eight parts showed increasing trends in December rainfall. Eastern region found no trend while insignificant decreasing trend was revealed in the western region.

Generally, increasing trends were found in most parts of the study area during March, April, July, September and December. Trends in opposite direction were shown in most regions during May, June, August and October. May, June and August are the monsoon months of SWM, which is considered the driest season among the four seasons. The decreasing trends found are similar to the report of IPCC (2014), which showed decreasing trend in total rainfall during SWM. Report of IPCC (2014) also highlighted that total rainfall and frequency of wet days decreased over the peninsular Malaysia

during SWM, but the rainfall intensity had increased significantly. This explained the increasing trend found in July, which is also monsoon month of the SWM. Rainfall was more concentrated in July over the study period. ITM1 and ITM2 are generally wet season in the whole peninsular Malaysia. The increasing trends in March and April showed that the wet period is getting period and the dry season (SWM) is getting drier.

4.3.2 Seasonal Rainfall Trend Analysis

More significant trends were shown in spatial variation map of seasonal rainfall trend analysis. As shown in Figure 4.16, rainfall was getting more concentrated in the middle part of the Langat River Basin during SWM for the study period. No trend was found in the most western region while decreasing trends were shown in other part of the study area. In the paper of Suhaila et al. (2010), it was also found that insignificant decreasing trend was shown in total amount of rainfall at most of the stations in Peninsular Malaysia. In ITM1 rainfall, most stations showed increasing trends. The only significant downward trend was discovered in the southeastern part.

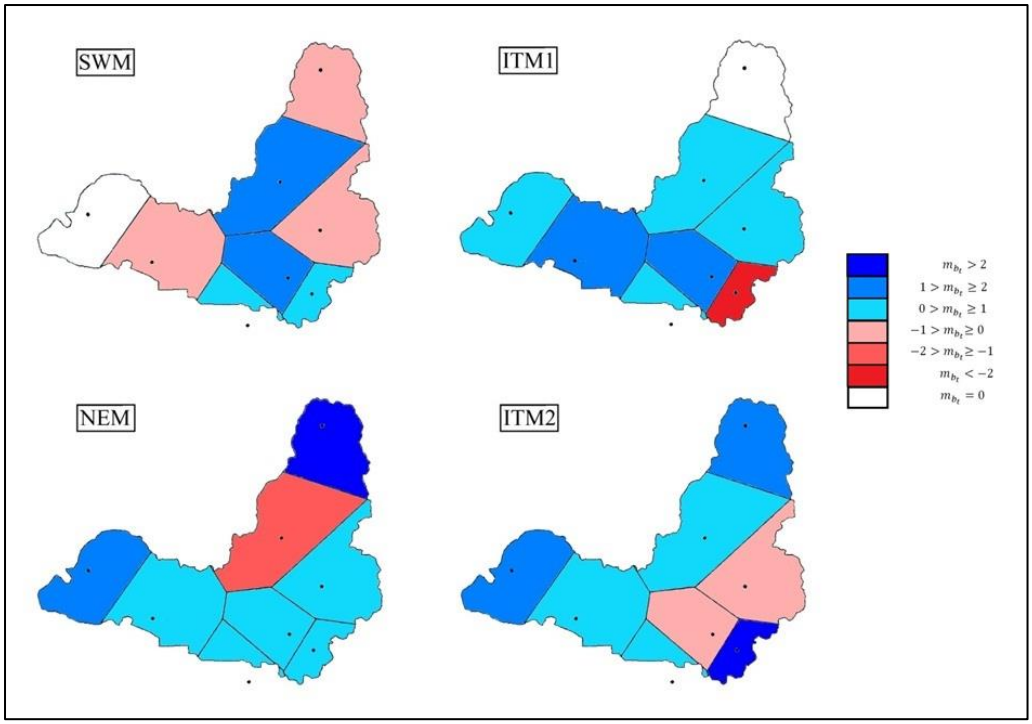

Figure 4.16: Spatial variation maps of seasonal rainfall trend analysis

Similar situation could be seen for NEM rainfall. Rainfall in all parts of the study area trended upward for the study period and significant one was found in the northeastern region, as shown in Figure 4.16. This result was consistent with the result from Suhaila et al. (2010) where increasing trend was found in most of the Peninsular Malaysia during NEM. There is only one part presented decreasing trend during NEM, which is in the eastern region. It was clearly shown in Figure 4.16 that upward trends were found in all area except some in the eastern region during ITM2.

Overall result showed that more increasing trends were discovered in spatial variation map of seasonal rainfall. Most parts in the study area showed increasing trend during ITM1, NEM and ITM2. This result suggested that the Langat River basin might get more rainfall during these few seasons in the future, flood protection should be planned in advance.

4.3.3 Rainfall Series Analysis

The second part of spatial variation map of rainfall series was developed using the result from Additive Holt-Winters method. Gradient of the best fitted line of the trend plot at each station was calculated. No significant trend was found in both monthly and seasonal rainfall series. Insignificant increasing rainfall trends were discovered in all parts except one in the west for monthly rainfall analysis, as shown in Figure 4.17. The only decreasing trend remained in the same direction for seasonal rainfall analysis. In addition, two more parts in the southern and southeastern region showed decreasing trends in seasonal spatial variation map.

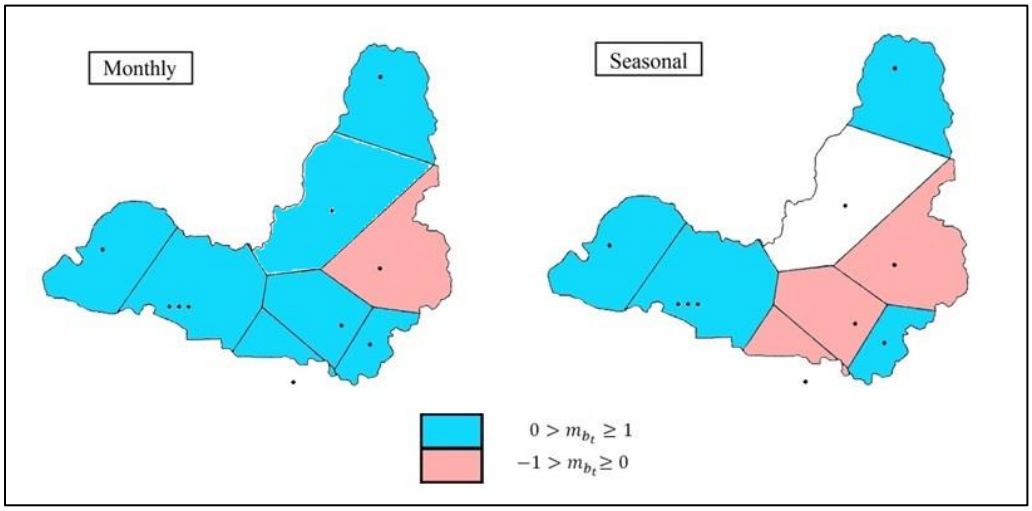

Figure 4.17: Spatial variation map of monthly and seasonal series analysis

CHAPTER 5

CONCLUSION

5.1 Summary

Holt-Winter's method is considered as a new method in rainfall trend analysis. It was widely used in stock forecasting but not in hydrological studies. It can be used on series with no trend, or linear or non-linear trend and non-seasonal series, or series with seasonal variation in additive or multiplicative patterns. On the other hand, the commonly-used non-parametric rank-based tests, Kendall's Tau and Spearman's Rho tests are capable to detect trend without making assumption on data distribution and less influenced by outliers in the data. However, these two tests could only provide a general conclusion of positive trend, negative trend or no trend. Instead of getting a single direction trend, the Holt's method models rainfall series to track the fluctuations during the study period.

Langat River Basin is the selected study area. Data from all rainfall stations in the study area were acquired from DID and MMD. Only 10 rainfall series with more than 25 years and less than 10% missing data were chosen. Missing data were checked and imputed using the IDW interpolation method to develop complete dataset for further analysis.

5.1.1 Rainfall Trend Analysis on Particular Month or Season

Rainfall trend analysis was done using the Holt's method, Kendall's Tau and Spearman's Rho test for rainfall series of specific month or season. Most series were found to be homogeneous. Thus, further investigation was done at all stations. It was assumed that the results are only acceptable if the Holt's, Kendall's Tau and Spearman's Rho tests give consistent results. From monthly rainfall trend analysis, it was discovered that March, July and November are among the months which have most of the stations with positive rainfall trends; while May and September are the months which have the highest number of station showing negative trends. Station 2815001 was the station with the highest number of months with changing rainfall trends throughout the year, which consisted of five months of decreasing trend and 3 months of increasing trend. Four months of upward trend and 2 months of downward trends were found at station 45254. The least number of months with changing trends was shown at station 45255. In seasonal rainfall trend analysis, there are seven stations in NEM showing increasing trend, and this result were consistent with result from monthly rainfall trend analysis for November, December, January and February. Also, it was mentioned in Chapter 3 that NEM was the wettest period for this study area, the increasing trend found in NEM suggested that more rainfall was received during the wettest period.

5.1.2 Rainfall Series Analysis on Monthly or Seasonal Series

Rainfall series analysis was carried out by modeling the rainfall series using the Additive Holt-Winters method. Homogeneity tests were first applied to the annual median and maximum of each rainfall series. Stations 2917001 which failed most of the homogeneity tests were excluded from further study. After modeling the rainfall series, the goodness of fit of each series was checked and it was found that the accuracy of the generated seasonal rainfall series was generally better than generated monthly rainfall series.

Most of the stations exhibited similar result in monthly and seasonal analyses. General increasing trends throughout the study period were shown at stations 2913001, 2815001 and 44256 in the western region except station 44255. Results from station 44255 revealed more fluctuations. From the result of series analysis at the three nearby stations 2815001, 44255 and 44256, it was noticed that the movement of trend depends on the length of the study period.

Different results were discovered in monthly and seasonal analyses at station 44239, which located in the southern region. Fluctuations were shown in the monthly analysis while a generally negative trend was found in the seasonal analysis. In the south-eastern region, both monthly and seasonal analyses at station 45254 and monthly analysis at station 45253 exhibited increasing trend. However, downward trend was found in the seasonal analysis at station 45253. The only station in the eastern region, station 2818110, showed result of downward trend in both monthly and seasonal analyses.

Positive trends in monthly and seasonal analyses were found at station 44320 in the north-eastern region for the whole study period.

5.1.3 Spatial variations of rainfall

As shown in the spatial variation maps developed from monthly rainfall trend analysis, it was found that most parts in the Langat River Basin showed increasing trend during March, April, July, September and December. In May, June, August and October, downward rainfall trends took place in most of the region. On the other hand, more increasing trends were discovered in spatial variation map of seasonal rainfall especially during ITM1, NEM and ITM2. From spatial variation analysis of monthly rainfall series, insignificant increasing rainfall trends were showed in the whole region except one in the west. Besides the only decreasing trend found in monthly rainfall, two more parts in the southern and south-eastern region showed decreasing trends in seasonal spatial variation map.

5.2 Recommendation

In accordance with data available in the study area, the study period used in this research was from 28 years to 43 years, which was considered short for assessment of climate change. Therefore, results from this research could only be treated as a reference and did not provide convincing evidence. Data with longer period should be used in order to get a more comprehensive picture of

rainfall pattern. Also, comparing results by analyzing on rainfall trend with other methods will present a more accurate scenario. Instead of rainfall amount, studies on other indices like rainfall intensity and frequency of wet days were recommended for climate change assessment.

In order to improve the accuracy of rainfall model, other factors like El Nino-Southern Oscillation (ENSO), evaporation rate and others should also be included in modeling rainfall. Understanding rainfall patterns is very important for forecasting future rainfall, which can be used in water resources planning and also flood protection.

LIST OF REFERENCES

Afzal, M., Mansell, M.G. and Gagnon, A. S., 2011. Trends and variability in daily precipitation in Scotland. *Procedia Environmental Sciences*, 6, pp. 15-26.

Basistha, A., Arya, D.S. and Goel, N.K., 2008. Spatial distribution of rainfall in Indian Himalayas – A Case Study of Uttarakhand Region. *Water Resources Management*, 22(10), pp. 1325-1346.

Bayazit, M. and Önöz, B., 2007. To prewhiten or not to prewhiten in trend analysis? *Hydrological Sciences*, 52(4), pp. 611-624.

Burn, D.H. and Elnur, M.A.H., 2002. Detection of hydrologic trends and variability. *Journal of Hydrology,* 255, pp. 107-122.

Caloiero, T. et al., 2011. Trend detection of annual and seasonal rainfall in Calabria (Southern Italy). *International Journal of Climatology*, 31, pp. 44-56.

Cannarozzo , M., Noto, L.V. and Viola, F., 2006. Spatial distribution of rainfall trends in Sicily (1921–2000). *Physics and Chemistry of the Earth*, 31(18), pp. 1201-1211.

Caramelo, L. and Orgaz, M. D. M., 2007. A study of precipitation variability in the Duero Basin (Iberian Peninsula). *International Journal of Climatology*, 27(3), pp. 327-339.

Chang, H. and Kwon, W. T., 2007. Spatial variations of summer precipitation trends in South Korea, 1973–2005. *Environmental Research Letters*, 2(4), pp. 1-9.

Cheung, W.H., Senay, G.B. and Singh,A., 2008. Trends and spatial distribution of annual and seasonal rainfall in Ethiopia. *International Journal of Climatology*, 28(13), pp. 1723-1734.

Del Río, S.D. et al., Spatial distribution of recent rainfall trends in Spain (1961–2006). *International Journal of Climatology*, 31, pp. 656-667.

Deni, S. M. et al., 2009, Trends of wet spells over Peninsular Malaysia during monsoon seasons. *Sains Malaysiana*, 38(2), pp. 133-142.

Deni, S. M. et al., 2010. Spatial trends of dry spells over Peninsular Malaysia during monsoon seasons. *Theoritical and Applied Climatology*, 99(3-4), pp. 357-371.

Department of Statistics, Malaysia, 2011. Population Distribution and Basic Demographic Characteristics 2010. Malaysia: Department of Statistics.

Department of Statistics, Malaysia, 2012. Demographic Indicators 2012, Malaysia. Putrajaya: Department of Statistics.

Du, J. et al., 2012. Assessing the effects of urbanization on annual runoff and flood events using an integrated hydrological modeling system for Qinhuai River basin, China. *Journal of Hydrology*, 464-465, pp. 127-139.

Ganesh, V. S., 2012. Chin: Langat 2 way behind schedule, *News Straits Times* 5 December. Available at http://www.nst.com.my/nation/general/chin-langat-2-way-behind-schedule-1.181365 [Accessed: 13 January 2013].

Ghahraman, B. and Taghvaeian, S., 2008. Investigation of annual rainfall trends in Iran. *Journal of Agricultural Science and Technology*, 10(1), pp. 93-97.

Gonzalez-Hidalgo, J. C., Brunetti, M. and de Luis, M., 2010. Precipitation trends in Spanish hydrological divisions, 1946–2005. *Climate Research,* 43(3), pp. 215-228.

Guhathakurta, P. and Rajeevan, M., 2008. Trends in the rainfall pattern over India. *International Journal of Climatology*, 28, pp. 1453-1469.

Hatzianastassiou, N. et al., 2008. Spatial and temporal variation of precipitation in Greece and surrounding regions based on Global Precipitation Climatology Project Data. *Journal of Climate*, 21(6), pp. 1349-1370.

Holt, C. C., 2004: Forecasting seasonals and trends by exponentially weighted moving averages. *International Journal of Forecasting*, 20, pp. 5-10.

IPCC, 2007: Climate Change 2007: The Physical Science Basis. Contribution of Working Group I to the Fourth Assessment Report of the Intergovernmental Panel on Climate Change. Cambridge University Press, Cambridge, United Kingdom and New York, USA.

IPCC, 2014: Climate Change 2014: Impacts, Adaptation, and Vulnerability. Part B: Regional Aspects. Contribution of Working Group II to the Fifth Assessment Report of the Intergovernmental Panel on Climate Change. Cambridge University Press, Cambridge, United Kingdom and New York, USA.

Jayawardene, H.K.W.I., Sonnadara, D.U.J. and Jayewardene, D. R., 2005: Trends in rainfall in Sri Lanka over the last century. *Sri Lankan Journal of Physics*, 6, pp. 7-17.

Juahir, H. et al., 2010. Hydrological trend analysis due to land use changes at Langat River Basin. *Environmental Asia*, 3, pp. 20-31.

Kamruzzaman, M., Beecham, S. and Metcalfe, A. V., 2011. Non-stationarity in rainfall and temperature in the Murray Darling Basin. *Hydrological Processes*, 25, pp. 1659-1675.

Kang, H.M. and Yusof, F., 2012. Homogeneity tests on daily rainfall series in Peninsular Malaysia. *International Journal of Comtemporary Mathematical Sciences*, 7, pp. 9-22.

Karpozos, D. K., Kavalieratou, S. and Babajimopoulos, C., 2010: Trend analysis of precipitation data in Pieria Region (Greece). *European Water*, 30, pp. 31-40.

Kavvas, M.L., Chen, Z.Q. and Ohara, N., 2006. Study of the Impact of Climate Change on the Hydrologic Regime and Water Resources of Peninsular Malaysia. California: NAHRIM.

Kumar, V. and Jain, S. K., 2011. Trends in rainfall amount and number of rainy days in river basins of India (1951–2004). *Hydrology Research*, 42(4), pp. 290-306.

Lewis, C. D., 1982: *Industrial and Business Forecasting Methods: A Practical Guide to Exponential Smoothing and Curve Fitting.* Butterworth Scientific.

Liu, Q., Yang, Z. and Cui, B., 2008. Spatial and temporal variability of annual precipitation during 1961–2006 in Yellow River Basin, China. *Journal of Hydrology*, 361(3-4), pp. 330-338.

Liu, Y., Xu, Y. and Shi, Y., 2012. Hydrological effects of urbanization in the Qinhuai River Basin, China. *Procedia Engineering*, 28, pp. 767-771.

Mahmood, M., 2012. Minister: Talk about water tariff later, *News Straits Times* 13 July. Available at http://www.nst.com.my/minister-talk-about-water-tariff-later-1.106804/facebook-comments-7.152175 [Accessed: 13 January 2013].

Obot, N. I. et al., 2010. Evaluation of rainfall trends in Nigeria for 30 years (1978-2007). *International Journal of the Physical Sciences*, 5(14), pp. 2217-2222.

Onyenechere, E.C., 2010. Climate change and spatial planning concerns in Nigeria: Remedial measures for more effective response. *Journal of Human Ecology*, 32(3), pp. 137-148.

Pfister, L. et al., 2004. Hydrological impacts of climate change at catchment scale: A case study in the Grand-Duchy of Luxembourg. *Geologica Acta*, 2(2), pp. 135-145.

Ratnayake, U and Herath,S. , 2005. Changing rainfall and its impact on landslides in Sri Lanka. *Journal of Mountain Science*, 2(3), pp. 218-224.

Sahin, S. and Cigizoglu, H.K., 2010. Homogeneity analysis of Turkish meteorological data set. *Hydrological Processes*, 24(8), pp. 981-992.

Seleshi, Y. and Zanke, U., 2004. Recent changes in rainfall and rainy days in Ethiopia. *International Journal of Climatology*, 24(8), pp. 973-983.

Soltani, S., Saboohi, R. and Yaghmaei, L., 2012. Rainfall and rainy days trend in Iran. *Climatic Change*, 110(1), pp. 187-213.

Suhaila, J. et al., 2010. Trends in Peninsular Malaysia rainfall data during the Southwest Monsoon and Northeast Monsoon Seasons: 1975–2004. *Sains Malaysiana*, 39(4), pp. 533-542.

Takahashi, H.G., 2011. Long-term changes in rainfall and tropical cyclone activity over South and Southeast Asia. *Advances in Geosciences*, 30, pp, 17-22.

Tangang, F.T. and Juneng, L., 2004. Mechanisms of Malaysian rainfall anomalies, Journal of Climate, 17(18), pp. 3616-3622.

Taschetto, A. S. and England, M. H., 2009. An analysis of late twentieth century trends in Australian rainfall. *International Journal of Climatology*, 29(6), pp. 791-807.

The Star, 2010. Selangor, KL and Putrajaya face risk of water shortage by 2014, 22 July. Available at http://www.thestar.com.my/story.aspx/?sec=nation&file=%2f2010%2f7%2f22%2fnation%2f6710750 [Accessed: 13 January 2013].

Wang, B.and Ding, Q., 2006. Changes in global monsoon precipitation over the past 56 years. *Geophysical Research Letters*, 33, pp. L06711.

Webster,P. J. et al., 2005. Changes in tropical cyclone number, duration, and intensity in a warming environment. *Science,* 309, pp. 1844-1846.

Wijingaard J.B., Klein Tank, A.M.G. and Können, G.P., 2003. Homogeneity of 20th century European daily temperature and precipitation series. *International Journal of Climatology*, 23, pp. 679-692.

Winters, P. R., 1960: Forecasting sales by exponentially weighted moving averages. *Management Science*, 6, pp. 324-342.

Wong,C. L. et al., 2009. Variability of rainfall in Peninsular Malaysia. *Hydrology and Earth System Sciences Discussions*, 6(4), pp. 5497-5503.

Yue, S. and Pilon, P., 2004, A comparison of the power of the *t* test, Mann-kendall and bootstrap tests for trend detection. *Hydrological Sciences*, 49(1), pp. 21-37.

APPENDIX A

Sample Calculation of Homogeneity Tests

(Monthly Median Series at Station 44255)

(i) Standard Normal Homogeneity Test

$$T_k = k\overline{z_1^2} + (n-k)\overline{z_2^2}, k = 1,2,\dots,n$$

where

$$\overline{z_1} = \frac{1}{k}\sum_{i=1}^{k}\frac{(Y_i - \bar{Y})}{s} \text{ and } \overline{z_2} = \frac{1}{n-k}\sum_{i=k+1}^{n}\frac{(Y_i - \bar{Y})}{s}$$

$$T_0 = \max_{1\le k\le n} T_k$$

45254			Standard normal homogeneity test					
k	Year	Median	$\frac{(Y_i-\bar{Y})}{s}$	$\sum_{i=1}^{k}\frac{(Y_i-\bar{Y})}{s}$	$\overline{z_1^2}$	$\sum_{i=k+1}^{n}\frac{(Y_i-\bar{Y})}{s}$	$\overline{z_2^2}$	T_k
1	1984	206.95	0.8996	0.899598	0.8093	-0.8996	0.001	0.84
2	1985	172.8	0.09628	0.99588	0.2479	-0.99588	0.0014	0.53
3	1986	178.1	0.22096	1.216836	0.1645	-1.21684	0.0022	0.55
4	1987	179.75	0.25977	1.476604	0.1363	-1.4766	0.0035	0.63
5	1988	195.35	0.62673	2.103334	0.177	-2.10333	0.0077	1.07
6	1989	156.85	-0.2789	1.824422	0.0925	-1.82442	0.0063	0.7
7	1990	102.35	-1.5609	0.2635	0.0014	-0.2635	0.0001	0.01
8	1991	182.7	0.32916	0.592661	0.0055	-0.59266	0.0008	0.06
9	1992	162.9	-0.1366	0.456065	0.0026	-0.45606	0.0005	0.03
10	1993	217.2	1.14071	1.596775	0.0255	-1.59677	0.0071	0.39
11	1994	163.35	-0.126	1.470764	0.0179	-1.47076	0.0067	0.32
12	1995	175.5	0.1598	1.630559	0.0185	-1.63056	0.0092	0.38
13	1996	164.8	-0.0919	1.538657	0.014	-1.53866	0.0092	0.33
14	1997	152.9	-0.3718	1.166829	0.0069	-1.16683	0.0061	0.19
15	1998	100	-1.6162	-0.44937	0.0009	0.449373	0.001	0.03
16	1999	109.55	-1.3916	-1.84093	0.0132	1.840929	0.0201	0.47
17	2000	251.4	1.9452	0.104272	4E-05	-0.10427	8E-05	0
18	2001	184.35	0.36797	0.472247	0.0007	-0.47225	0.0018	0.03
19	2002	149.55	-0.4506	0.021617	1E-06	-0.02162	5E-06	0
20	2003	203.1	0.80903	0.830651	0.0017	-0.83065	0.0085	0.11
21	2004	120.1	-1.1434	-0.31274	0.0002	0.312736	0.0015	0.02
22	2005	106.25	-1.4692	-1.78192	0.0066	1.781918	0.0648	0.6

23	2006	123.2	-1.0705	-2.85238	0.0154	2.852383	0.226	1.71
24	2007	118.1	-1.1904	-4.04282	0.0284	4.042816	0.6538	3.95
25	2008	190.25	0.50676	-3.53605	0.02	3.536055	0.7815	3.63
26	2009	170.6	0.04453	-3.49152	0.018	3.491523	1.3545	4.53
27	2010	270.4	2.39214	-1.09938	0.0017	1.099382	0.3022	0.65
28	2011	168.75	0.00101	-1.09837	0.0015	1.098368	1.2064	1.25
29	2012	215.4	1.09837	4.88E-15	3E-32			
							T_0 =	4.53

(ii) The Buishand Range Test

$$S_0^* = 0 \text{ and } S_k^* = \sum_{i=1}^{k} (Y_i - \bar{Y}), k = 1,2, \dots, n$$

$$R = \frac{\left(\max_{0 \le k \le n} S_k^* - \min_{0 \le k \le n} S_k^* \right)}{s}$$

	45254		Buishand Range	
k	Year	Median	$(Y_i - \bar{Y})$	S_k^*
0		-		0
1	1984	206.95	38.2431	38.2431034
2	1985	172.8	4.093103	42.3362069
3	1986	178.1	9.393103	51.7293103
4	1987	179.75	11.0431	62.7724138
5	1988	195.35	26.6431	89.4155172
6	1989	156.85	-11.8569	77.5586207
7	1990	102.35	-66.3569	11.2017241
8	1991	182.7	13.9931	25.1948276
9	1992	162.9	-5.8069	19.387931
10	1993	217.2	48.4931	67.8810345
11	1994	163.35	-5.3569	62.5241379
12	1995	175.5	6.793103	69.3172414
13	1996	164.8	-3.9069	65.4103448
14	1997	152.9	-15.8069	49.6034483
15	1998	100	-68.7069	-19.103448
16	1999	109.55	-59.1569	-78.260345
17	2000	251.4	82.6931	4.43275862
18	2001	184.35	15.6431	20.0758621
19	2002	149.55	-19.1569	0.91896552
20	2003	203.1	34.3931	35.312069
21	2004	120.1	-48.6069	-13.294828
22	2005	106.25	-62.4569	-75.751724
23	2006	123.2	-45.5069	-121.25862
24	2007	118.1	-50.6069	-171.86552
25	2008	190.25	21.5431	-150.32241
26	2009	170.6	1.893103	-148.42931
27	2010	270.4	101.6931	-46.736207
28	2011	168.75	0.043103	-46.693103
29	2012	215.4	46.6931	1.9895E-13
			max	89.4155172

min	-171.86552
R	6.14614997
R/√n	1.1413114

(iii) The Pettitt Test

$$X_k = 2\sum_{i=1}^{k} r_i - k(n+1)\ , k = 1,2, \dots, n$$

$$X_E = \max_{1 \le k \le n} |X_k|$$

45254			Pettitt test				
k	Year	Median	r_i	$\sum_{i=1}^{k} r_i$	$2\sum_{i=1}^{k} r_i$	X_k	$\lvert X_k \rvert$
1	1984	206.95	5	5	10	-20	20
2	1985	172.8	14	19	38	-22	22
3	1986	178.1	12	31	62	-28	28
4	1987	179.75	11	42	84	-36	36
5	1988	195.35	7	49	98	-52	52
6	1989	156.85	20	69	138	-42	42
7	1990	102.35	28	97	194	-16	16
8	1991	182.7	10	107	214	-26	26
9	1992	162.9	19	126	252	-18	18
10	1993	217.2	3	129	258	-42	42
11	1994	163.35	18	147	294	-36	36
12	1995	175.5	13	160	320	-40	40
13	1996	164.8	17	177	354	-36	36
14	1997	152.9	21	198	396	-24	24
15	1998	100	29	227	454	4	4
16	1999	109.55	26	253	506	26	26
17	2000	251.4	2	255	510	0	0
18	2001	184.35	9	264	528	-12	12
19	2002	149.55	22	286	572	2	2
20	2003	203.1	6	292	584	-16	16
21	2004	120.1	24	316	632	2	2
22	2005	106.25	27	343	686	26	26
23	2006	123.2	23	366	732	42	42
24	2007	118.1	25	391	782	62	62
25	2008	190.25	8	399	798	48	48
26	2009	170.6	15	414	828	48	48
27	2010	270.4	1	415	830	20	20
28	2011	168.75	16	431	862	22	22
29	2012	215.4	4	435	870	0	0
						max	62

(iv) The Von Neumann Ratio Test

$$N = \frac{\sum_{i=1}^{n-1}(Y_i - Y_{i+1})^2}{\sum_{i=1}^{n}(Y_i - \bar{Y})^2}$$

	45254		Von Neumann Ratio Test	
k	Year	Median	$(Y_i - Y_{i+1})^2$	$(Y_i - \bar{Y})^2$
1	1984	206.95	1166.2225	1462.53496
2	1985	172.8	28.09	16.7534958
3	1986	178.1	2.7225	88.2303924
4	1987	179.75	243.36	121.950134
5	1988	195.35	1482.25	709.854961
6	1989	156.85	2970.25	140.585996
7	1990	102.35	6456.1225	4403.23772
8	1991	182.7	392.04	195.806944
9	1992	162.9	2948.49	33.7200476
10	1993	217.2	2899.8225	2351.58108
11	1994	163.35	147.6225	28.6963407
12	1995	175.5	114.49	46.1462545
13	1996	164.8	141.61	15.2638407
14	1997	152.9	2798.41	249.857979
15	1998	100	91.2025	4720.63763
16	1999	109.55	20121.4225	3499.53841
17	2000	251.4	4495.7025	6838.14936
18	2001	184.35	1211.04	244.706685
19	2002	149.55	2867.6025	366.986685
20	2003	203.1	6889	1182.88556
21	2004	120.1	191.8225	2362.63039
22	2005	106.25	287.3025	3900.86393
23	2006	123.2	26.01	2070.87763
24	2007	118.1	5205.6225	2561.05798
25	2008	190.25	386.1225	464.105306
26	2009	170.6	9960.04	3.58384067
27	2010	270.4	10332.7225	10341.4873
28	2011	168.75	2176.2225	0.00185791
29	2012	215.4		2180.24591
		sum	86033.3375	50601.9786
			N	1.7001971

APPENDIX B

Trend plot of each month at each station

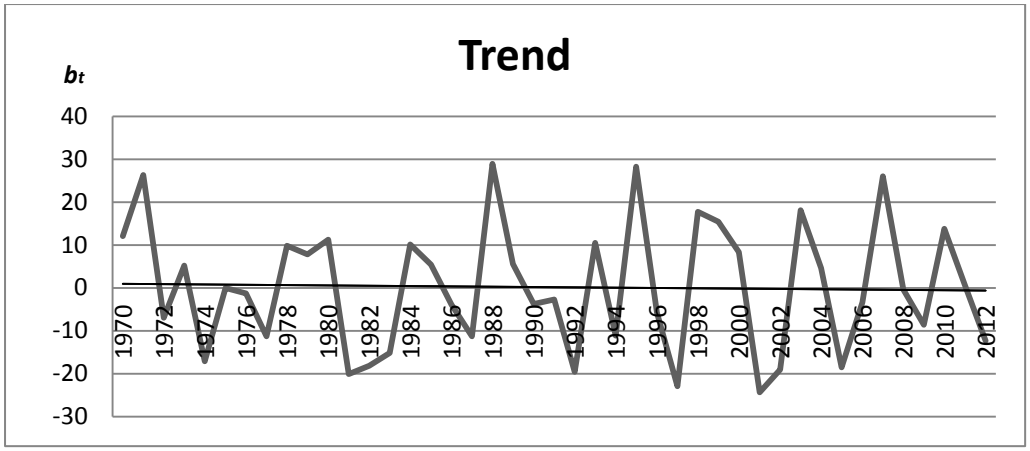

Trend plot of January series using Holt's method at station 2815001.

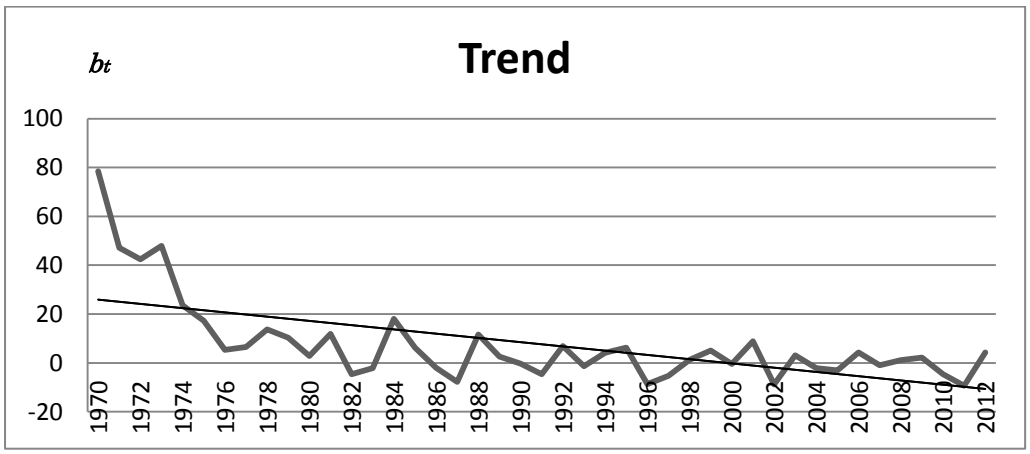

Trend plot of February series using Holt's method at station 2815001.

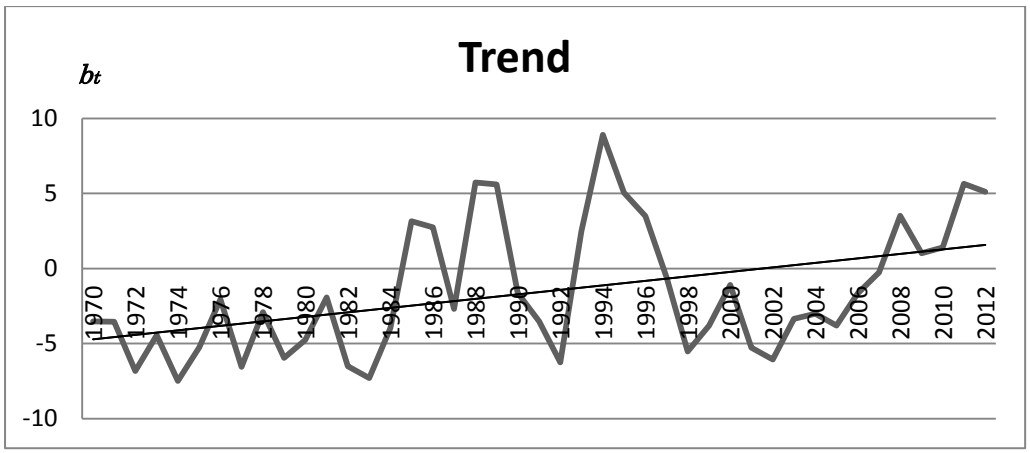

Trend plot of March series using Holt's method at station 2815001.

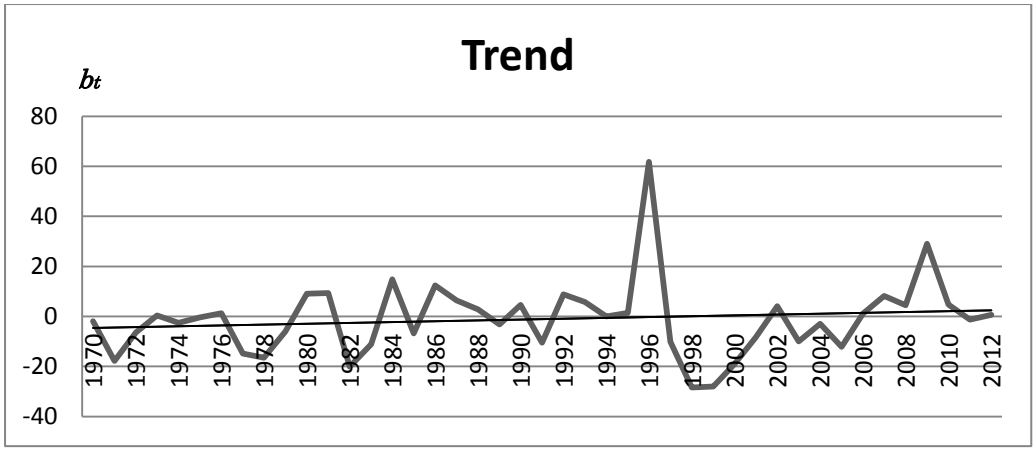

Trend plot of April series using Holt's method at station 2815001.

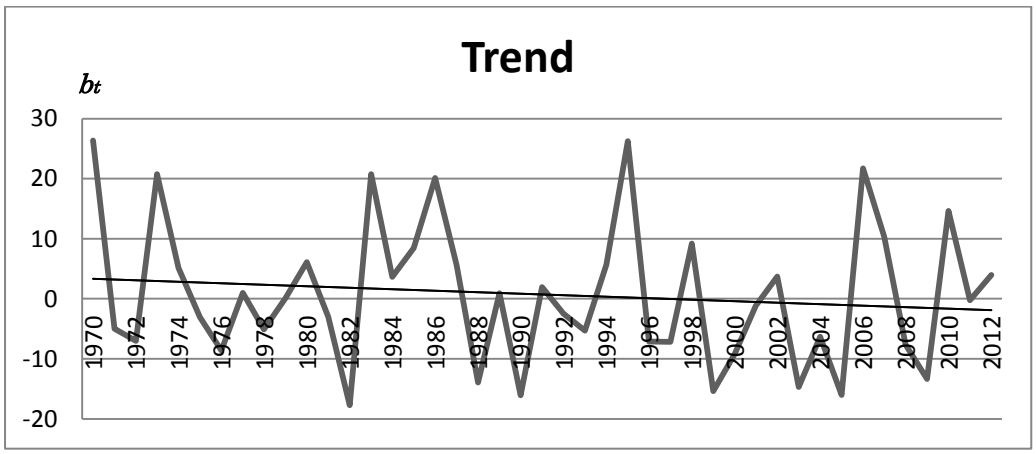

Trend plot of May series using Holt's method at station 2815001.

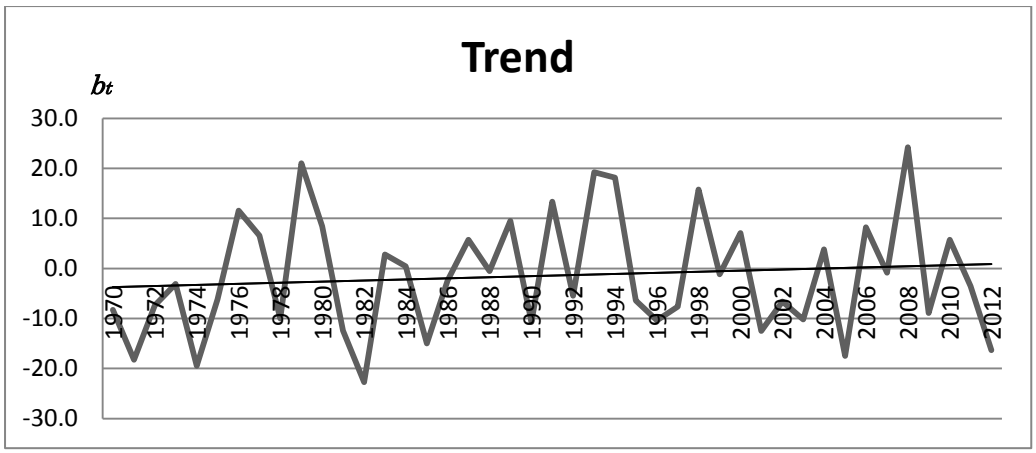

Trend plot of June series using Holt's method at station 2815001.

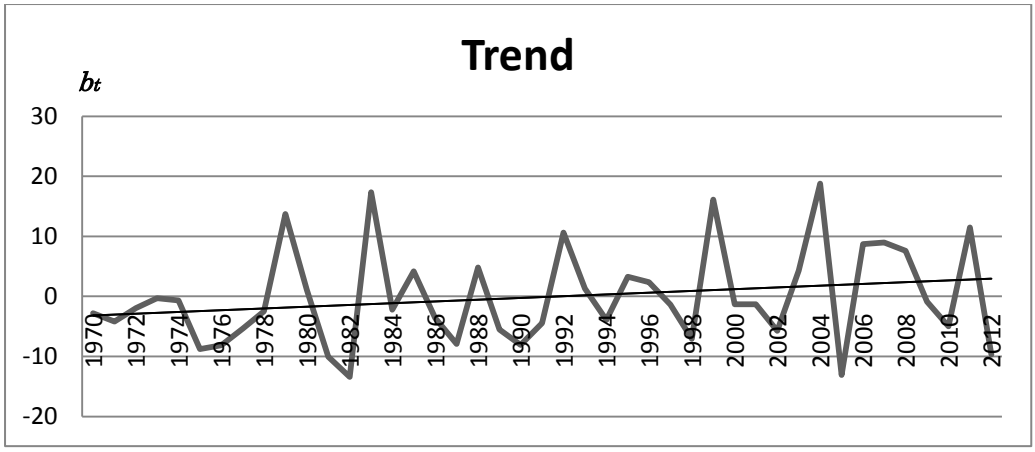

Trend plot of July series using Holt's method at station 2815001.

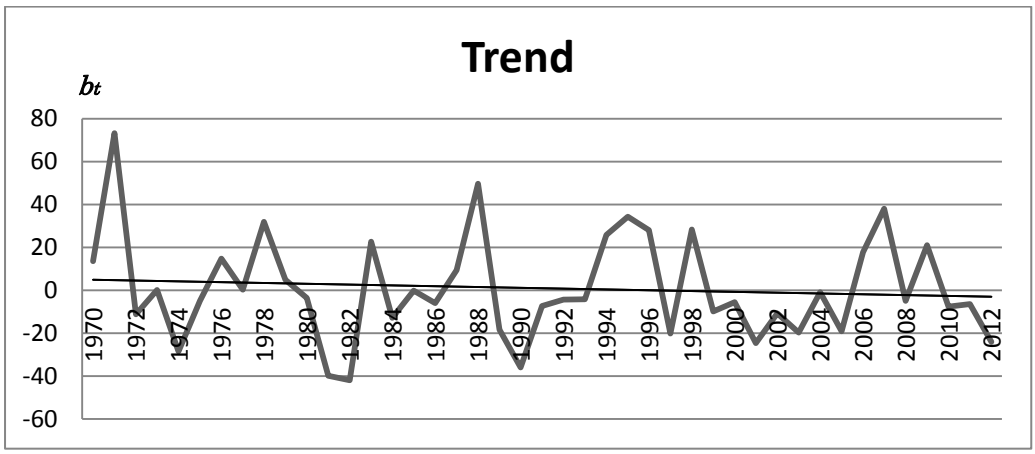

Trend plot of August series using Holt's method at station 2815001.

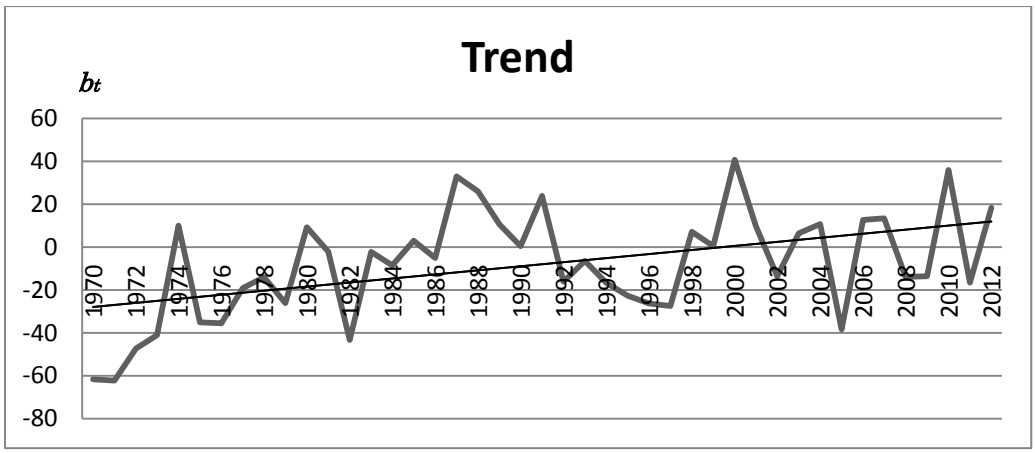

Trend plot of September series using Holt's method at station 2815001.

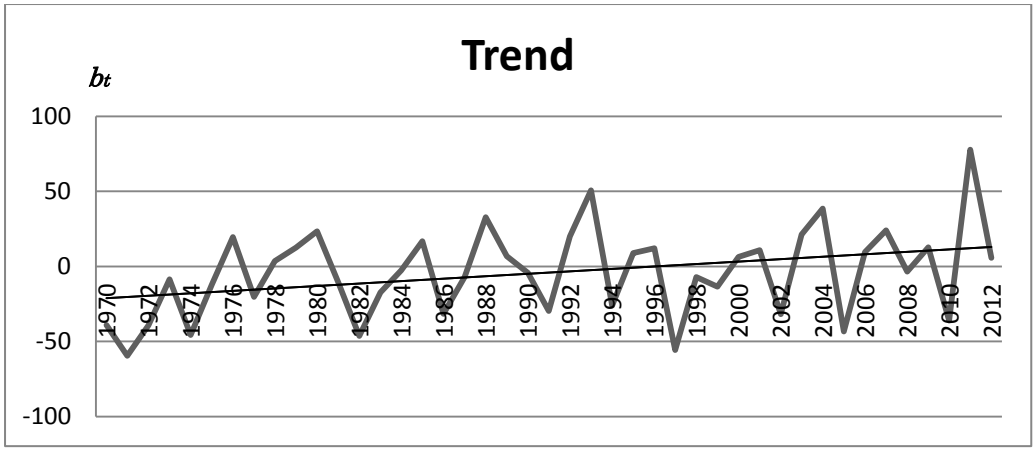

Trend plot of October series using Holt's method at station 2815001.

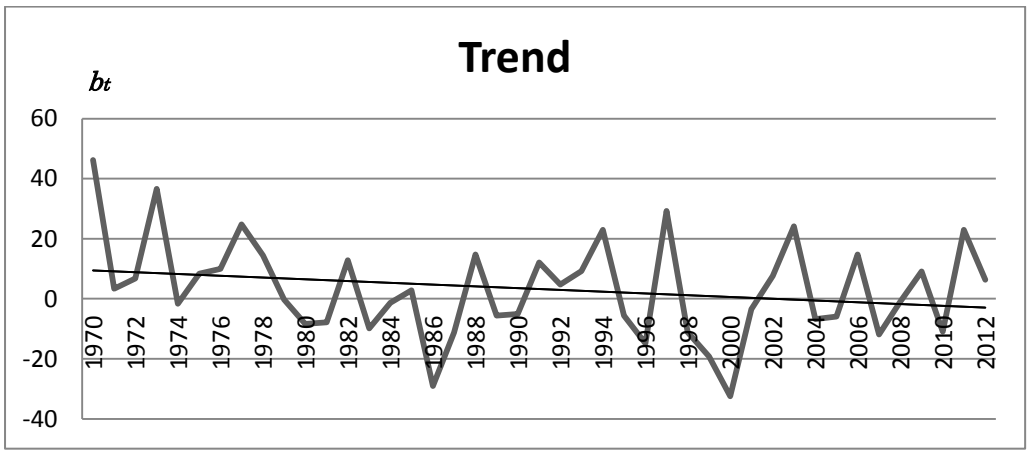

Trend plot of November series using Holt's method at station 2815001.

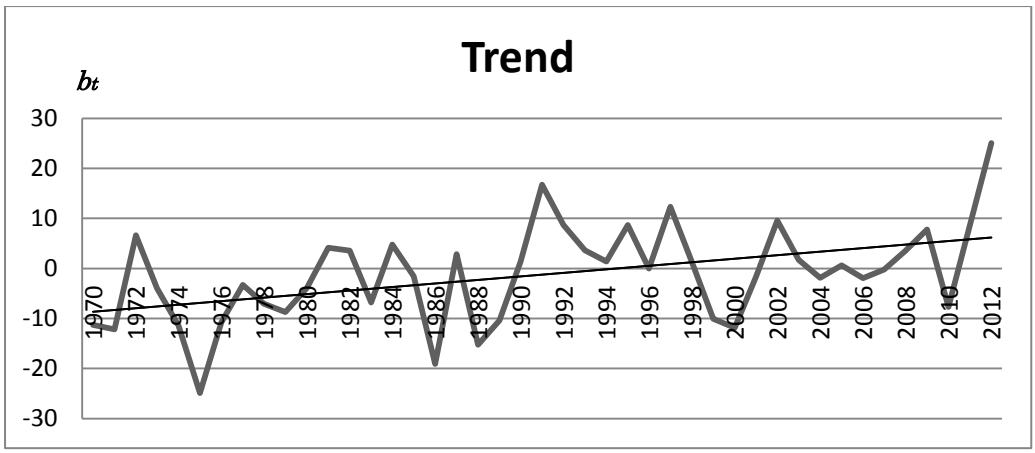

Trend plot of December series using Holt's method at station 2815001.

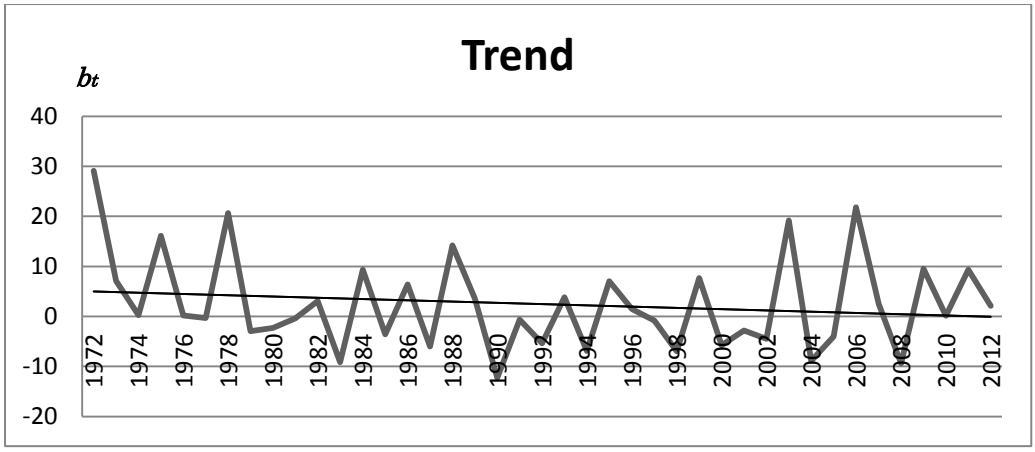

Trend plot of January series using Holt's method at station 2818110.

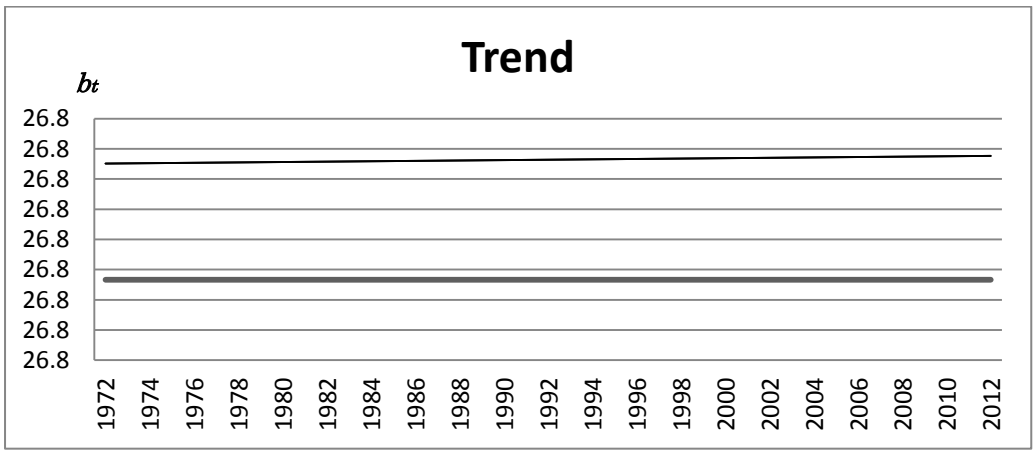

Trend plot of February series using Holt's method at station 2818110.

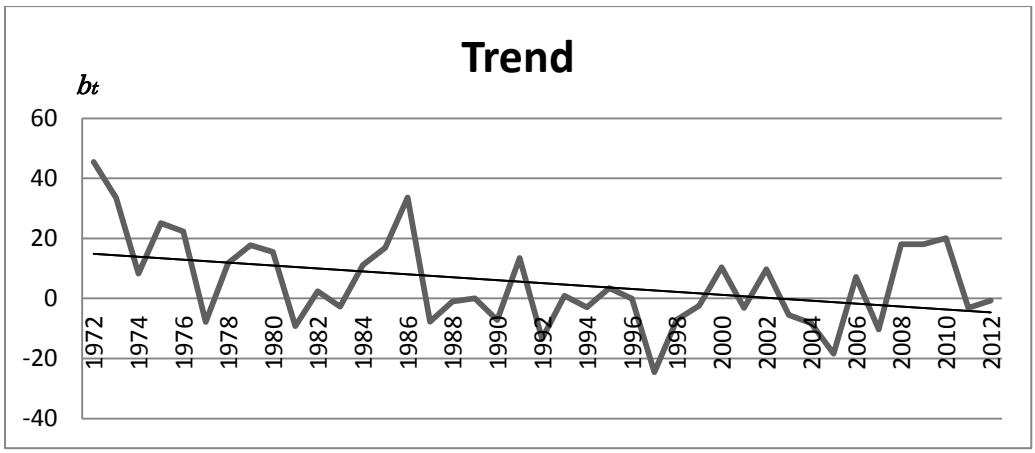

Trend plot of March series using Holt's method at station 2818110.

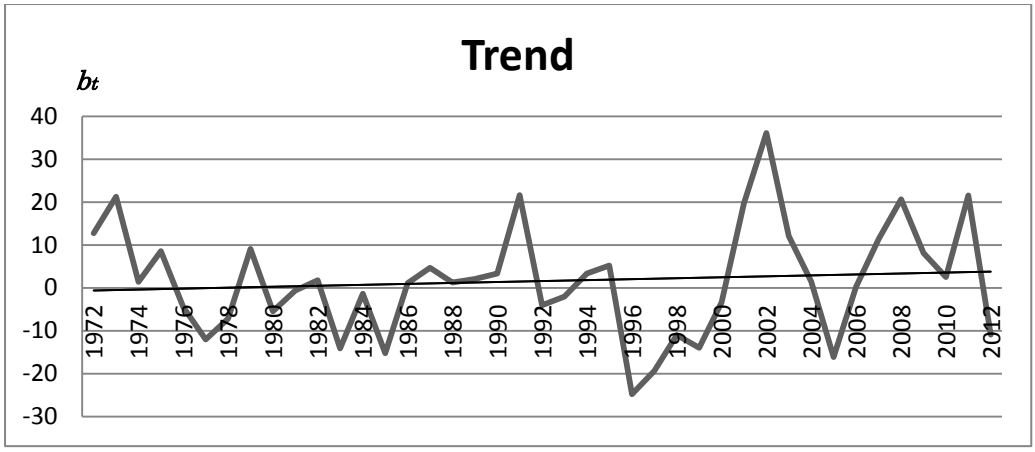

Trend plot of April series using Holt's method at station 2818110.

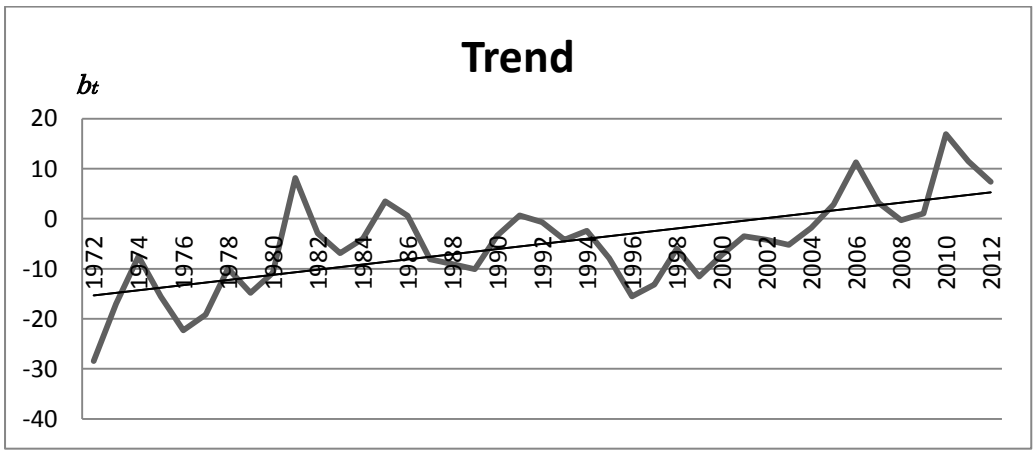

Trend plot of May series using Holt's method at station 2818110.

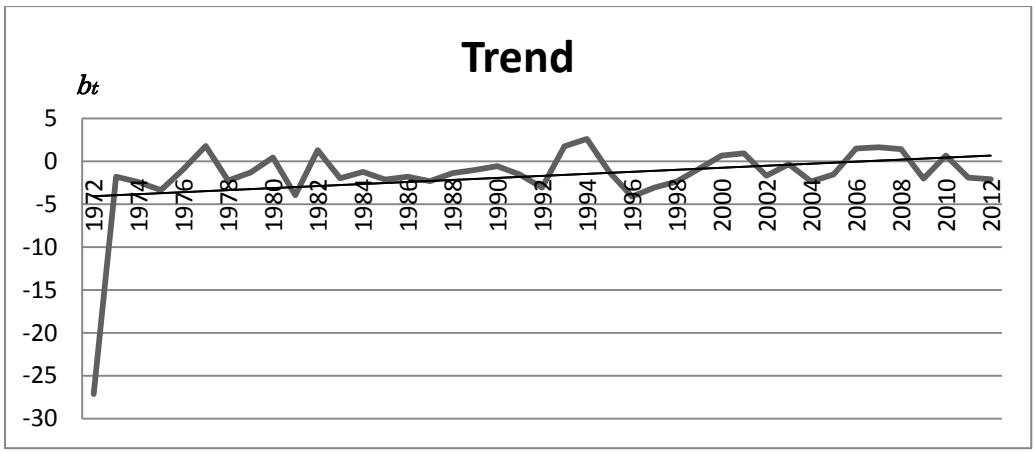

Trend plot of June series using Holt's method at station 2818110.

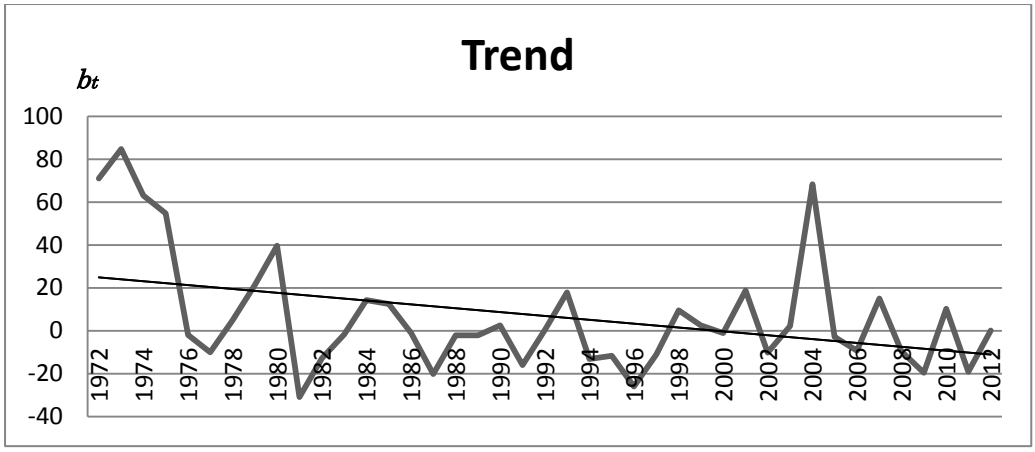

Trend plot of July series using Holt's method at station 2818110.

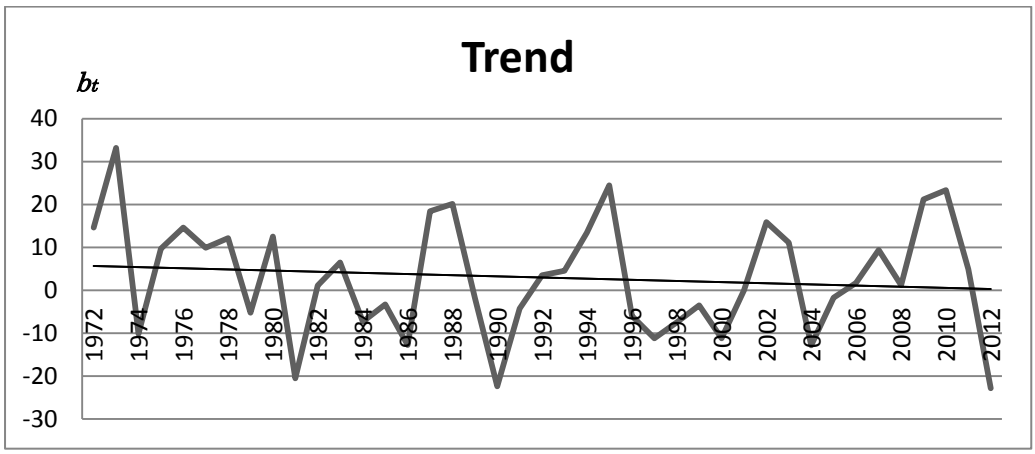

Trend plot of August series using Holt's method at station 2818110.

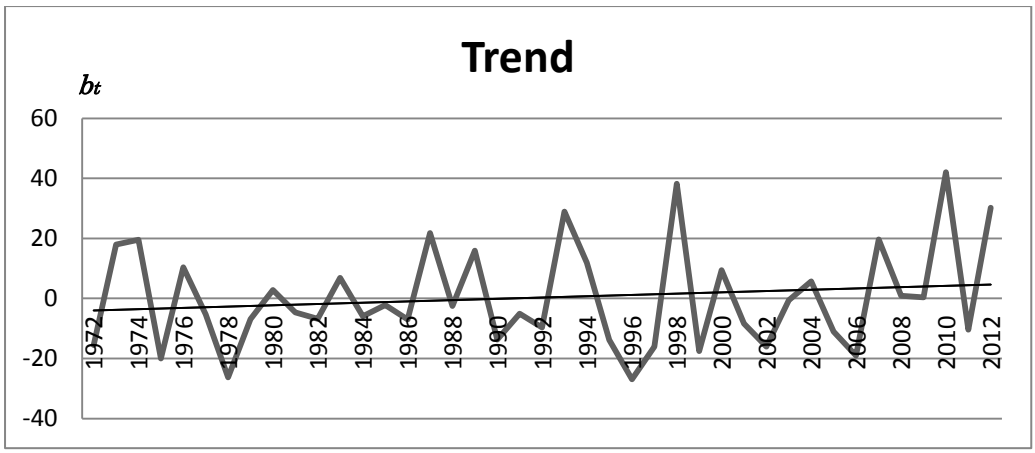

Trend plot of September series using Holt's method at station 2818110.

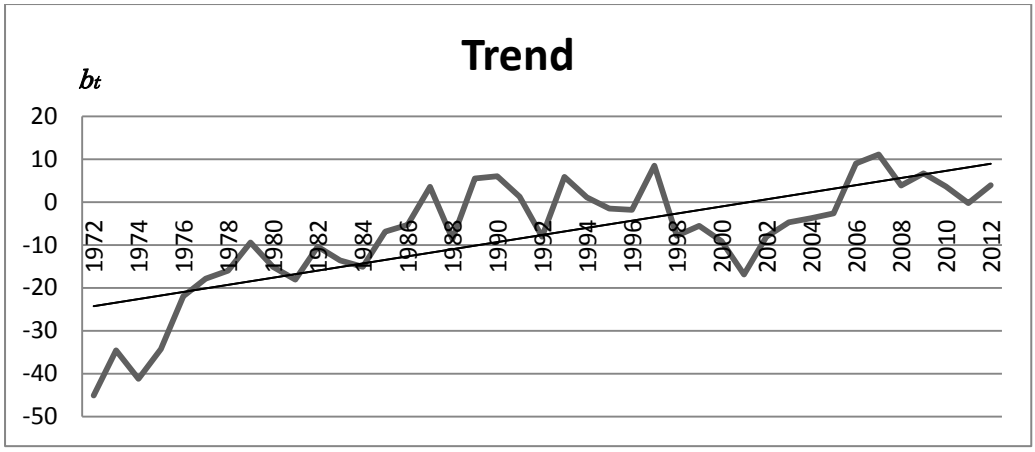

Trend plot of October series using Holt's method at station 2818110.

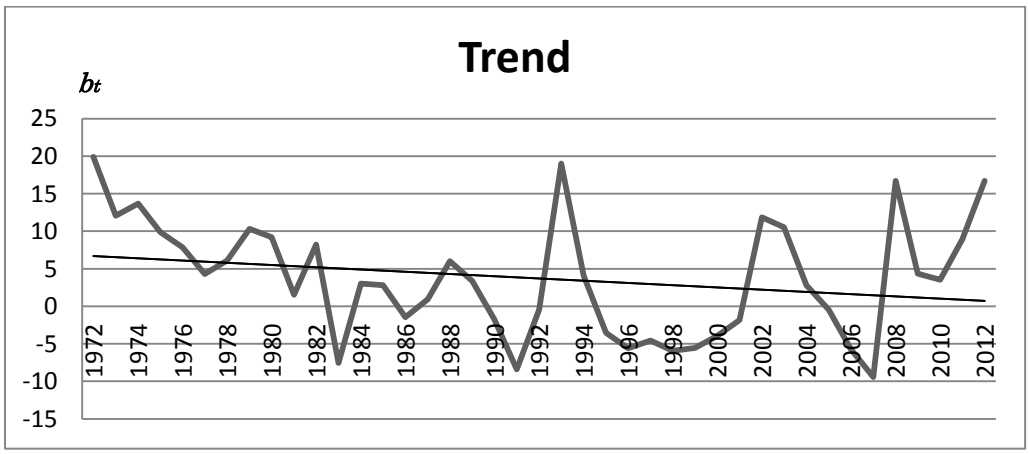

Trend plot of November series using Holt's method at station 2818110.

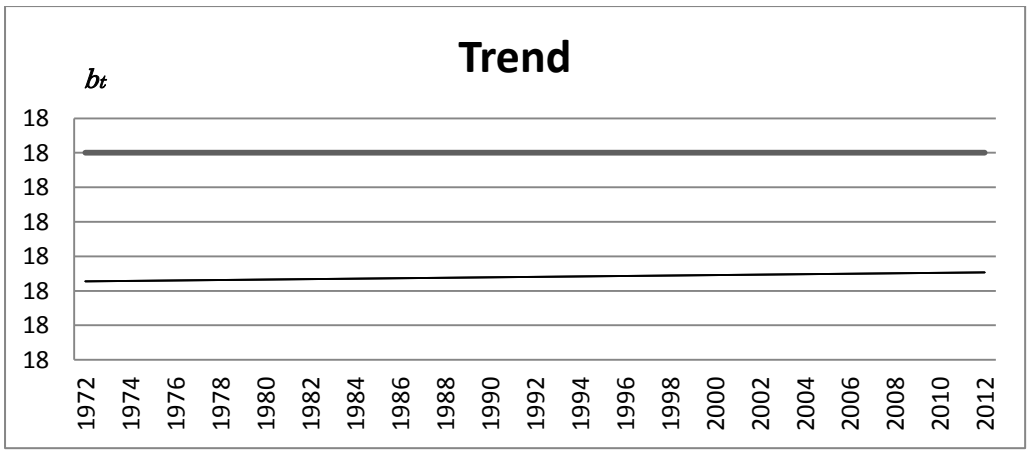

Trend plot of December series using Holt's method at station 2818110.

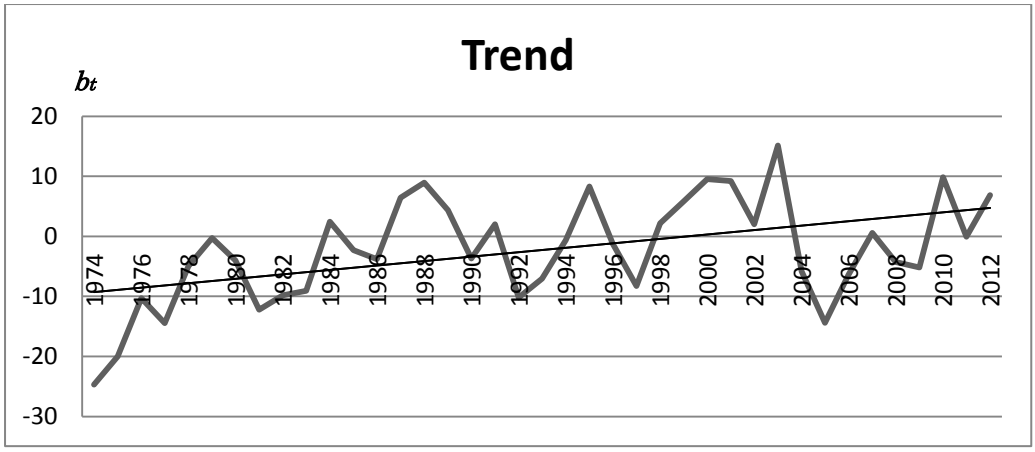

Trend plot of January series using Holt's method at station 2913001.

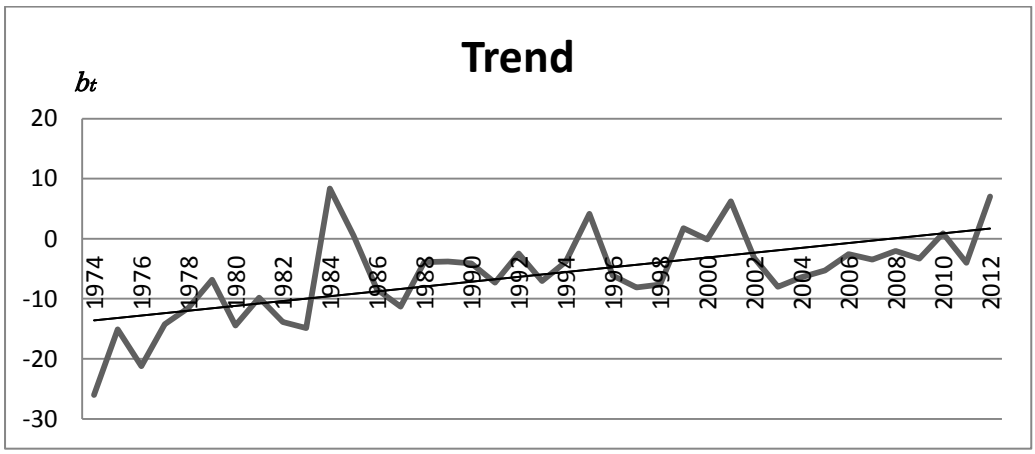

Trend plot of February series using Holt's method at station 2913001.

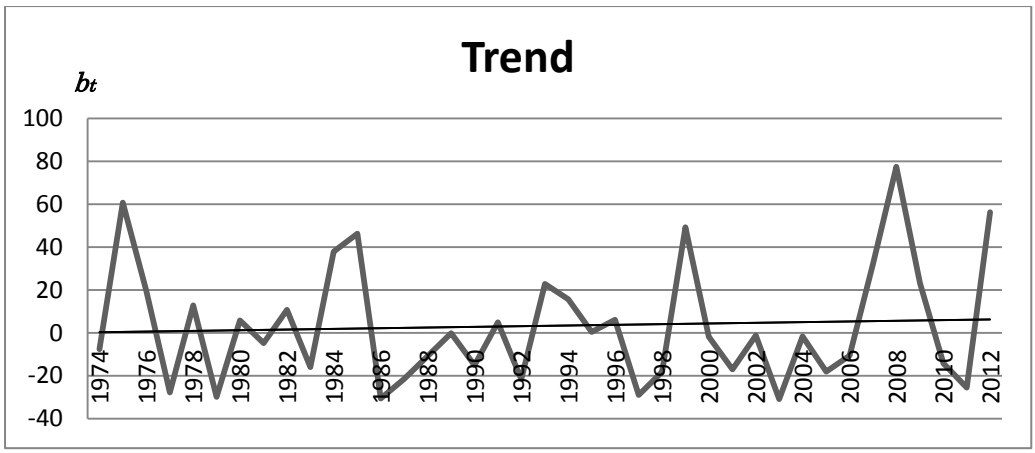

Trend plot of March series using Holt's method at station 2913001.

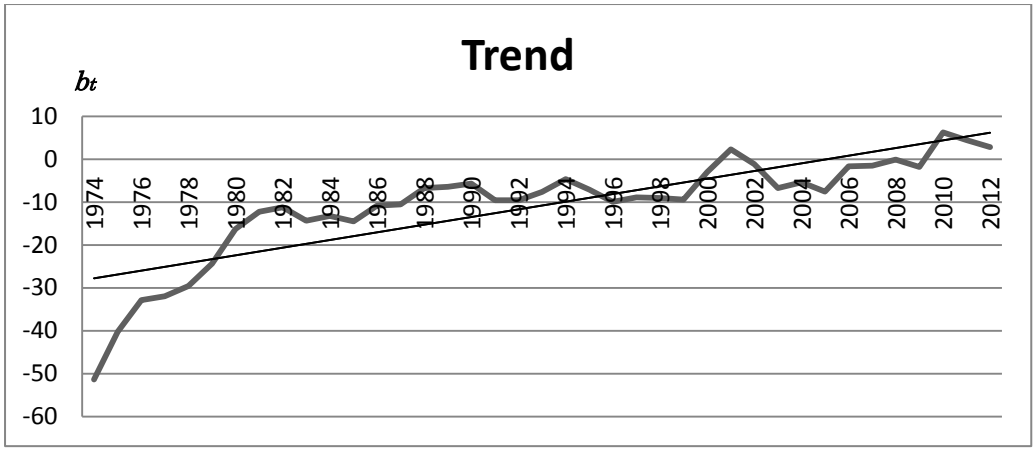

Trend plot of April series using Holt's method at station 2913001.

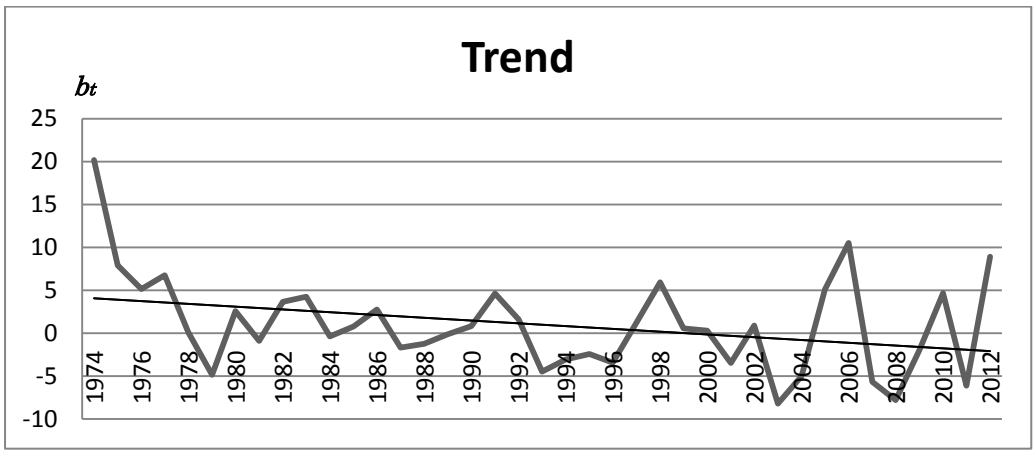

Trend plot of May series using Holt's method at station 2913001.

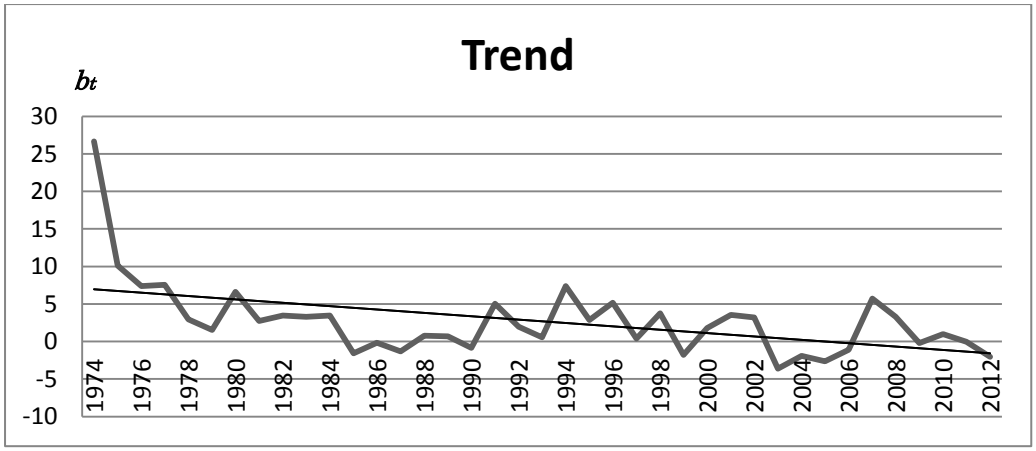

Trend plot of June series using Holt's method at station 2913001.

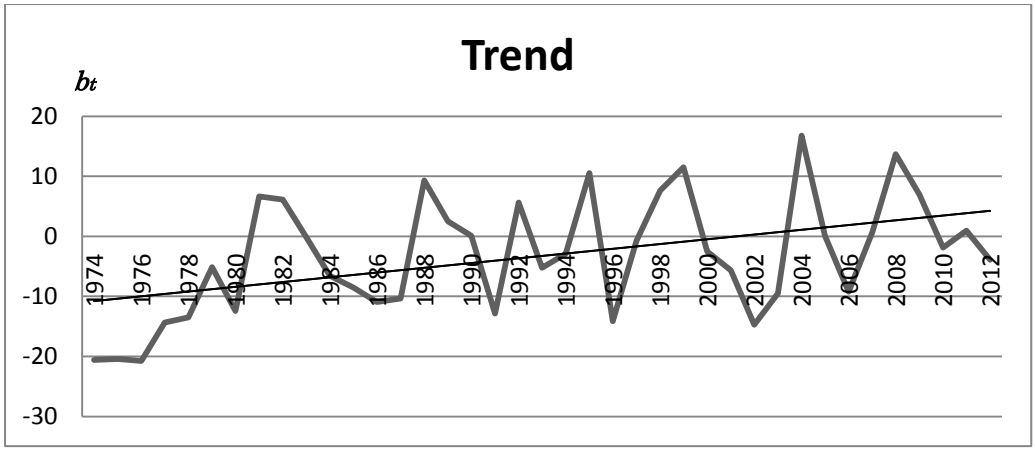

Trend plot of July series using Holt's method at station 2913001.

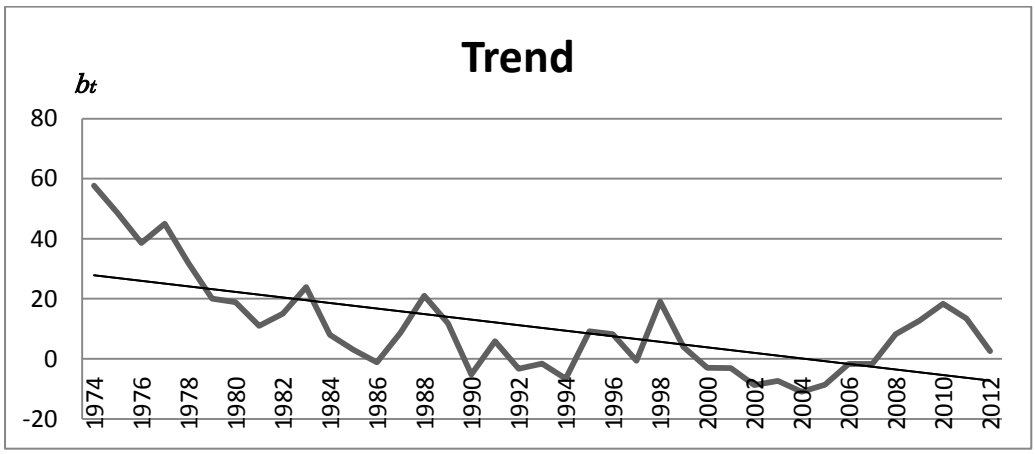

Trend plot of August series using Holt's method at station 2913001.

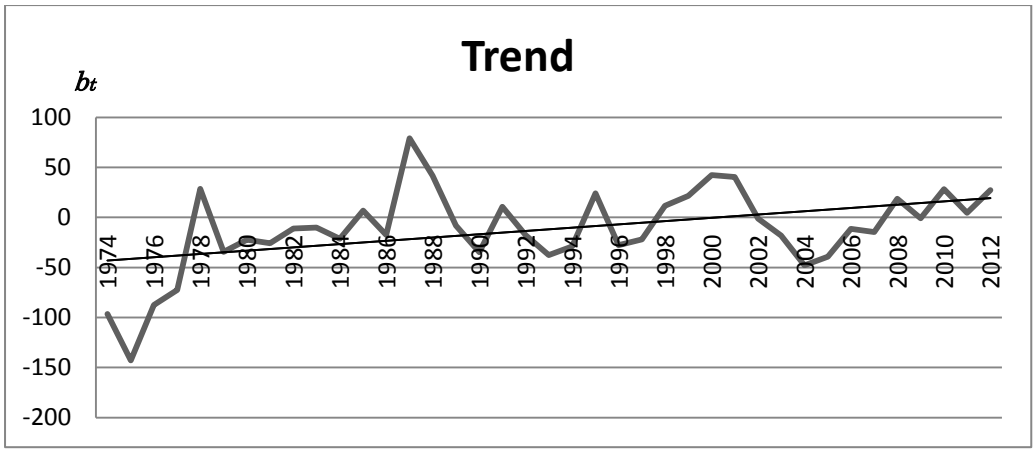

Trend plot of September series using Holt's method at station 2913001.

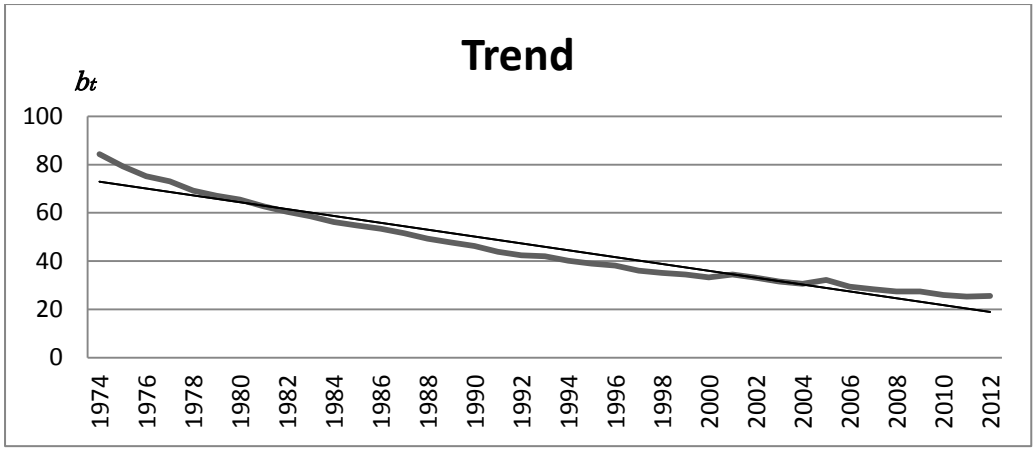

Trend plot of October series using Holt's method at station 2913001.

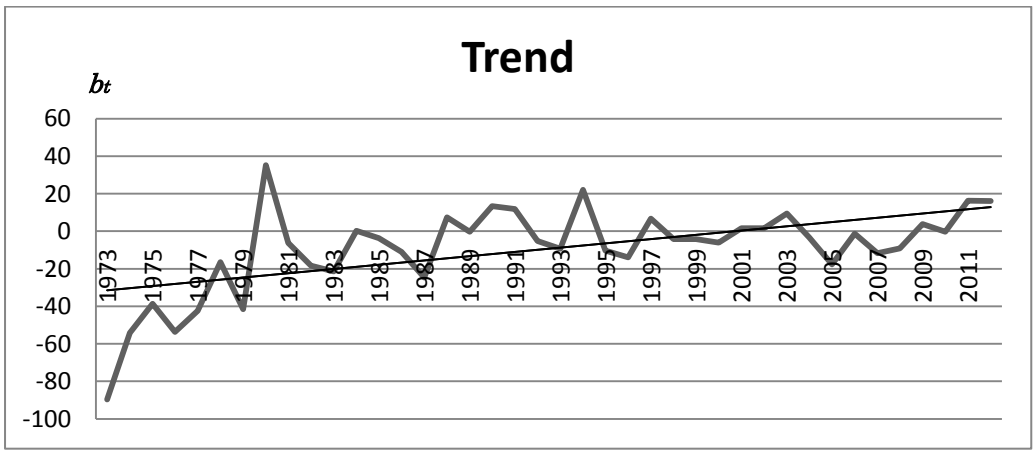

Trend plot of November series using Holt's method at station 2913001.

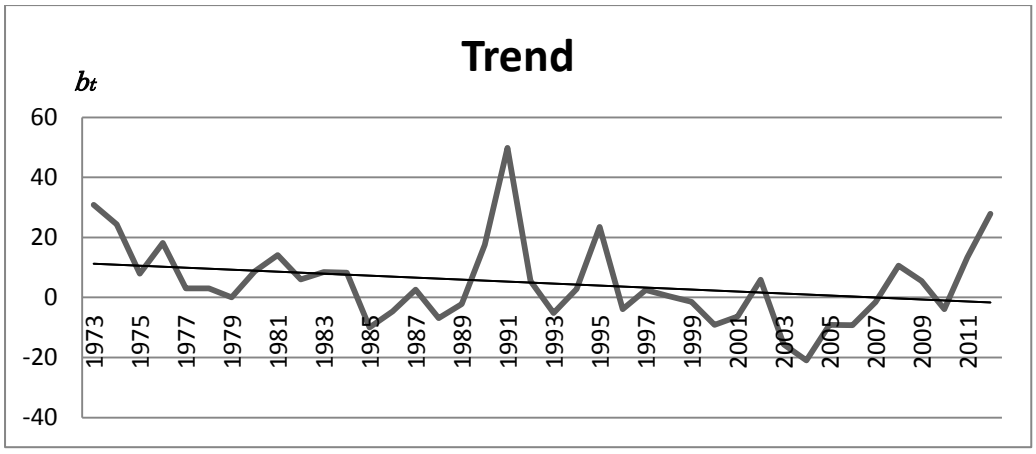

Trend plot of December series using Holt's method at station 2913001.

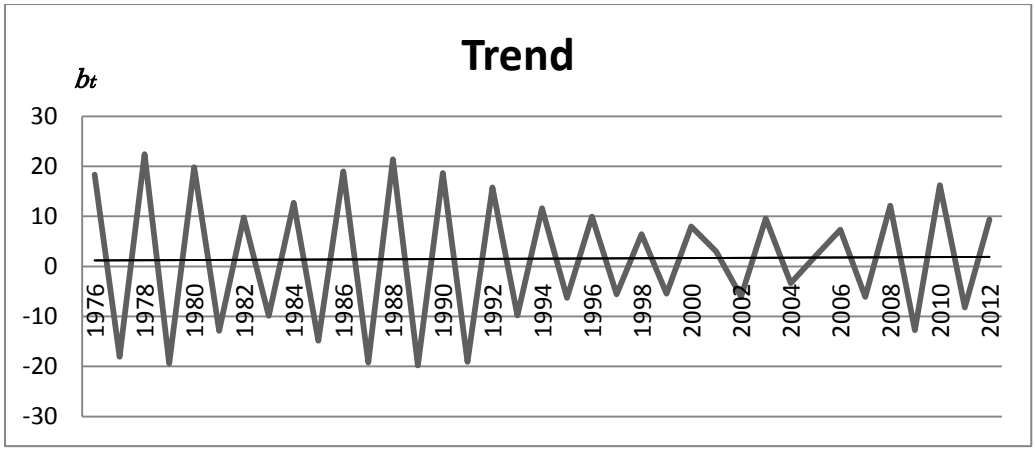

Trend plot of January series using Holt's method at station 2917001.

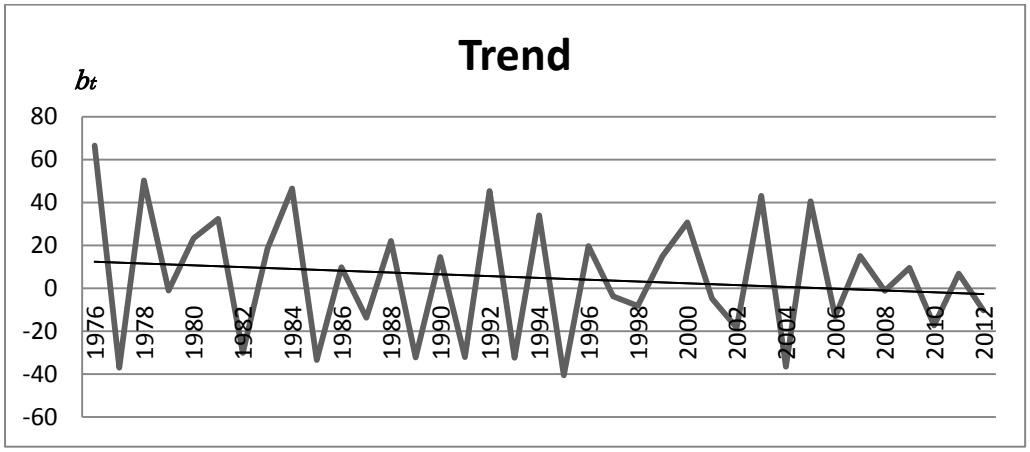

Trend plot of February series using Holt's method at station 2917001.

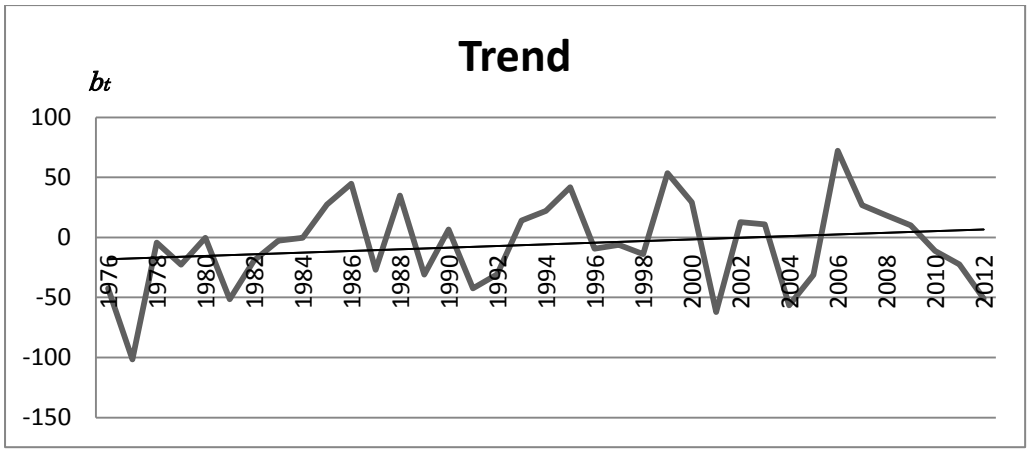

Trend plot of March series using Holt's method at station 2917001.

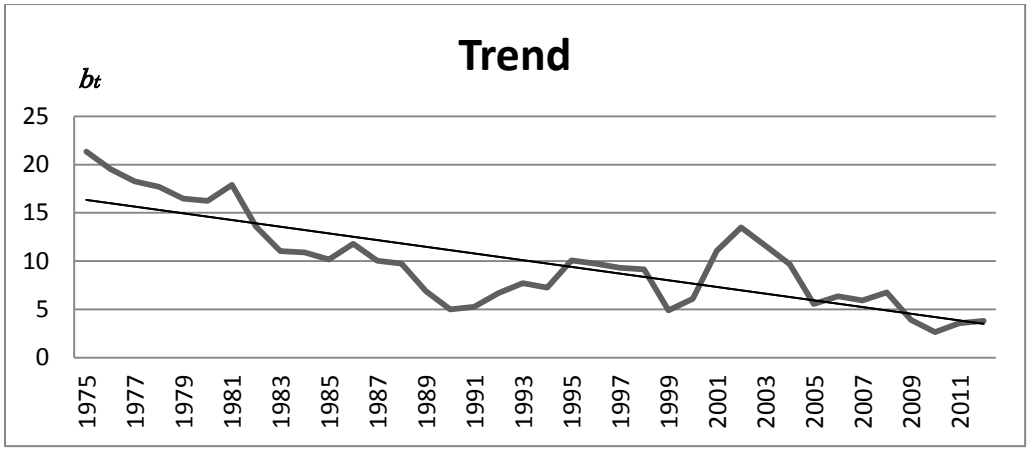

Trend plot of April series using Holt's method at station 2917001.

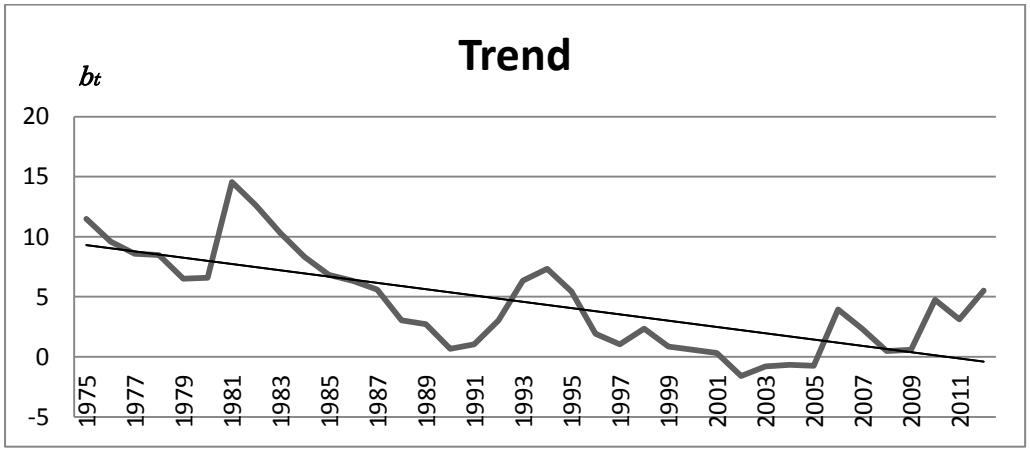

Trend plot of May series using Holt's method at station 2917001.

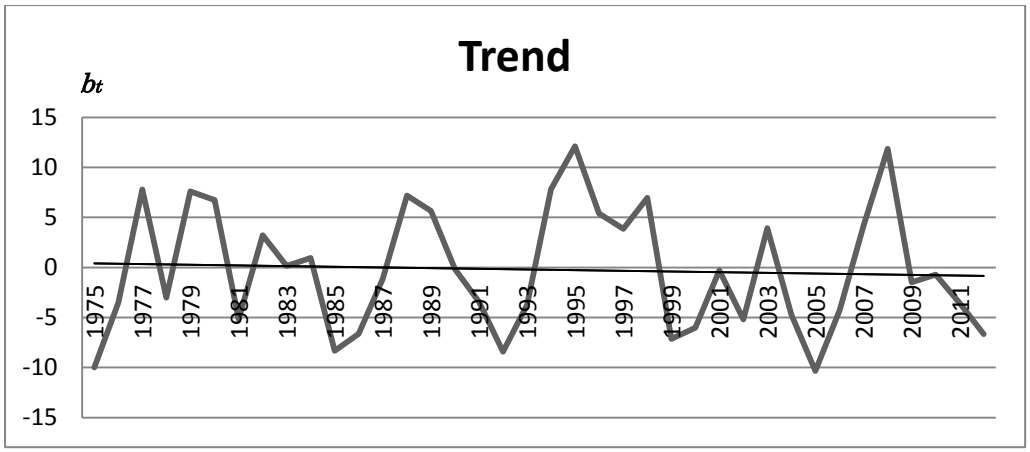

Trend plot of June series using Holt's method at station 2917001.

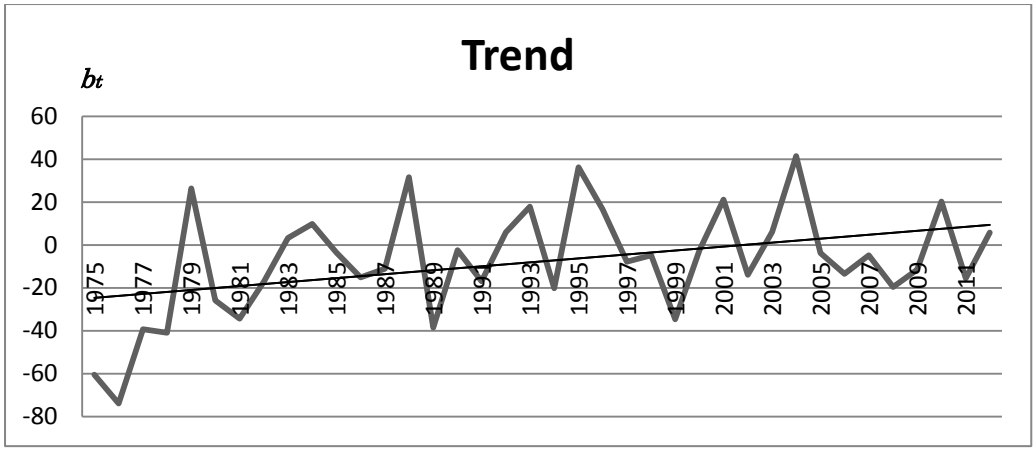

Trend plot of July series using Holt's method at station 2917001.

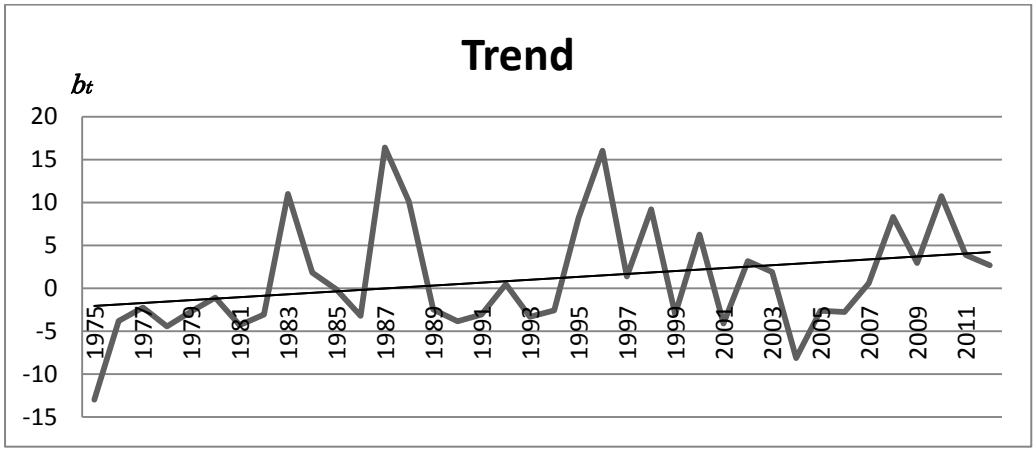

Trend plot of August series using Holt's method at station 2917001.

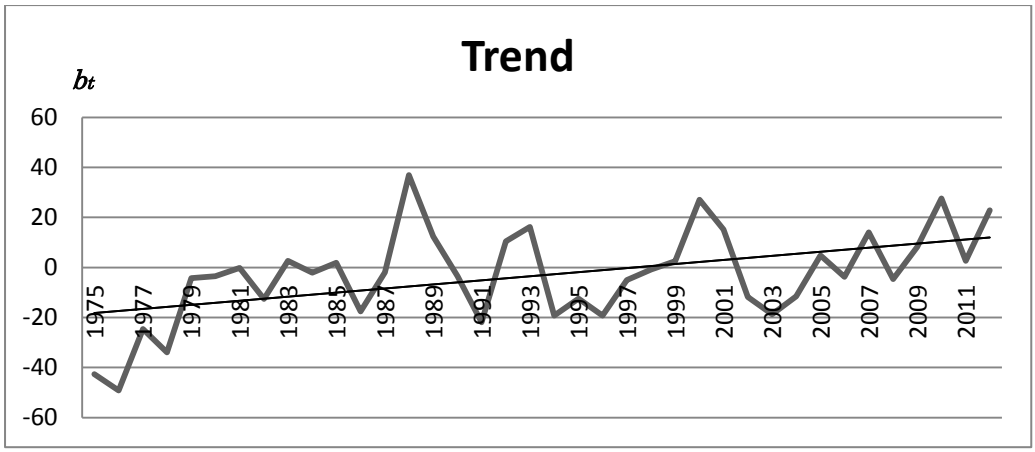

Trend plot of September series using Holt's method at station 2917001.

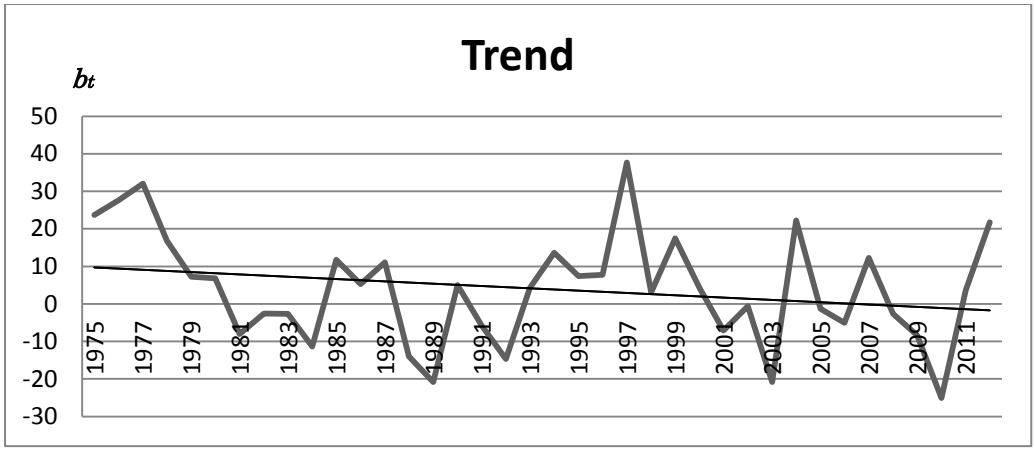

Trend plot of October series using Holt's method at station 2917001.

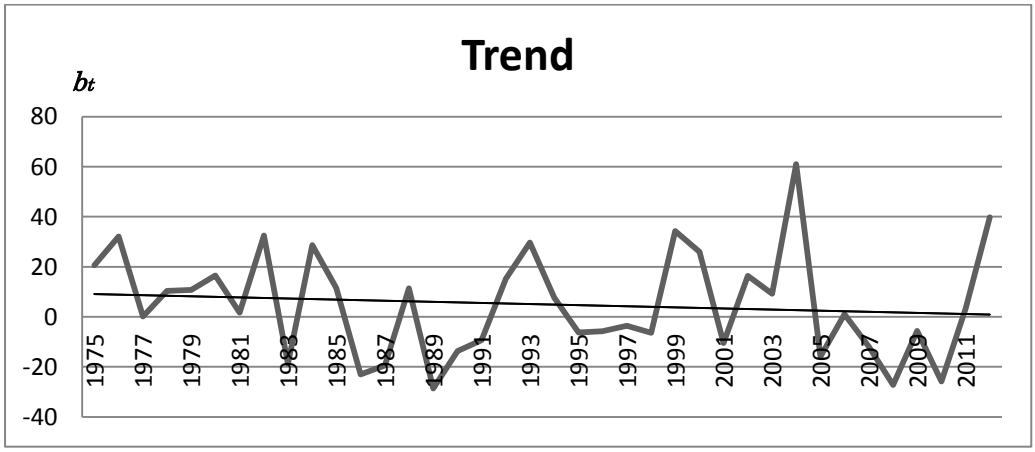

Trend plot of November series using Holt's method at station 2917001.

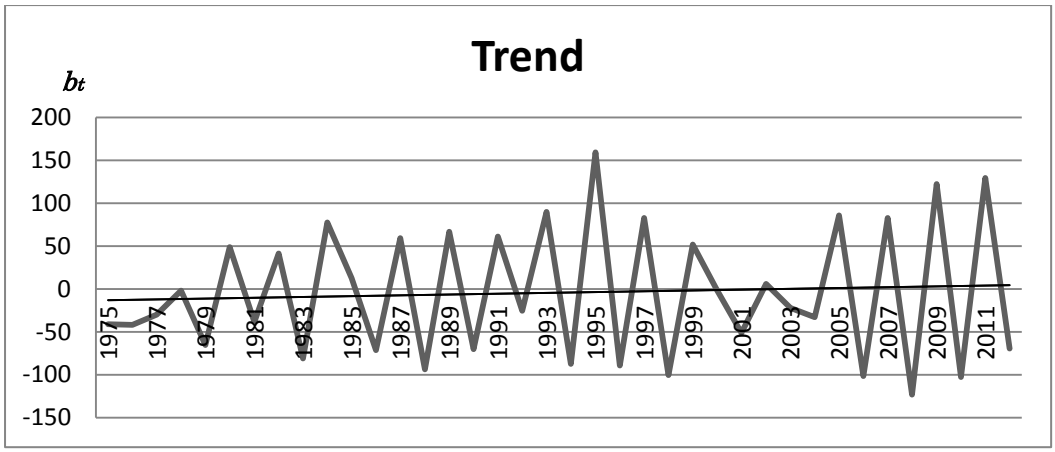

Trend plot of December series using Holt's method at station 2917001.

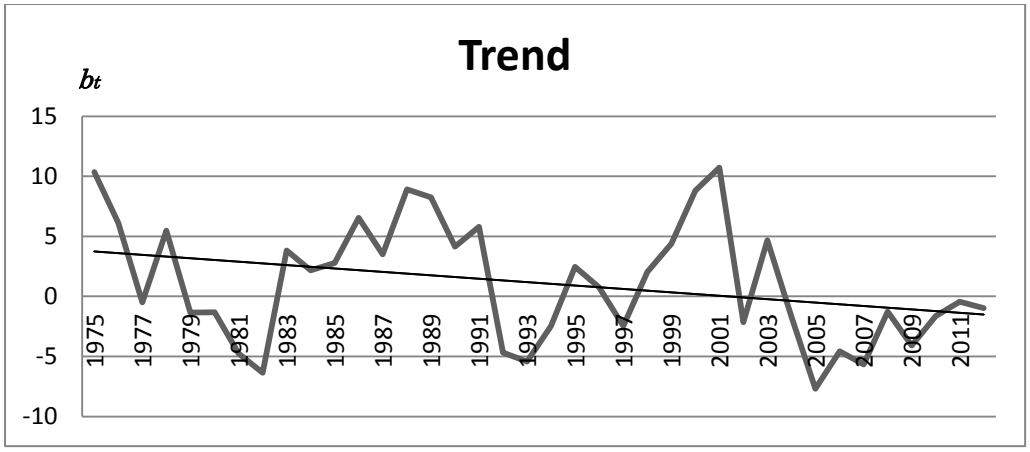

Trend plot of January series using Holt's method at station 44239.

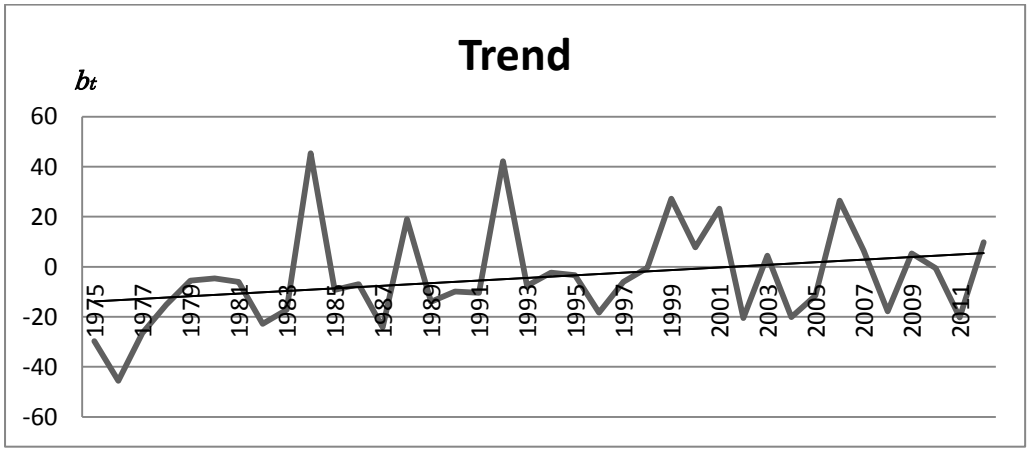

Trend plot of February series using Holt's method at station 44239.

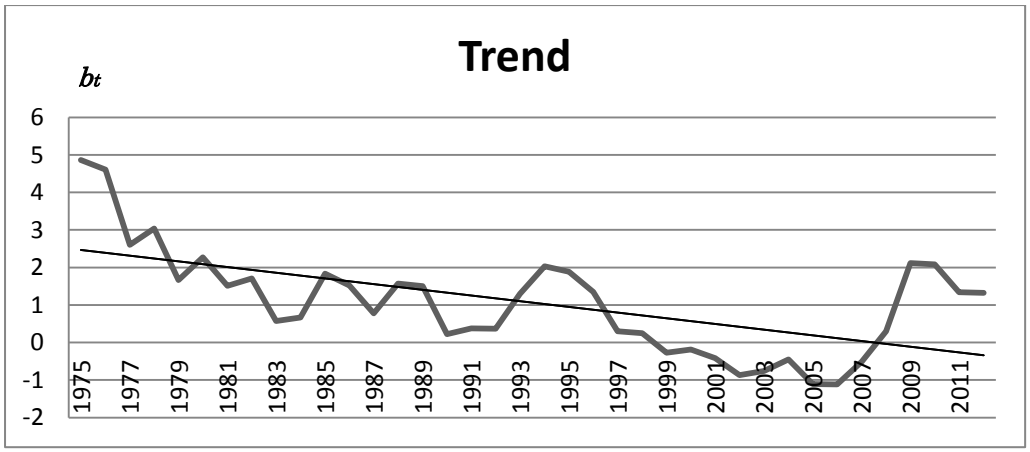

Trend plot of March series using Holt's method at station 44239.

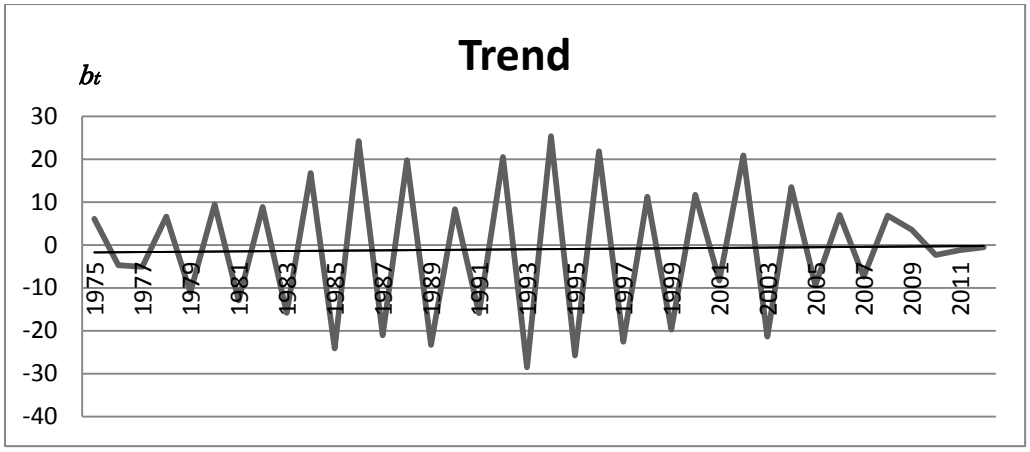

Trend plot of April series using Holt's method at station 44239.

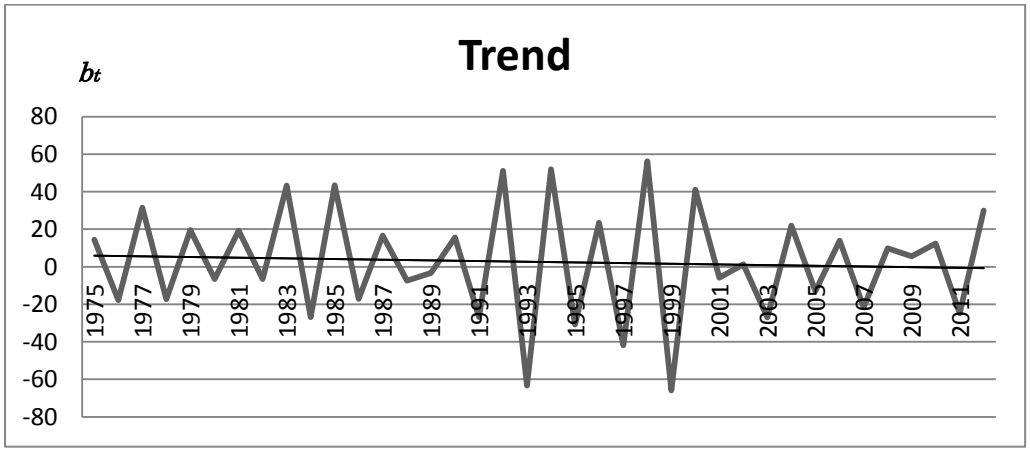

Trend plot of May series using Holt's method at station 44239.

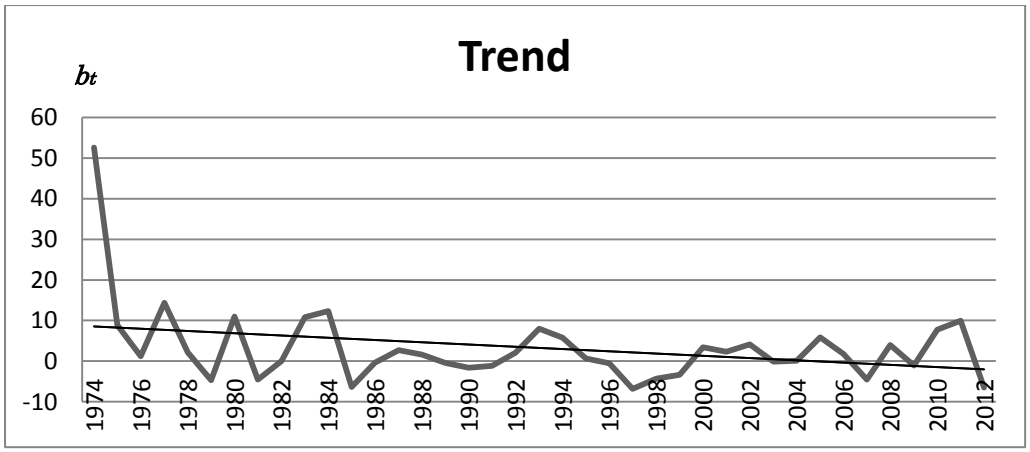

Trend plot of June series using Holt's method at station 44239.

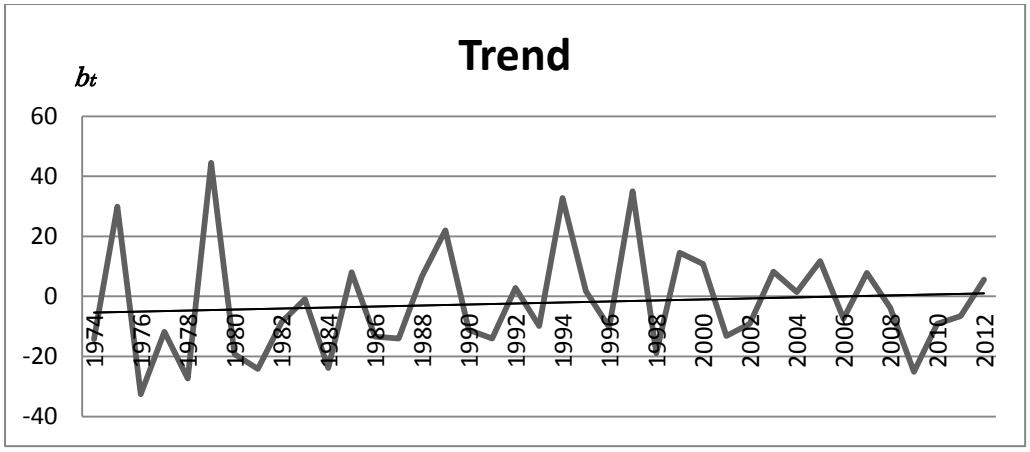

Trend plot of July series using Holt's method at station 44239.

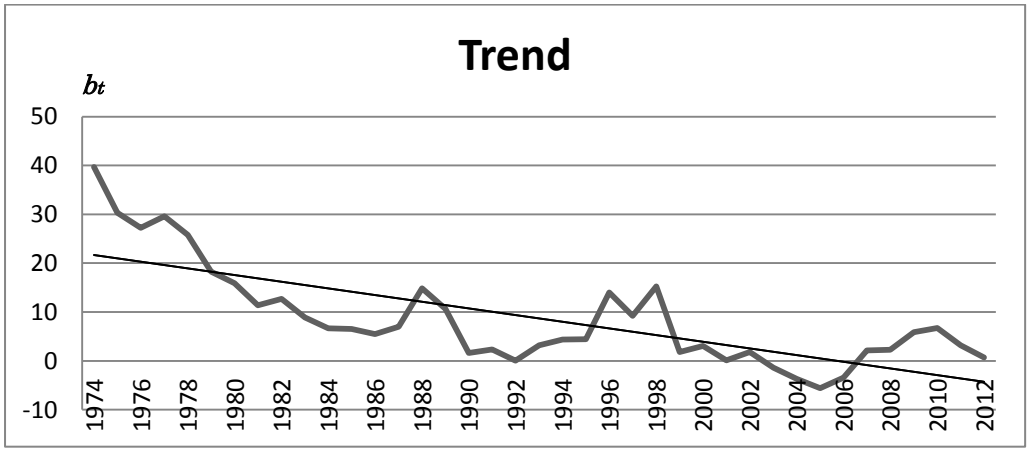

Trend plot of August series using Holt's method at station 44239.

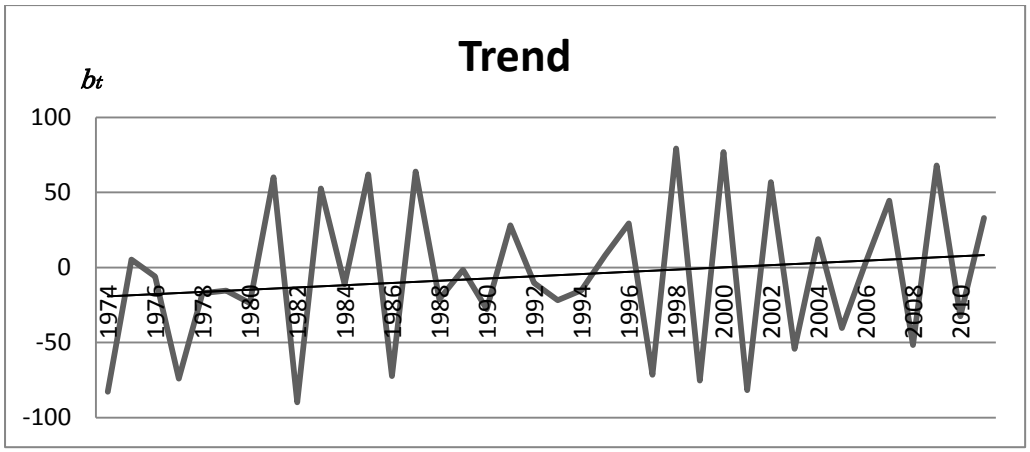

Trend plot of September series using Holt's method at station 44239.

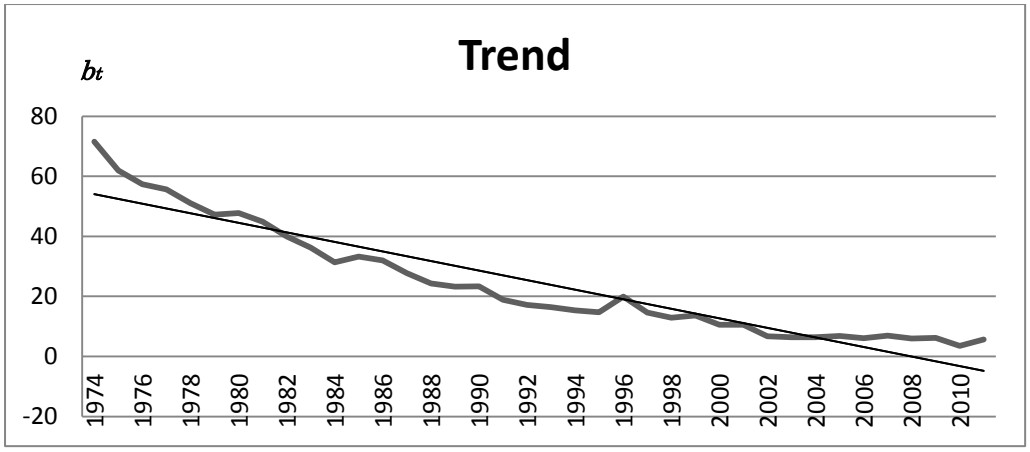

Trend plot of October series using Holt's method at station 44239.

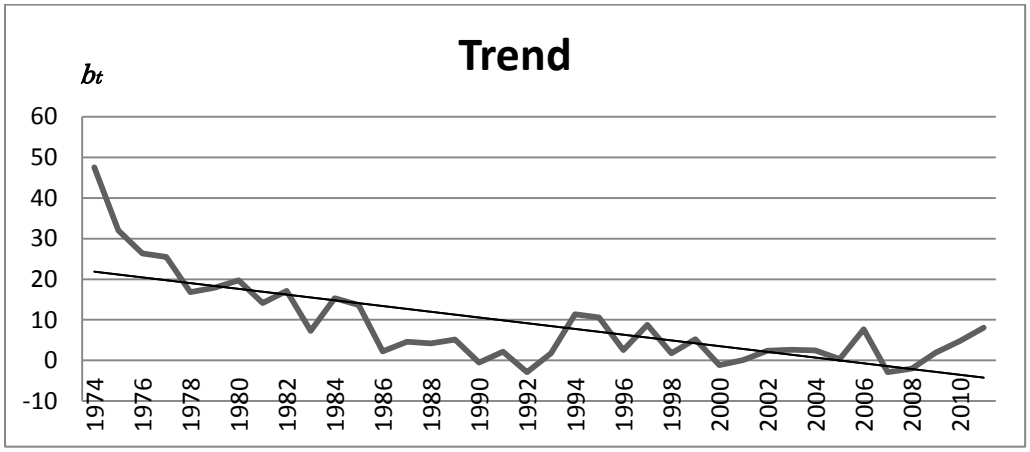

Trend plot of November series using Holt's method at station 44239.

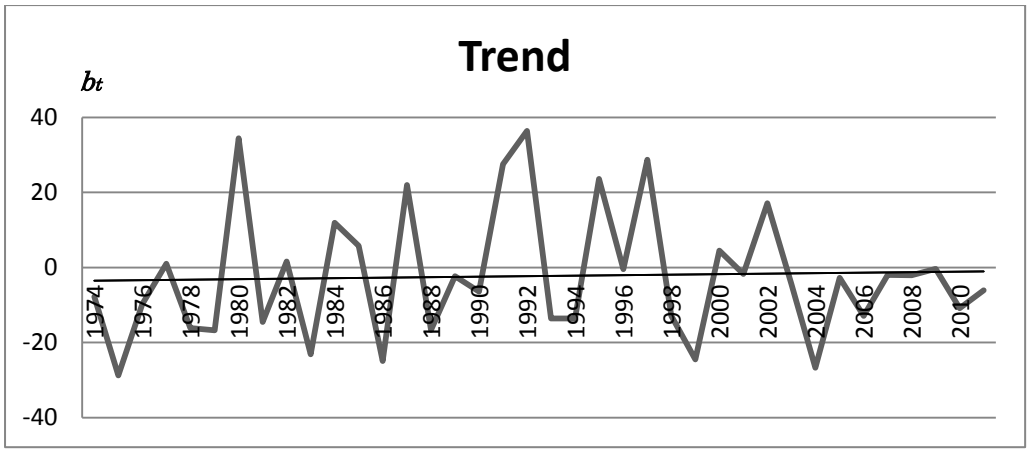

Trend plot of December series using Holt's method at station 44239.

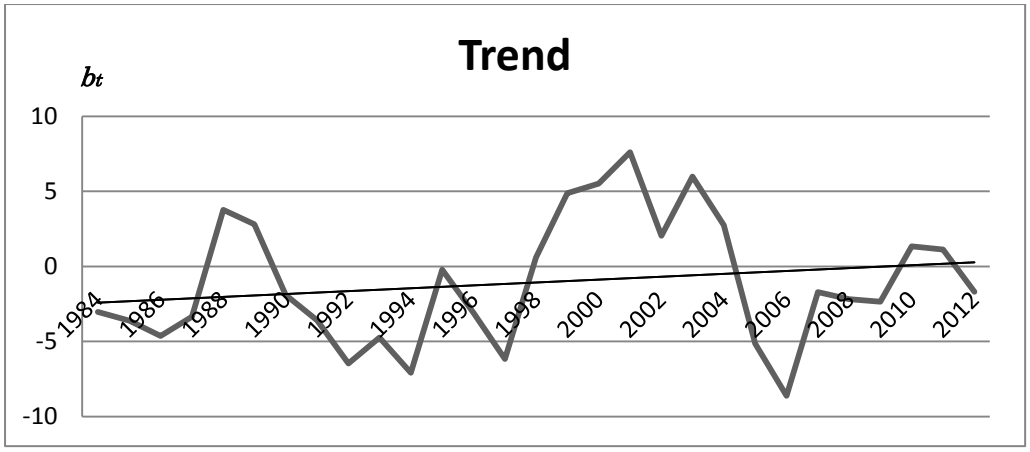

Trend plot of January series using Holt's method at station 44255.

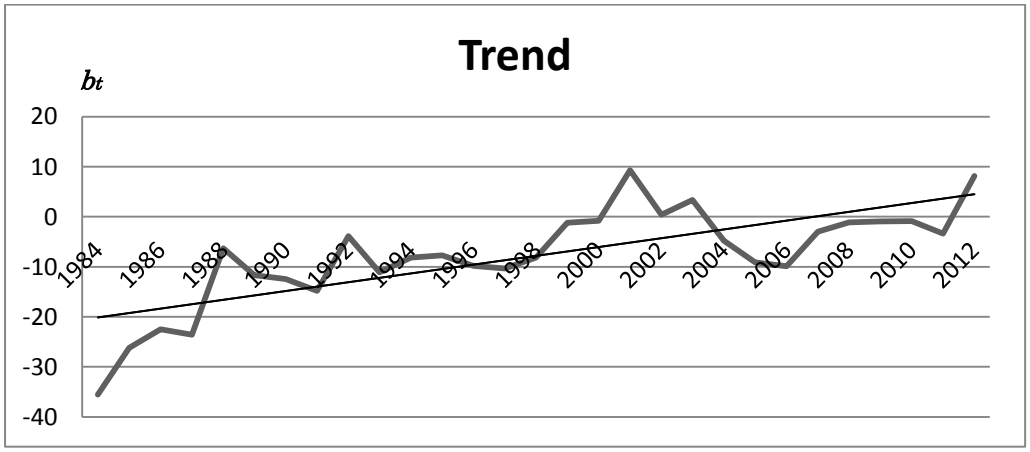

Trend plot of February series using Holt's method at station 44255.

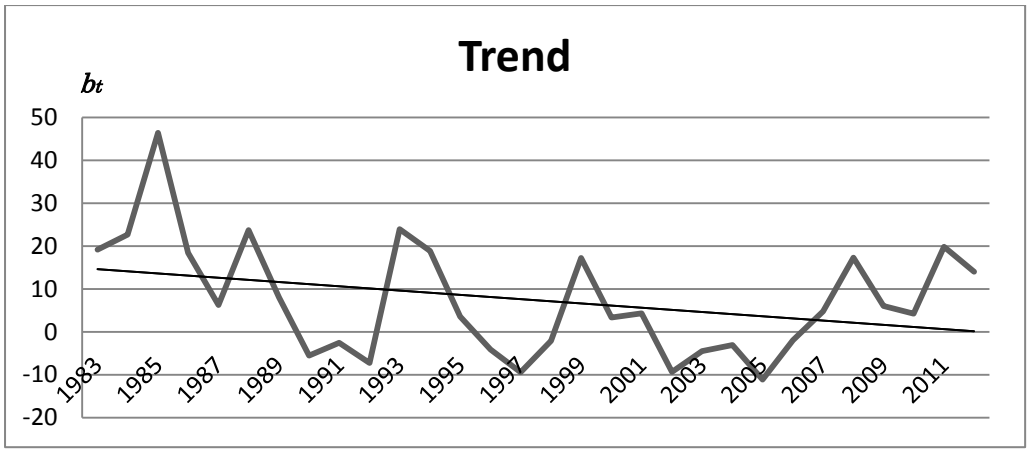

Trend plot of March series using Holt's method at station 44255.

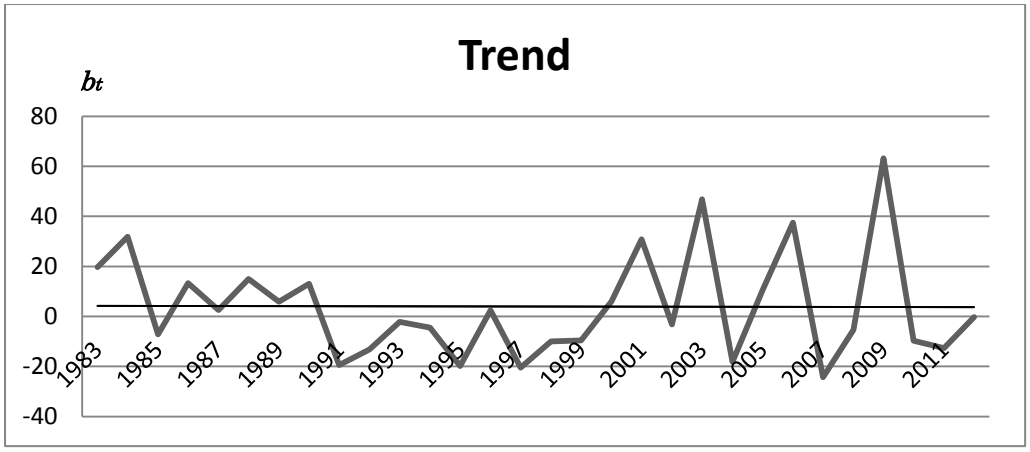

Trend plot of April series using Holt's method at station 44255.

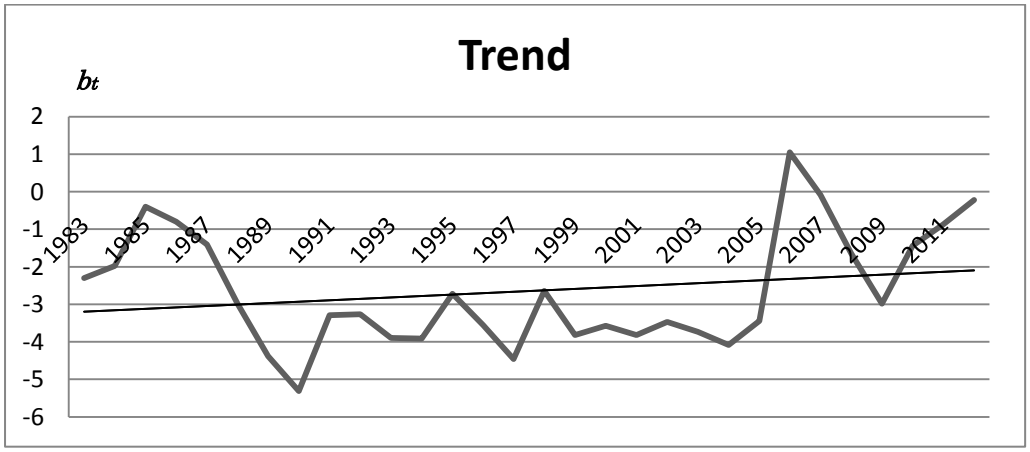

Trend plot of May series using Holt's method at station 44255.

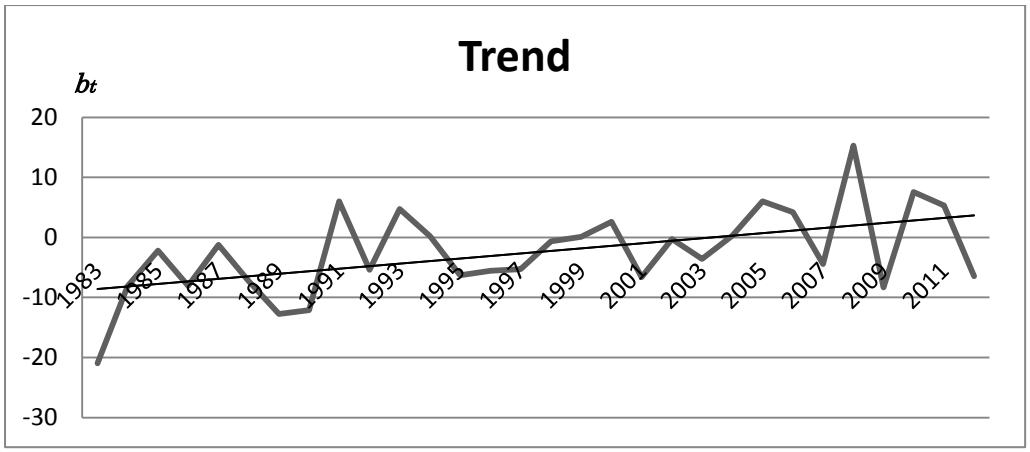

Trend plot of June series using Holt's method at station 44255.

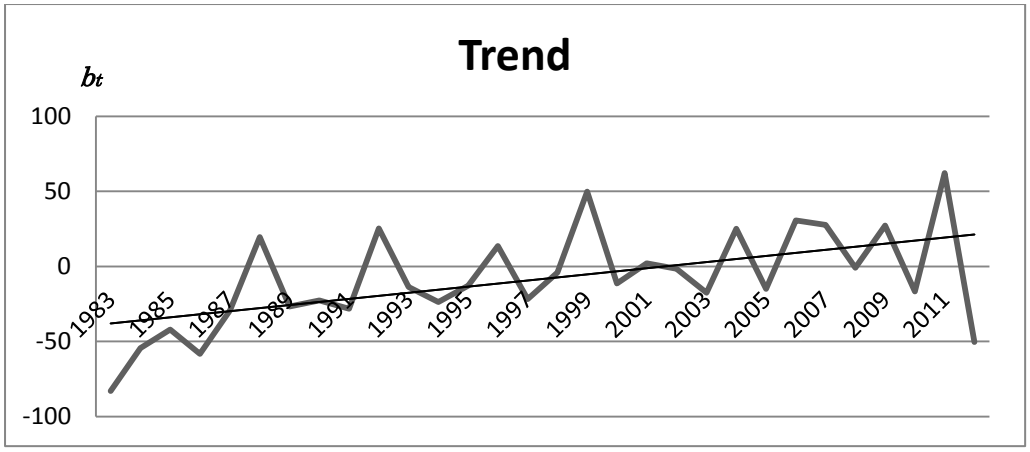

Trend plot of July series using Holt's method at station 44255.

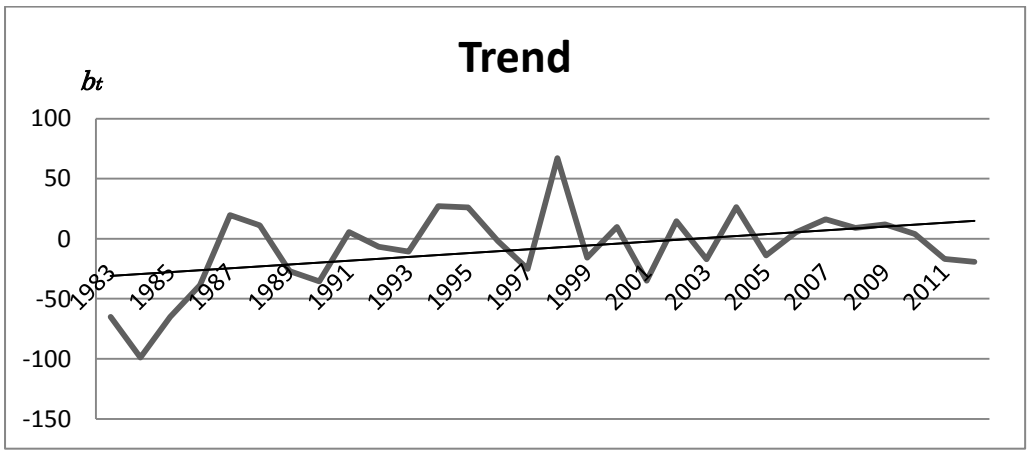

Trend plot of August series using Holt's method at station 44255.

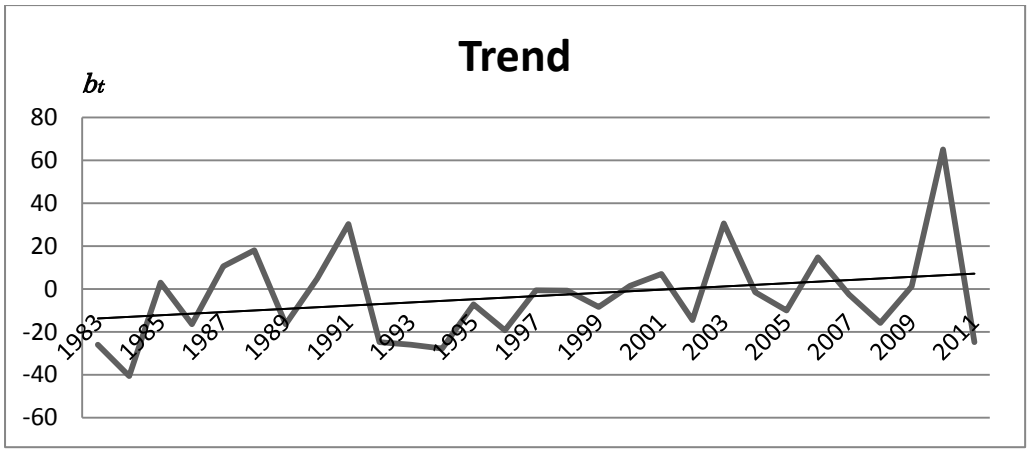

Trend plot of September series using Holt's method at station 44255.

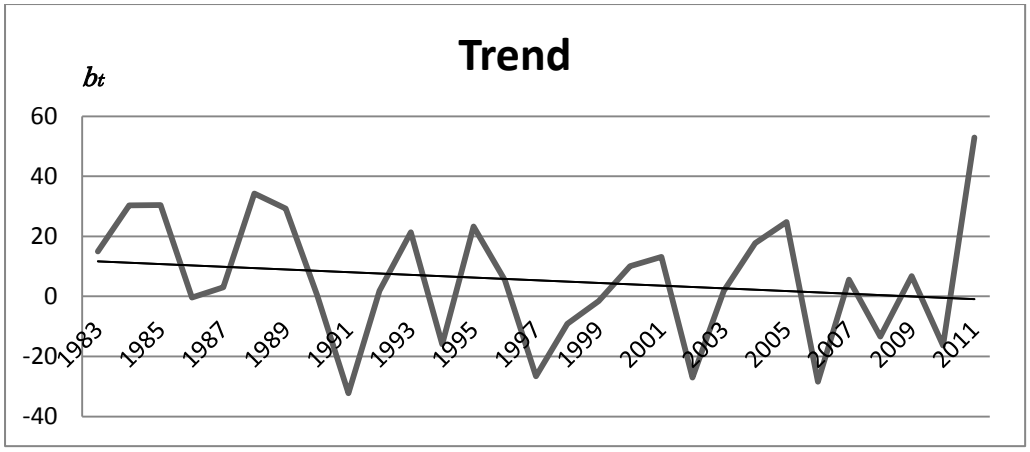

Trend plot of October series using Holt's method at station 44255.

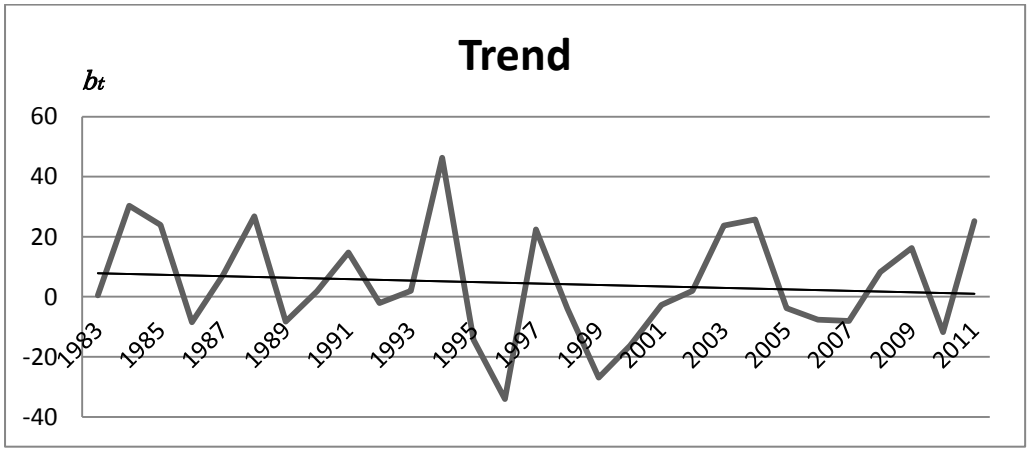

Trend plot of November series using Holt's method at station 44255.

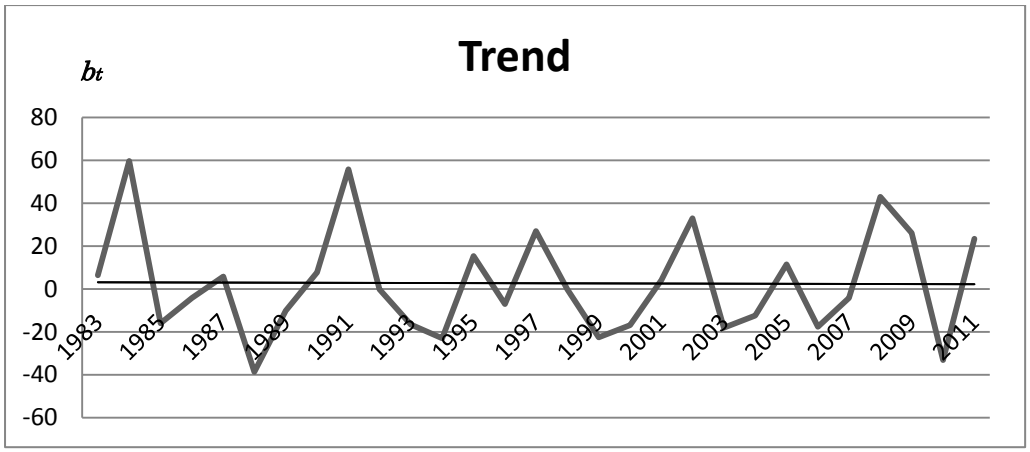

Trend plot of December series using Holt's method at station 44255.

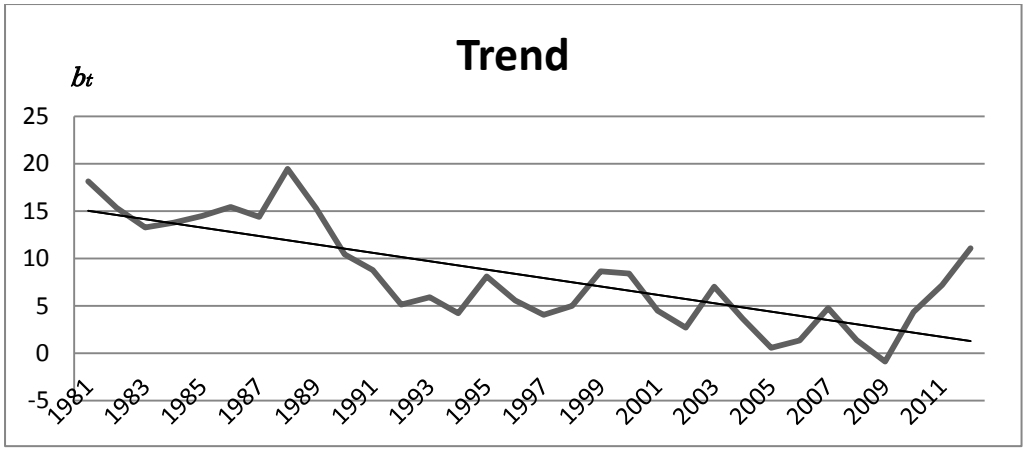

Trend plot of January series using Holt's method at station 44256.

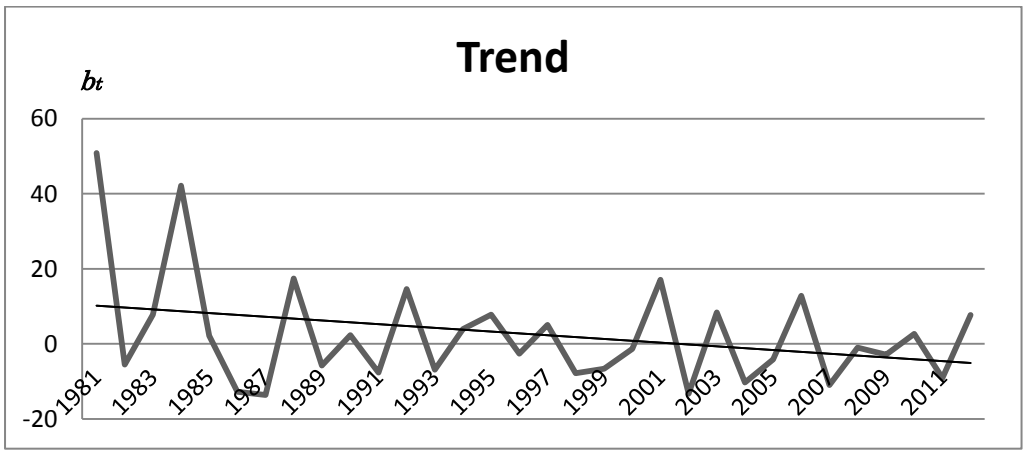

Trend plot of February series using Holt's method at station 44256.

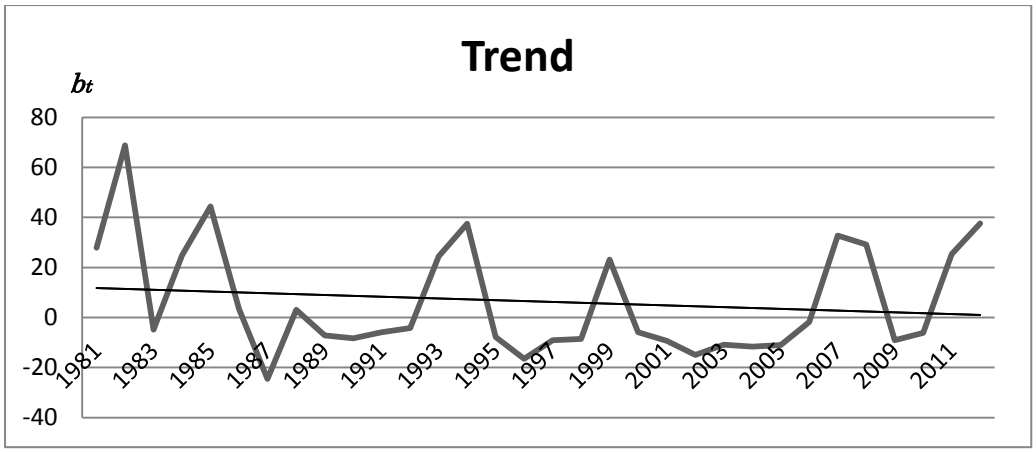

Trend plot of March series using Holt's method at station 44256.

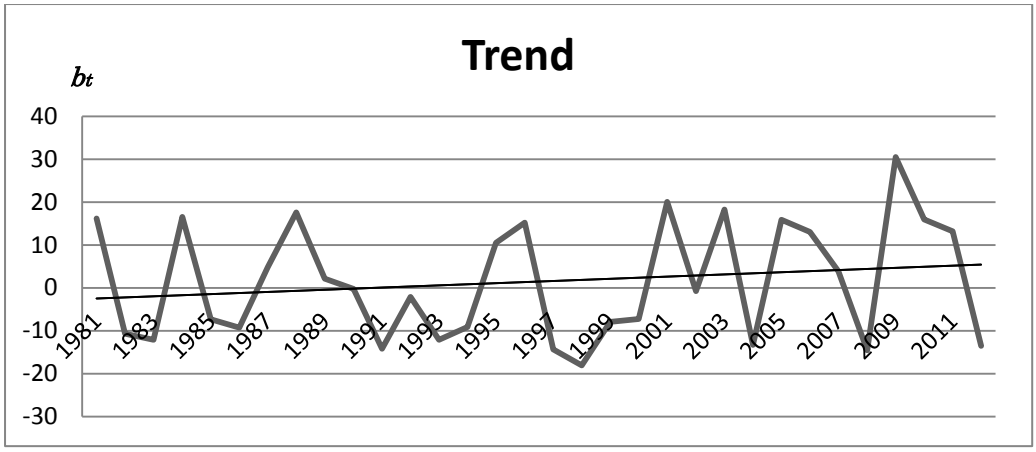

Trend plot of April series using Holt's method at station 44256.

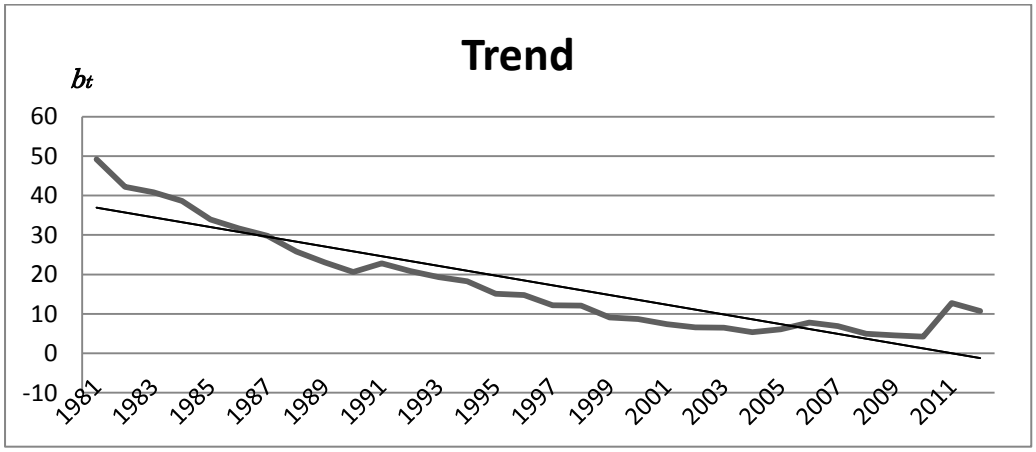

Trend plot of May series using Holt's method at station 44256.

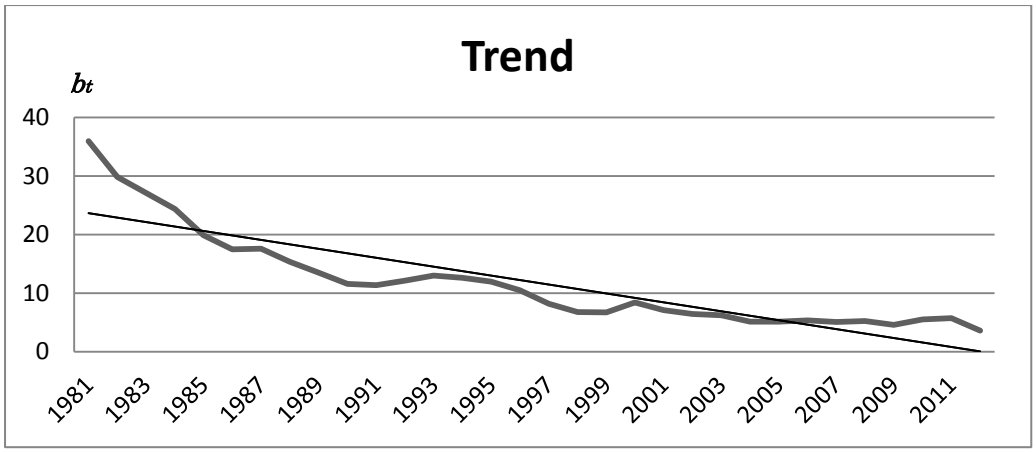

Trend plot of June series using Holt's method at station 44256.

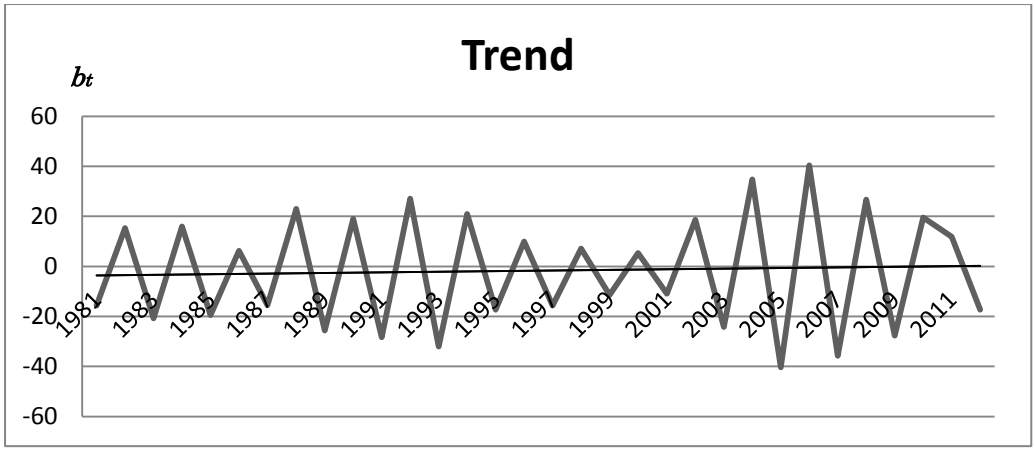

Trend plot of July series using Holt's method at station 44256.

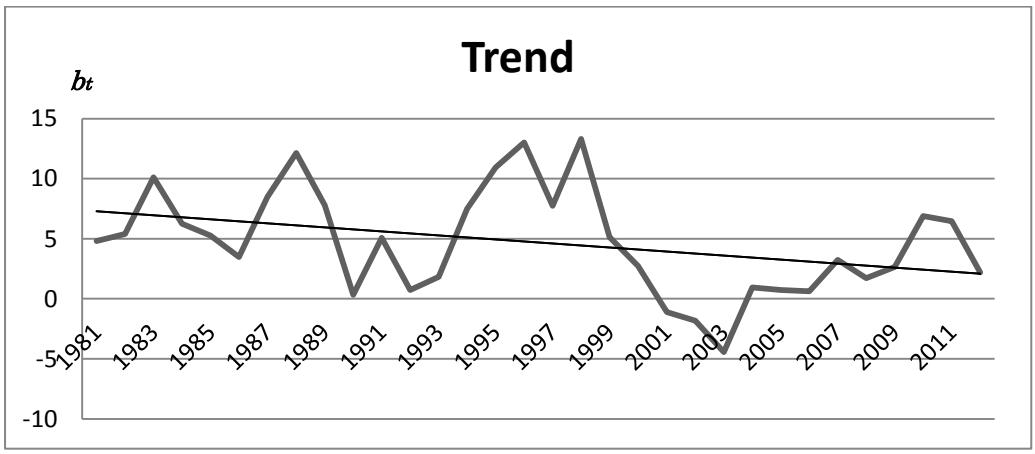

Trend plot of August series using Holt's method at station 44256.

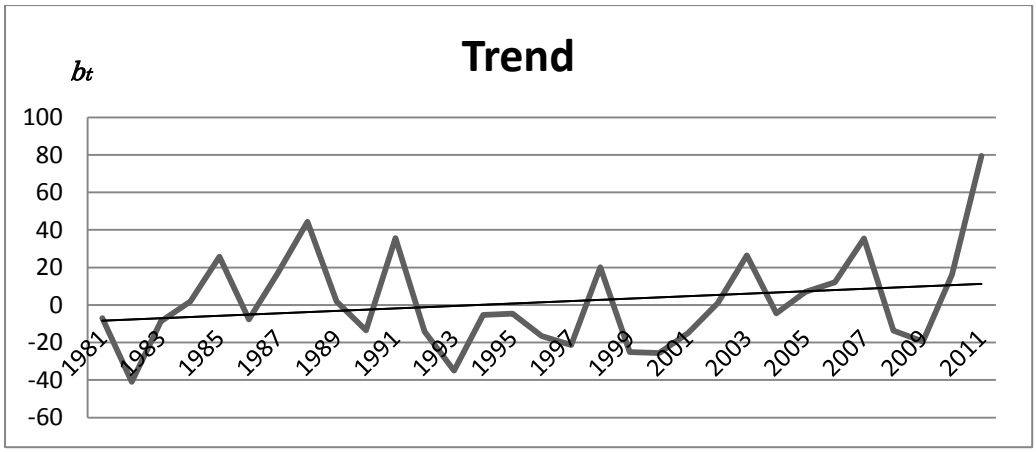

Trend plot of September series using Holt's method at station 44256.

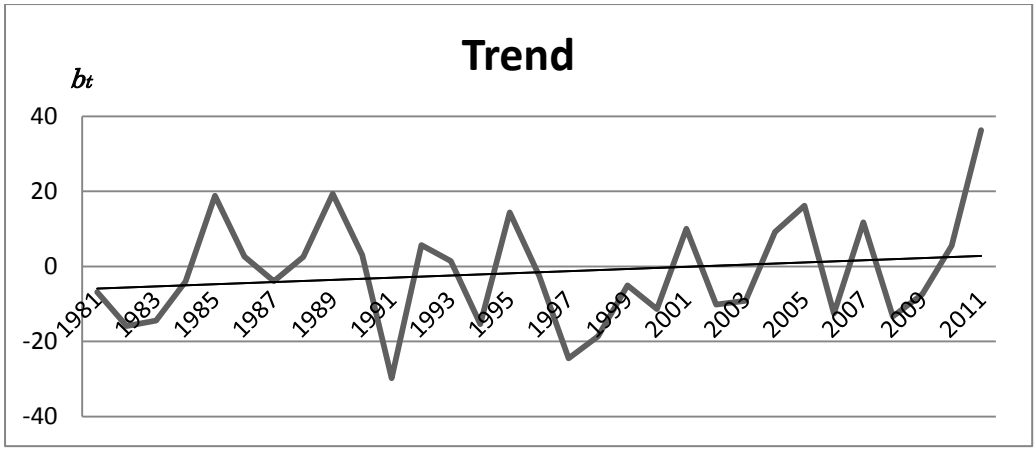

Trend plot of October series using Holt's method at station 44256.

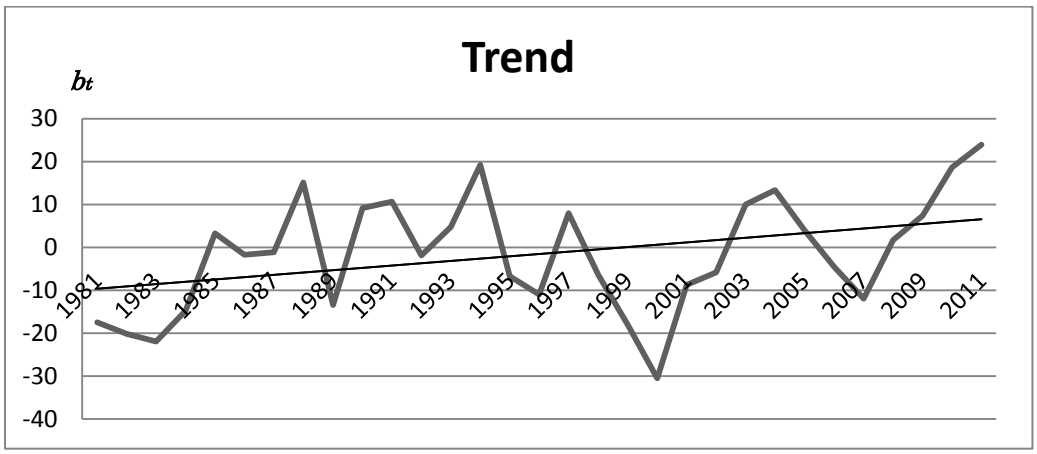

Trend plot of November series using Holt's method at station 44256.

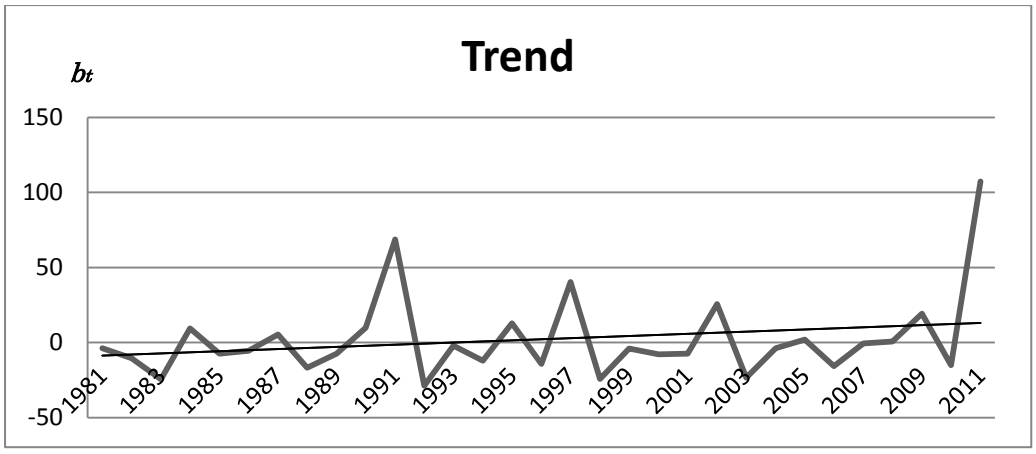

Trend plot of December series using Holt's method at station 44256.

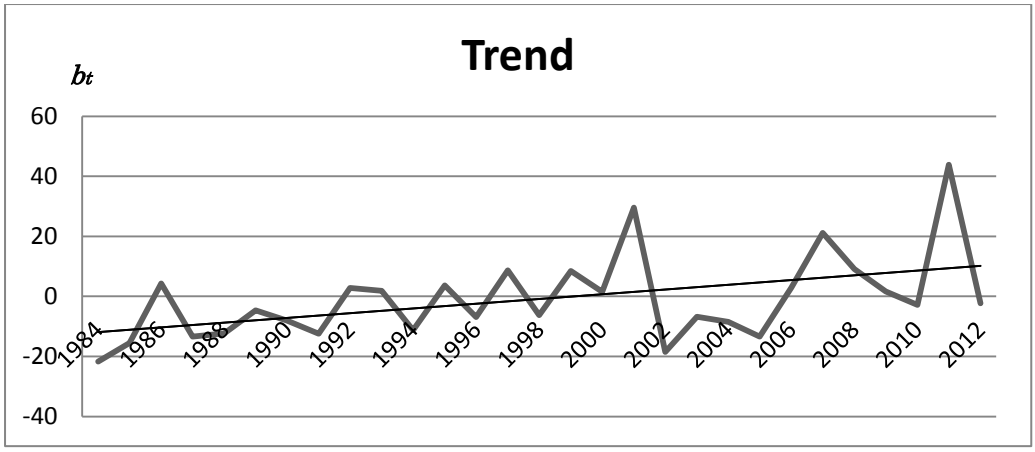

Trend plot of January series using Holt's method at station 44320.

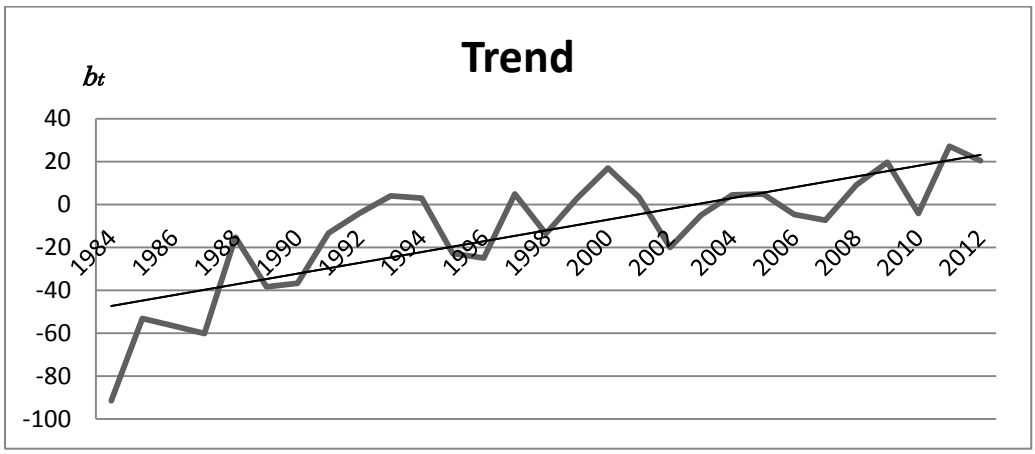

Trend plot of February series using Holt's method at station 44320.

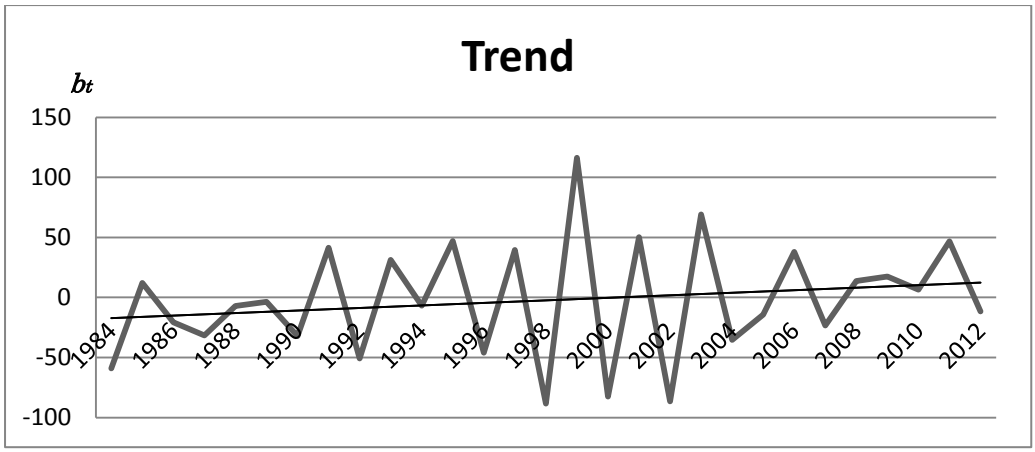

Trend plot of March series using Holt's method at station 44320.

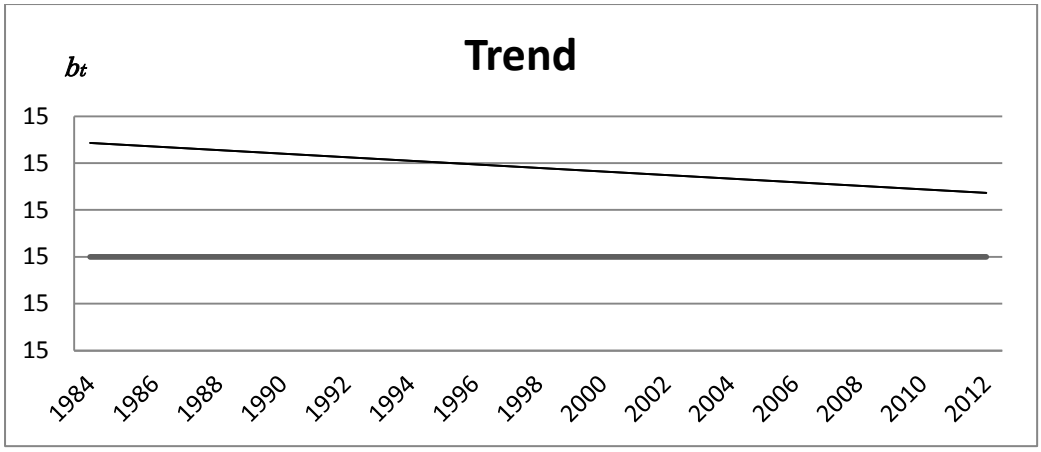

Trend plot of April series using Holt's method at station 44320.

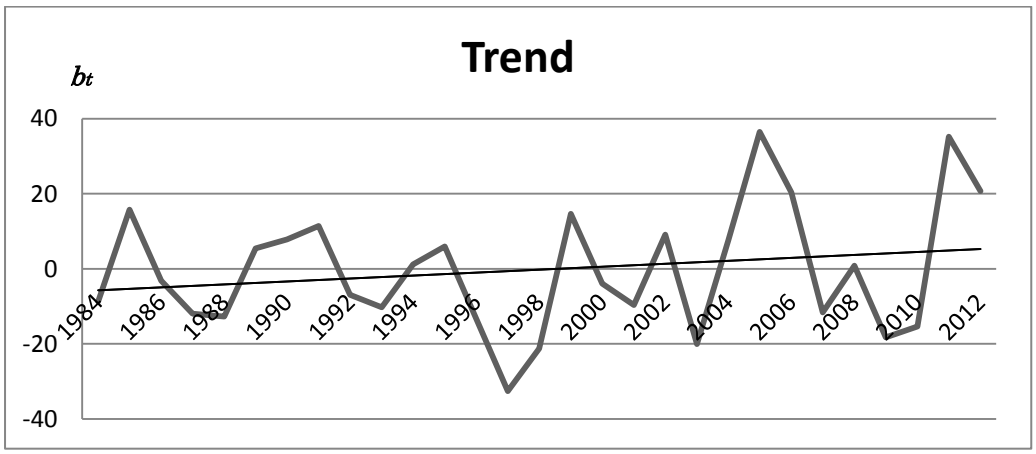

Trend plot of May series using Holt's method at station 44320.

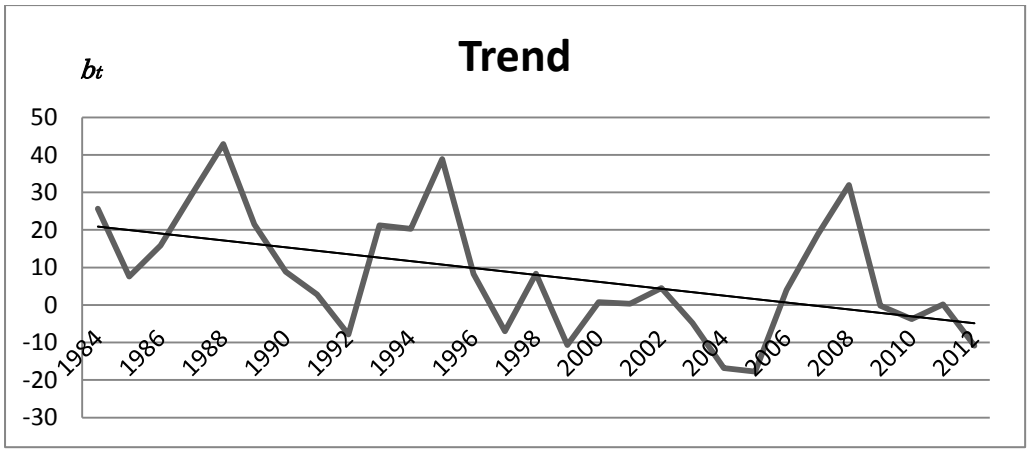

Trend plot of June series using Holt's method at station 44320.

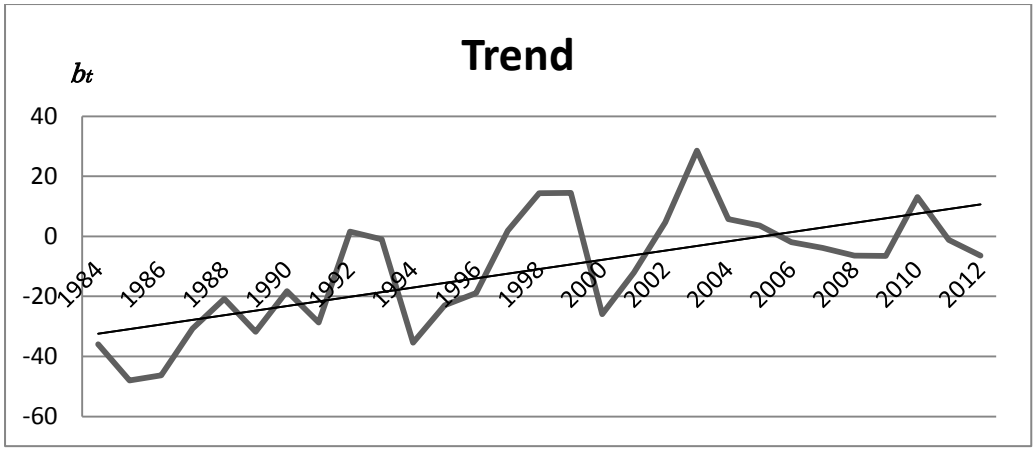

Trend plot of July series using Holt's method at station 44320.

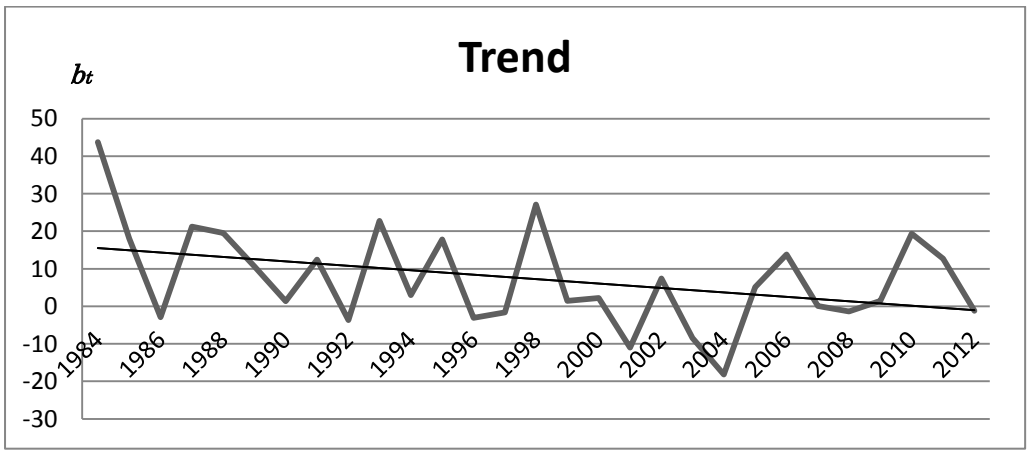

Trend plot of August series using Holt's method at station 44320.

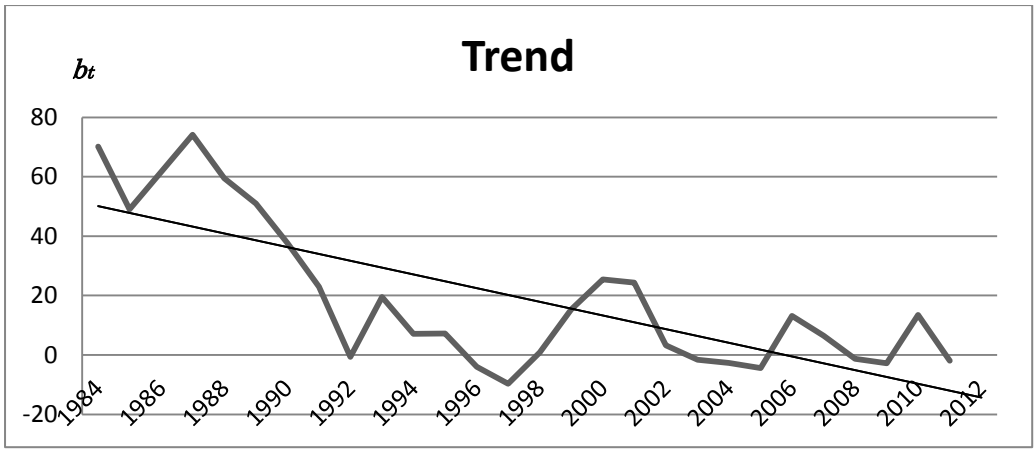

Trend plot of September series using Holt's method at station 44320.

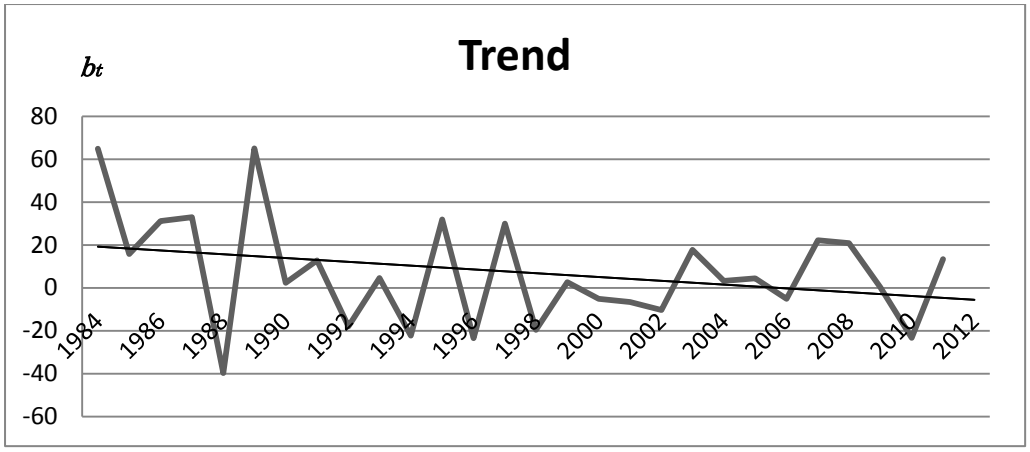

Trend plot of October series using Holt's method at station 44320.

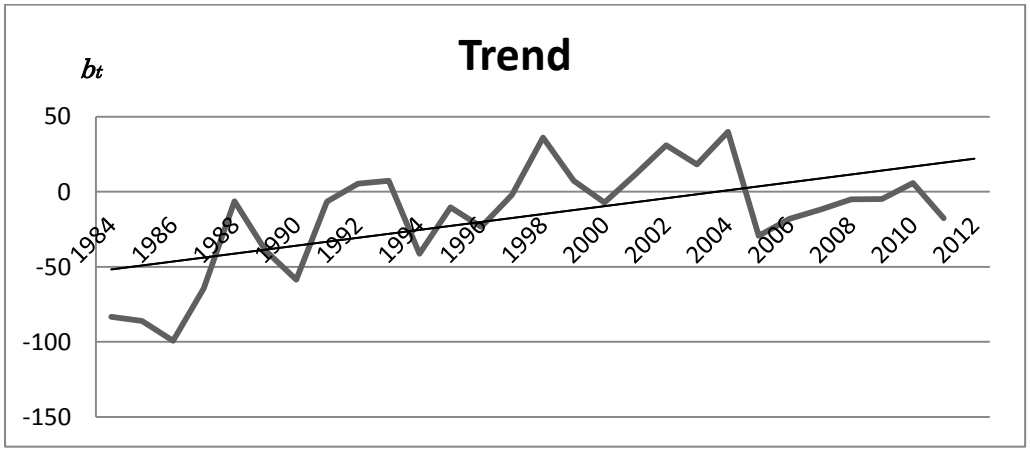

Trend plot of November series using Holt's method at station 44320.

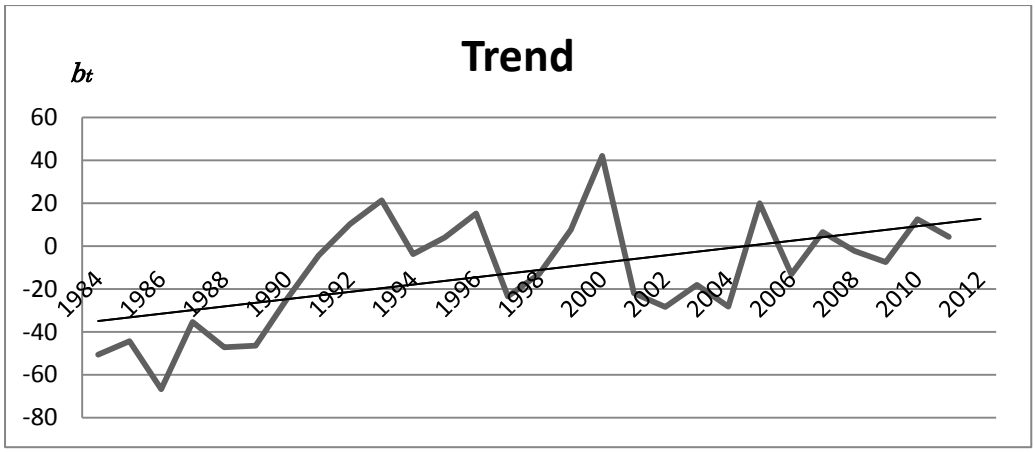

Trend plot of December series using Holt's method at station 44320.

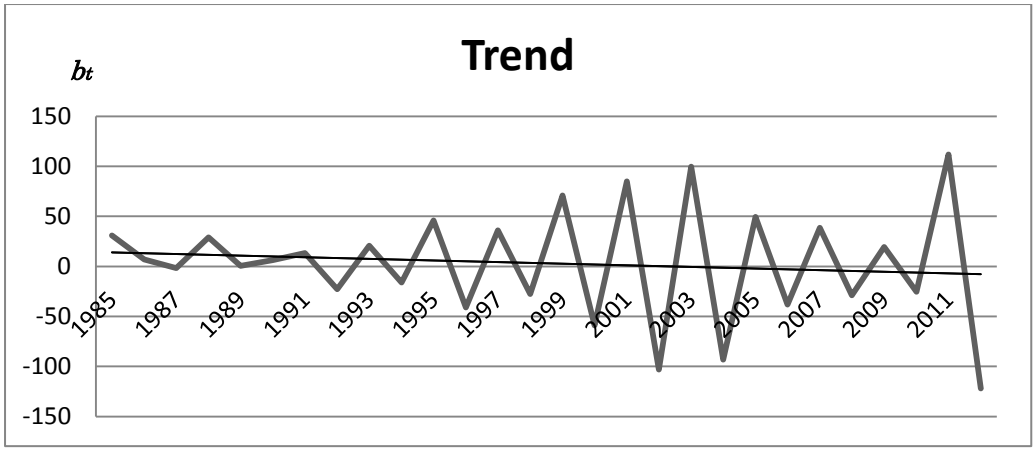

Trend plot of January series using Holt's method at station 45253.

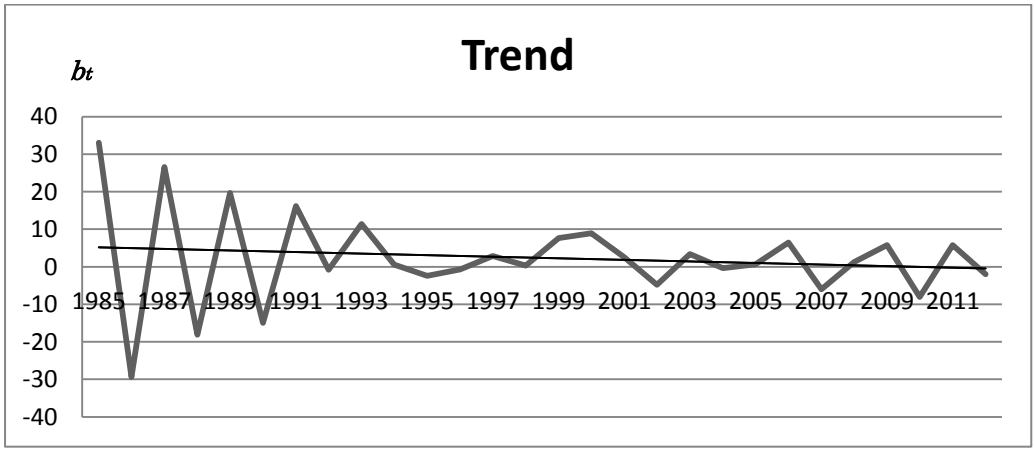

Trend plot of February series using Holt's method at station 45253.

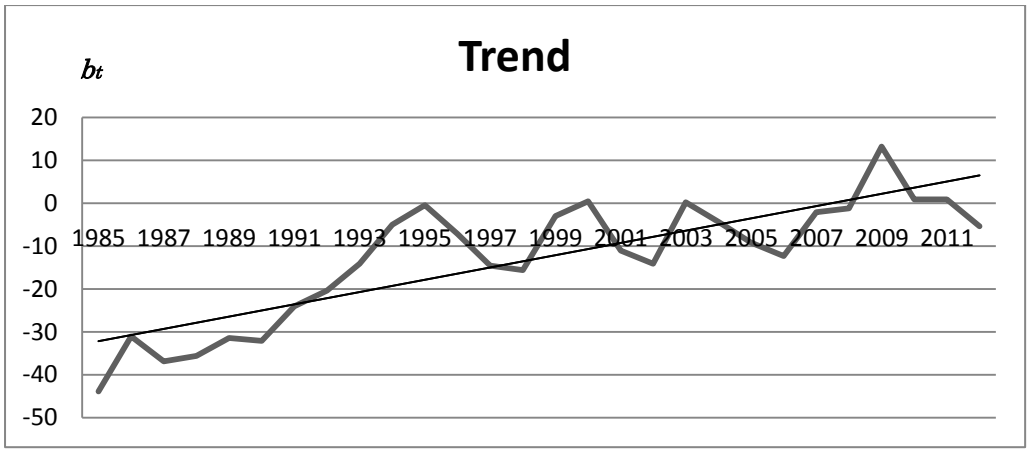

Trend plot of March series using Holt's method at station 45253.

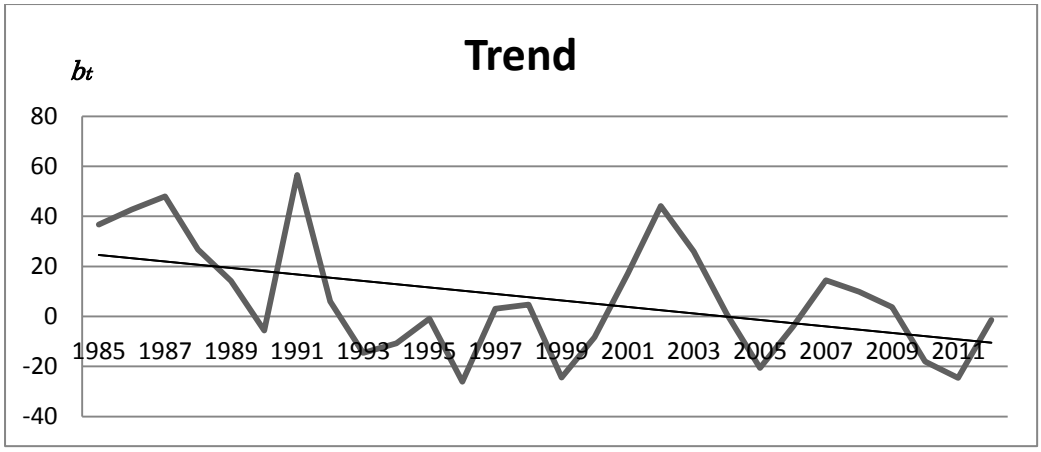

Trend plot of April series using Holt's method at station 45253.

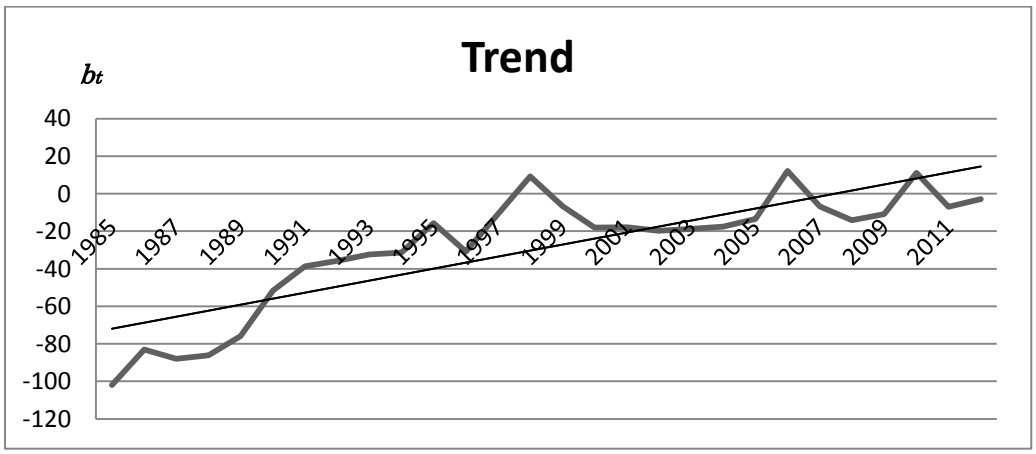

Trend plot of May series using Holt's method at station 45253.

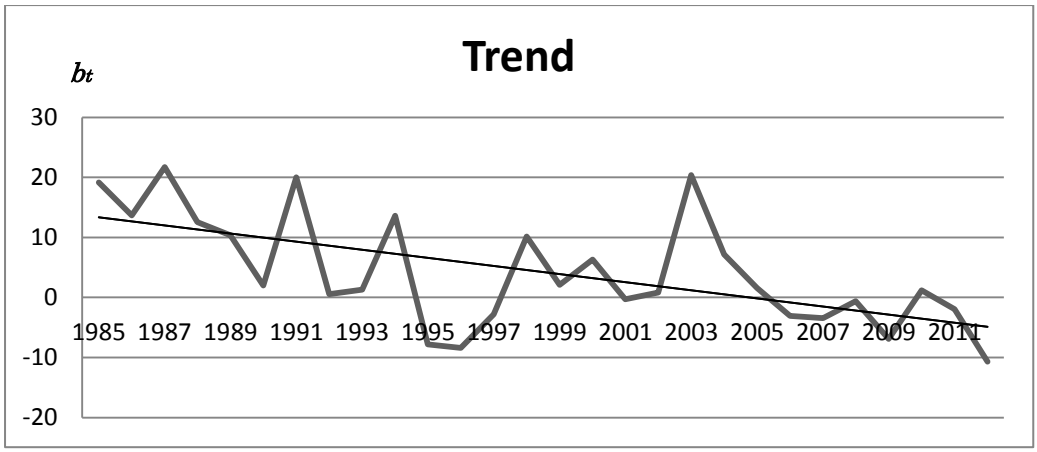

Trend plot of June series using Holt's method at station 45253.

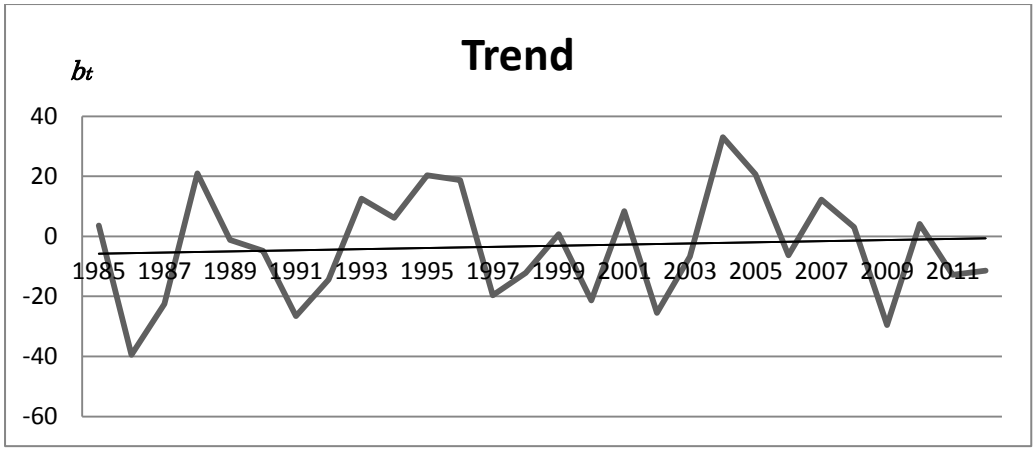

Trend plot of July series using Holt's method at station 45253.

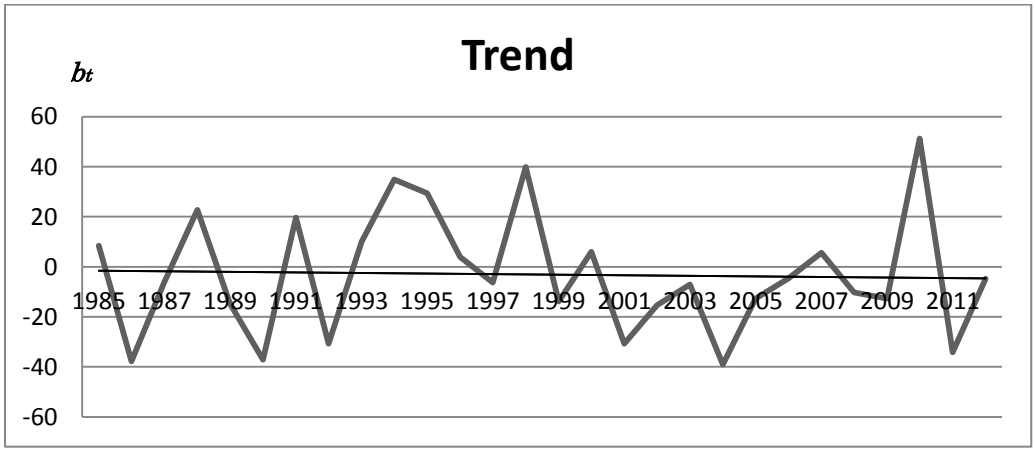

Trend plot of August series using Holt's method at station 45253.

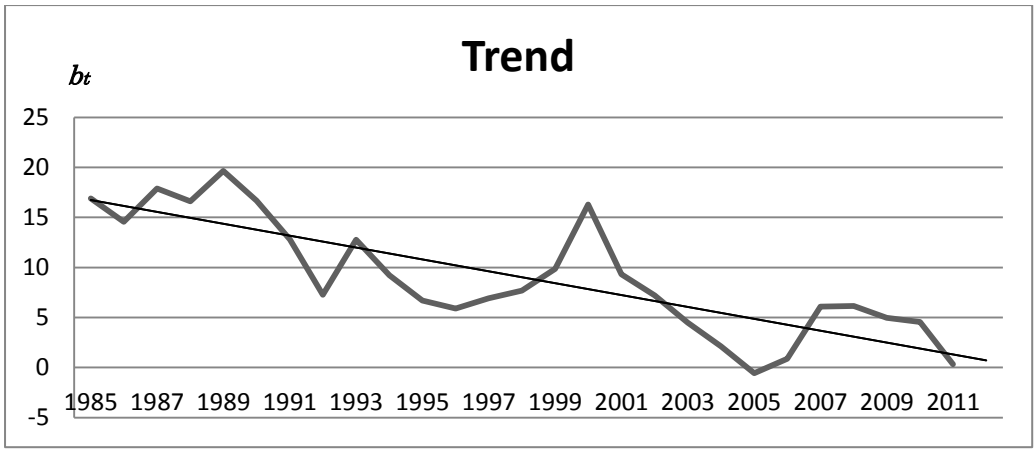

Trend plot of September series using Holt's method at station 45253.

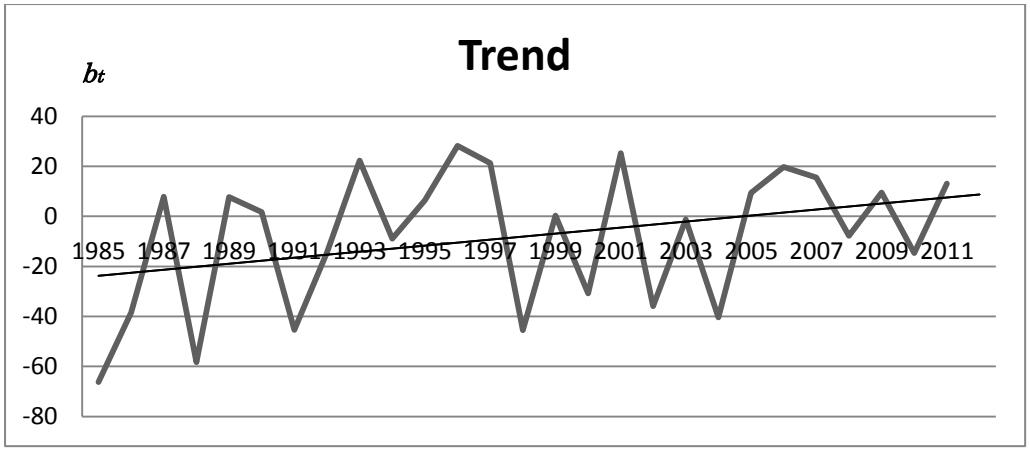

Trend plot of October series using Holt's method at station 45253.

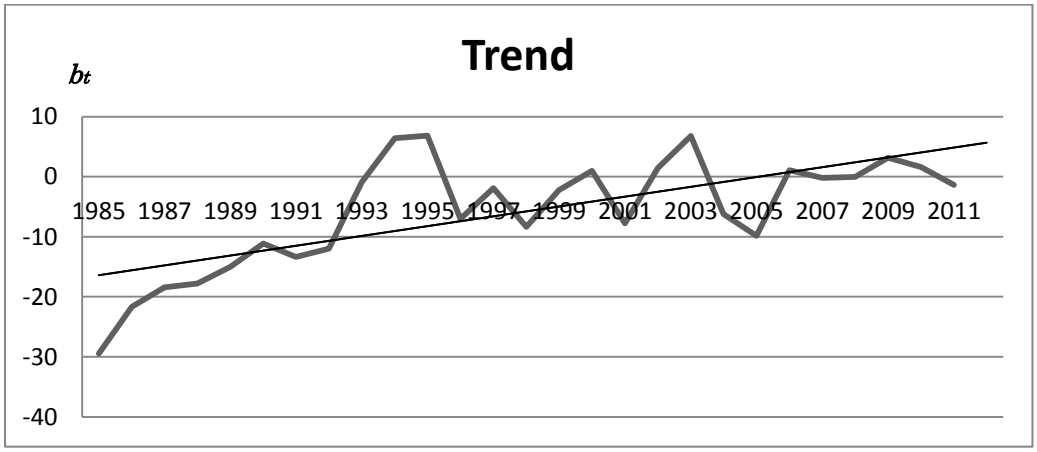

Trend plot of November series using Holt's method at station 45253.

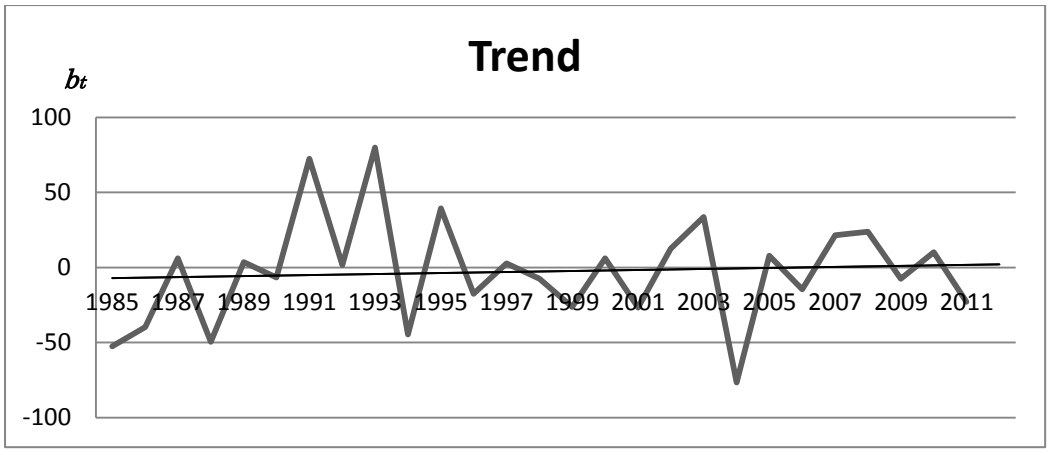

Trend plot of December series using Holt's method at station 45253.

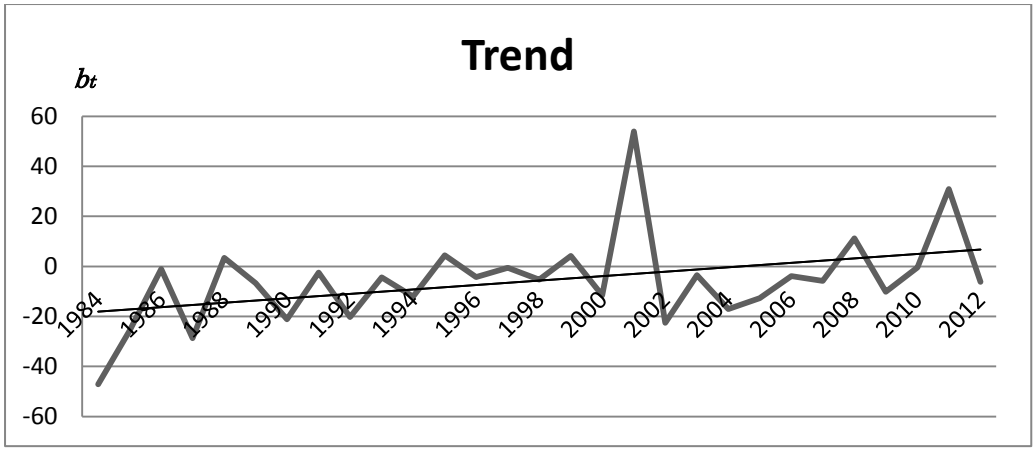

Trend plot of January series using Holt's method at station 45254.

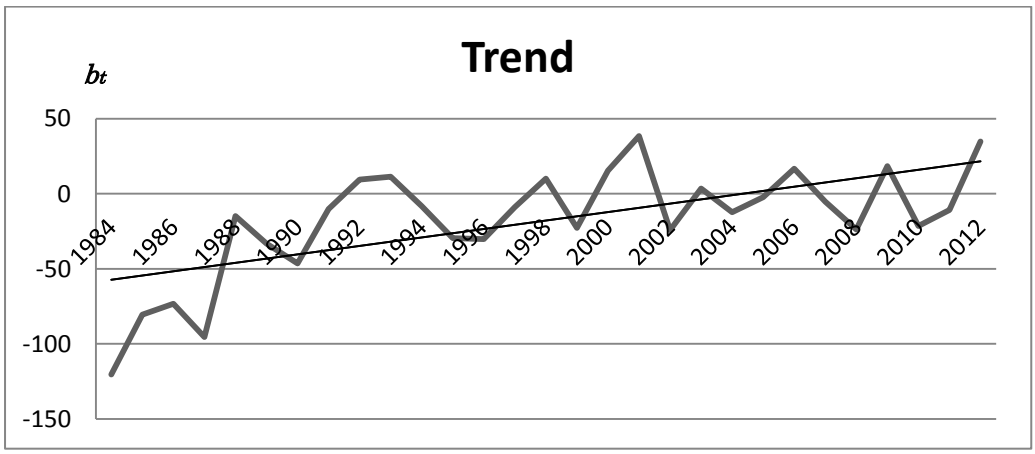

Trend plot of February series using Holt's method at station 45254.

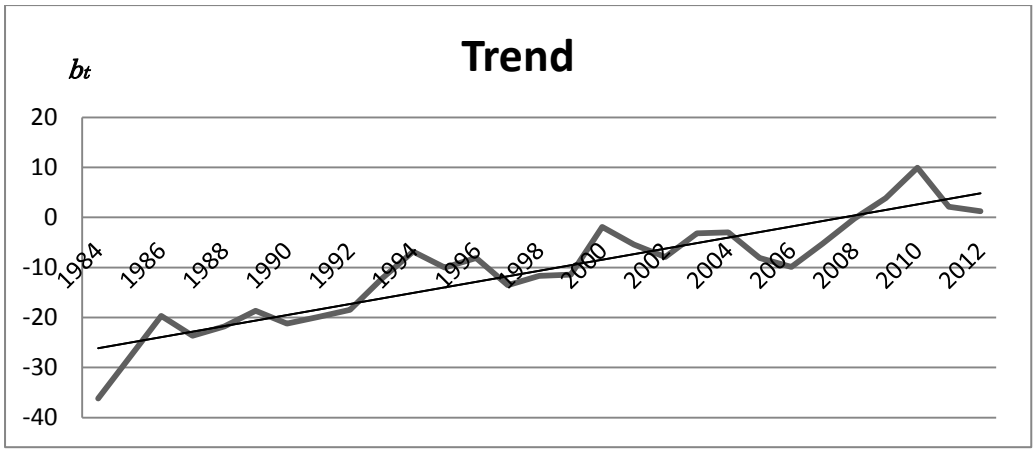

Trend plot of March series using Holt's method at station 45254.

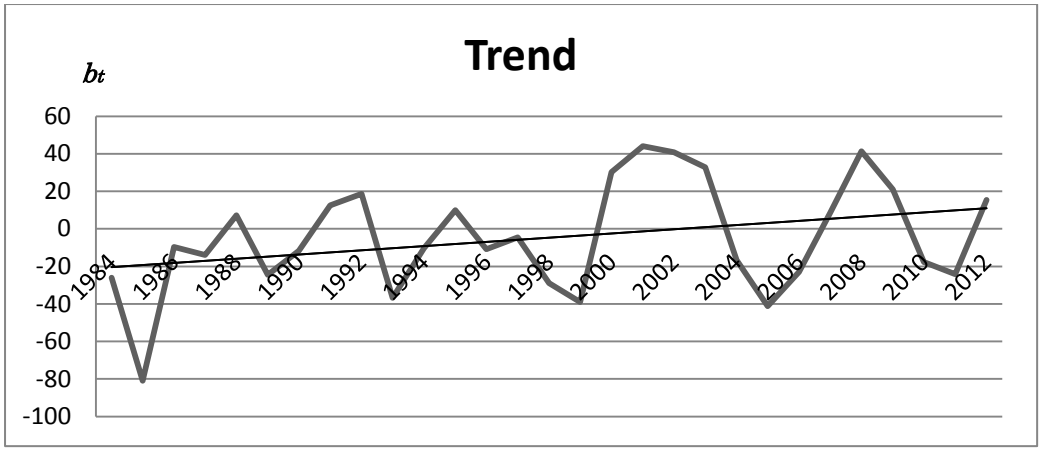

Trend plot of April series using Holt's method at station 45254.

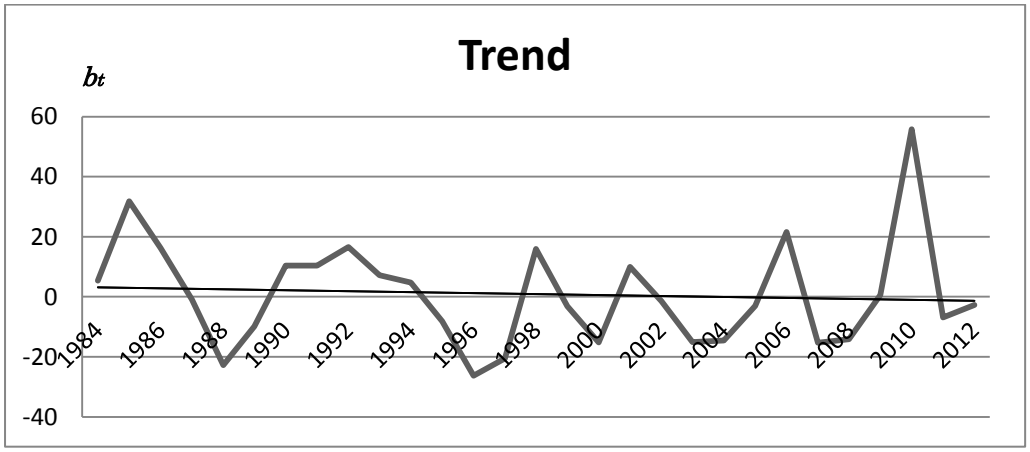

Trend plot of May series using Holt's method at station 45254.

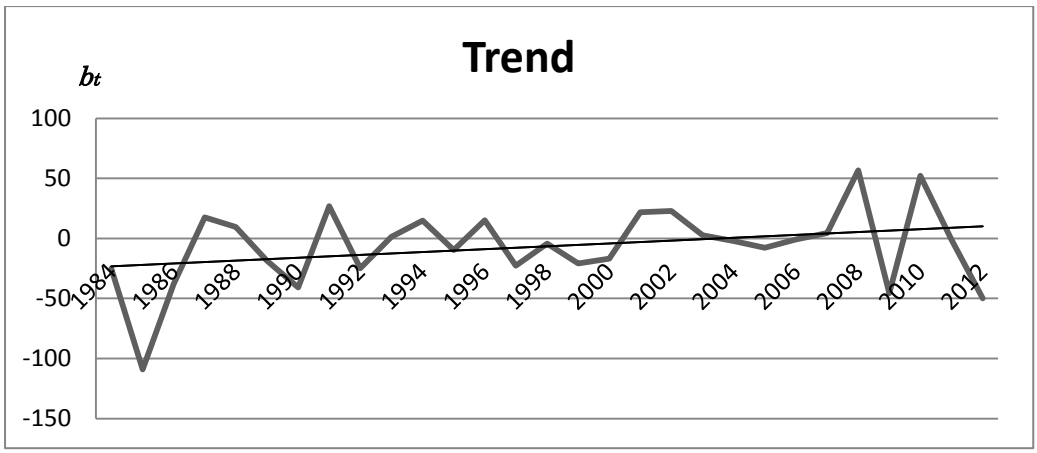

Trend plot of June series using Holt's method at station 45254.

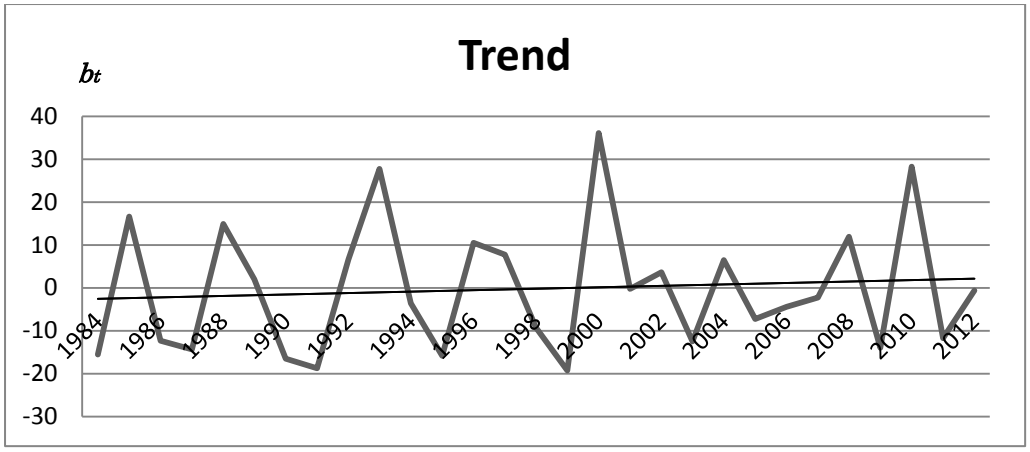

Trend plot of July series using Holt's method at station 45254.

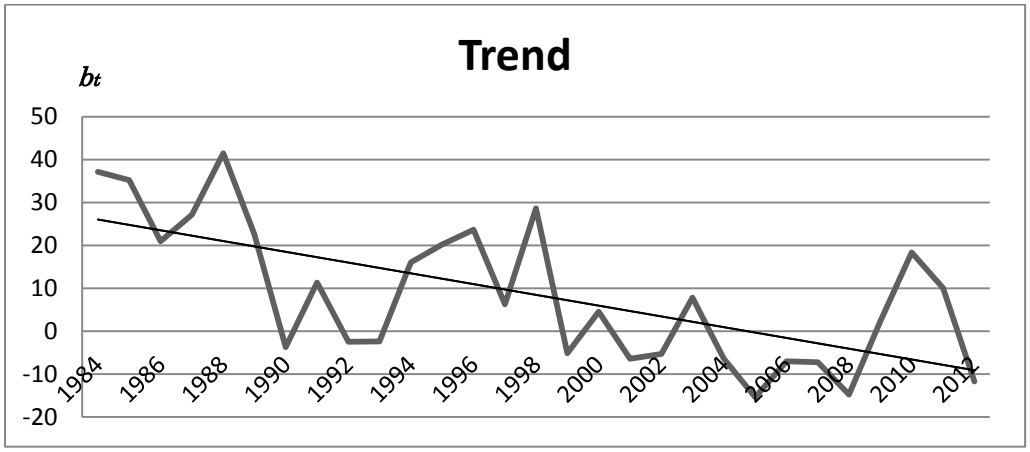

Trend plot of August series using Holt's method at station 45254.

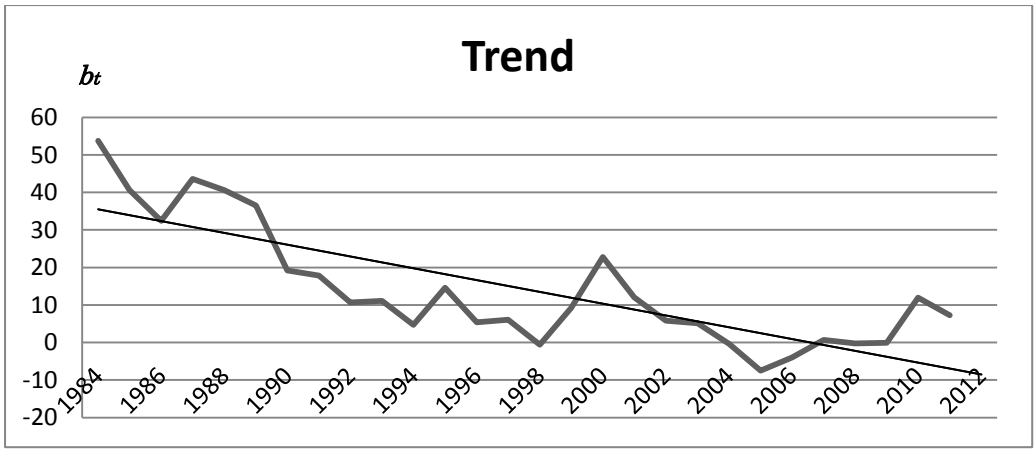

Trend plot of September series using Holt's method at station 45254.

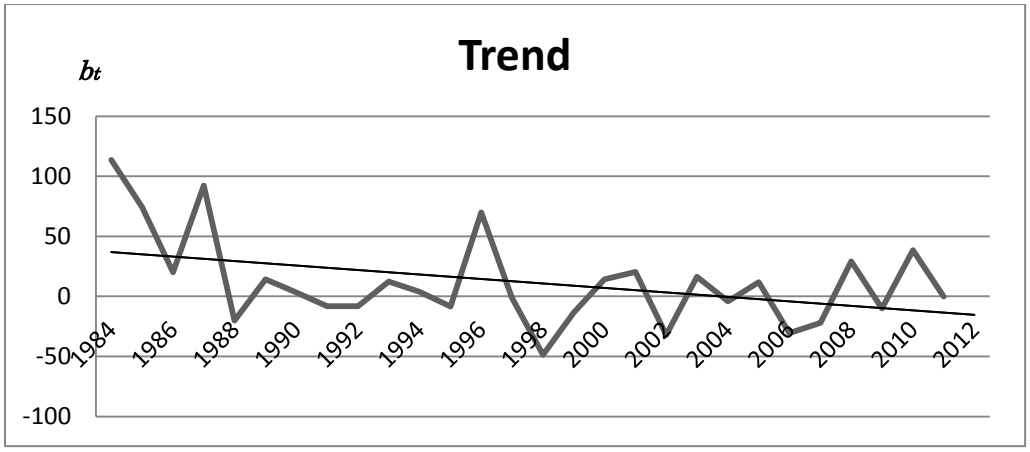

Trend plot of October series using Holt's method at station 45254.

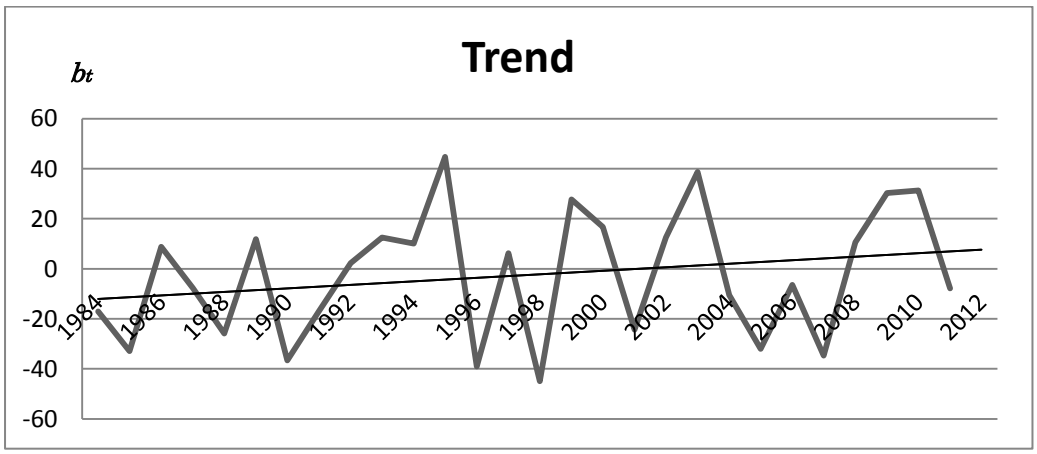

Trend plot of November series using Holt's method at station 45254.

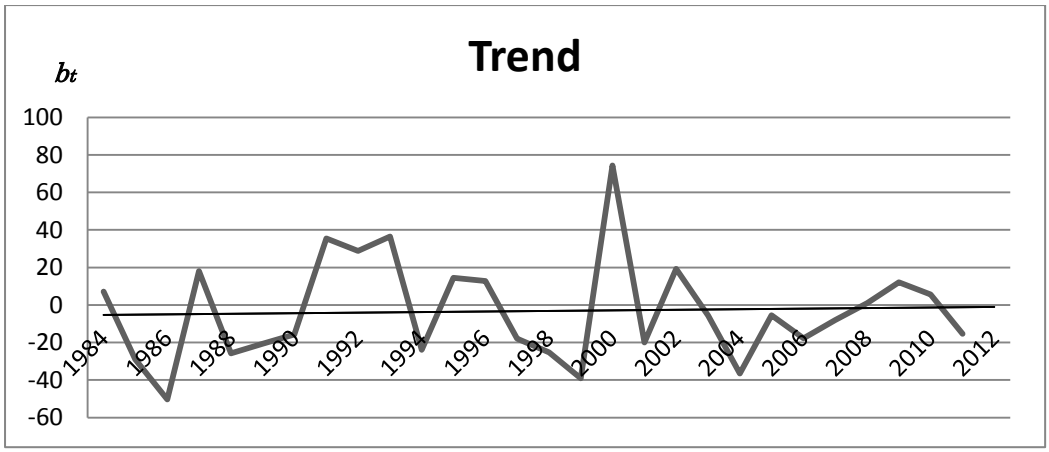

Trend plot of December series using Holt's method at station 45254.

APPENDIX C

Percentage of MAD to Average Rainfall for Rainfall Series Analysis

Stations Code		Average	MAD	Percentage
44239	Monthly	170.9	65.5	38.33%
	Seasonal	509.7	119.3	23.41%
44255	Seasonal	476.8	133.8	28.06%
44256	Monthly	170.7	72.4	42.41%
	Seasonal	511.3	141.2	27.62%
44320	Monthly	215	84.8	39.44%
	Seasonal	640.8	161.8	25.25%
45253	Monthly	174.3	76.2	43.72%
	Seasonal	517	152	29.40%
45254	Monthly	180.7	79.4	43.94%
	Seasonal	536.5	154.3	28.76%
2815001	Monthly	147.7	66.6	45.09%
	Seasonal	440.8	142.5	32.33%
2818110	Monthly	162.5	64.2	39.51%
	Seasonal	485.8	133.5	27.48%
2913001	Monthly	160	70.7	44.19%
	Seasonal	475.6	133.5	28.07%
2917001	Monthly	567.3	78.1	13.77%

APPENDIX D

LIST OF PUBLICATION

Huang, Y.F., Puah, Y.J., Chua, K.C. and Lee, T.S., 2014. Analysis of monthly and seasonal rainfall trends using the Holt's test. *International Journal of Climatology*, Published online in Wiley Online Library (wileyonlinelibrary.com). DOI: 10.1002/joc.4071.